

REPUBLIC OF THE PHILIPPINES

DEPARTMENT OF NATURAL RESOURCES

BUREAU OF MINES

REPORT ON GEOLOGICAL SURVEY

OF

NORTHEASTERN LUZON

PHASE I

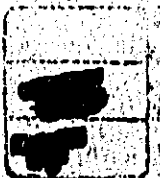
GEOLOGICAL, GEOCHEMICAL AND AEROMAGNETIC SURVEYS

OCT. 1975

METAL MINING AGENCY

JAPAN INTERNATIONAL COOPERATION AGENCY

GOVERNMENT OF JAPAN



REPUBLIC OF THE PHILIPPINES

DEPARTMENT OF NATURAL RESOURCES

BUREAU OF MINES

REPORT ON GEOLOGICAL SURVEY

OF

JICA LIBRARY



1046619[1]

NORTHEASTERN LUZON

PHASE I

GEOLOGICAL, GEOCHEMICAL AND AEROMAGNETIC SURVEYS

OCT. 1975

METAL MINING AGENCY

JAPAN INTERNATIONAL COOPERATION AGENCY

GOVERNMENT OF JAPAN

国際協力事業団	
輸入 月日 84. 3. 28	118
登録No. 02143	66.1
	MP

PREFACE

The Government of Japan, in response to the request of the Government of the Republic of the Philippines, decided to conduct a geological survey for mineral exploration in Northeastern Luzon of the Philippines, and commissioned its implementation to the Japan International Cooperation Agency.

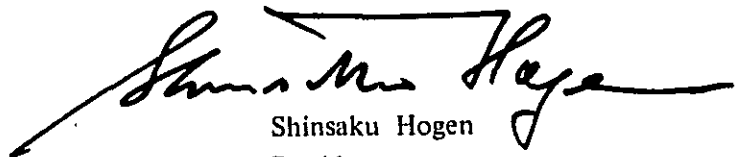
The Agency, taking into consideration of the importance of technical nature of the survey work, in turn sought the Metal Mining Agency of Japan for its cooperation to accomplish the task within a period of three years.

This year was for the first phase survey, and as for this current year, a survey team was formed consisting of fifteen (15) members headed by Mr. Hiroshi Fuchimoto, Staff of the Metal Mining Agency of Japan, and sent to the Philippines on January 4, 1975. The team stayed there for ninety-two (92) days from January 4, 1975 to April 5, 1975. During the period of its stay, the team, in close collaboration with the Government of the Republic of the Philippines and its various authorities, was able to complete survey works on schedule.

This report submitted hereby summarizes the results of the survey performed for the first-phase survey, and it will be also formed a portion of the final report that will be prepared with regard to the results obtained in the second and the third phases.

I wish to take this opportunity to express my heartfelt gratitude to the Government of the Republic of the Philippines and the other authorities concerned for their kind cooperation and support extended to the Japanese survey team.

October 1975



Shinsaku Hogen
President
Japan International Cooperation
Agency

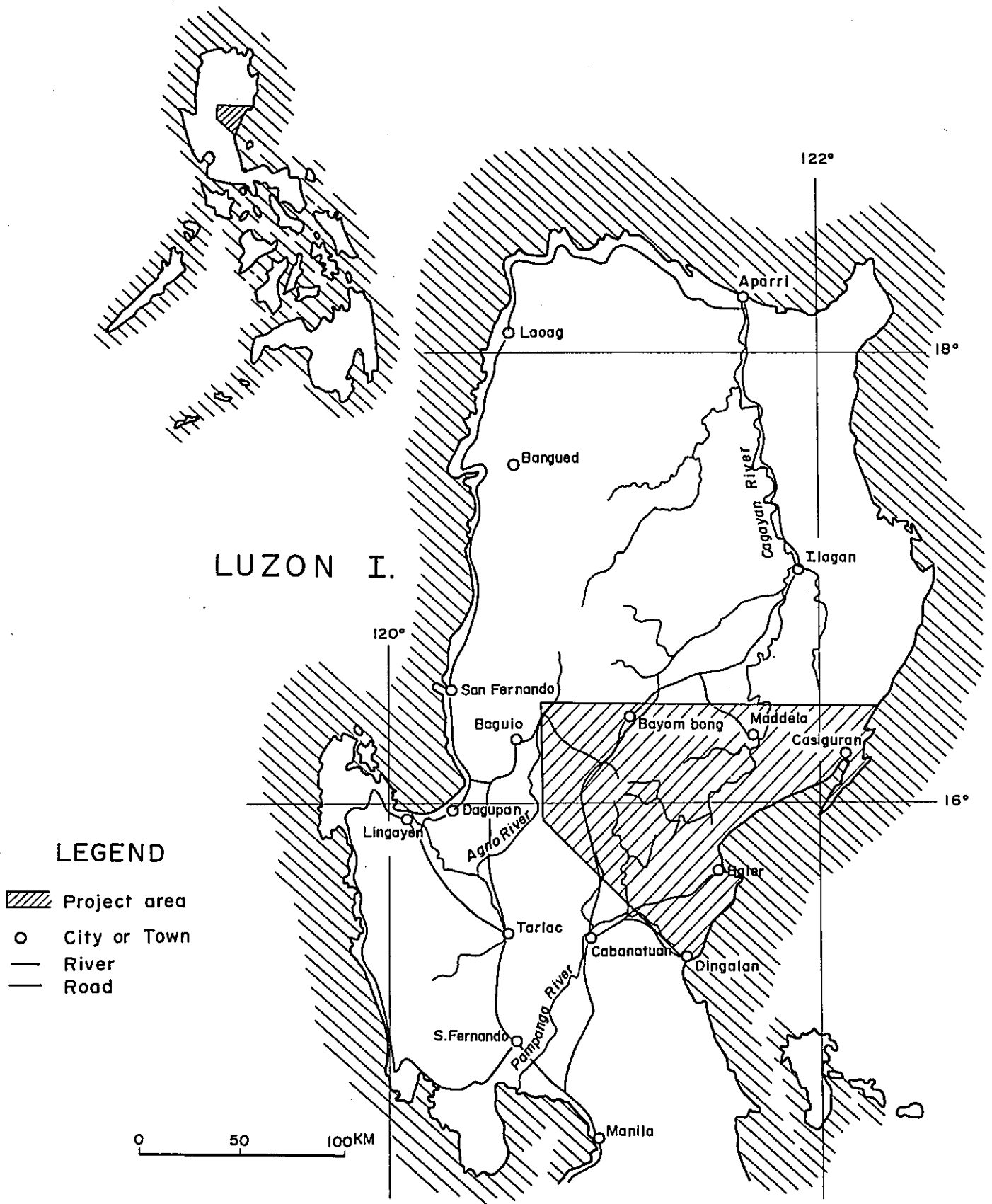


Fig. 1 Location map of the Survey area

CONTENTS

PREFACE	1
LOCATION MAP OF SURVEY AREA	2
ABSTRACT	11

GENERAL INFORMATION

1. Introduction	12
1-1 Purpose of Survey	12
1-2 Outline of Survey	12
1-3 List of Members	14
1-4 Reference	15
2. General Information	18
2-1 Location and Accessibility	18
2-2 Topography	18
2-3 Climate and Vegetation	21
3. General Discussion	22
3-1 Natures of dioritic rocks	22
3-2 Geochemical survey results	25
3-3 Aeromagnetic survey results	26
3-4 Summary	27
4. Conclusions and Future Problems	29

PART I GEOLOGICAL SURVEY

1. Geology	31
1-1 Previous Works	31
1-2 Stratigraphy	32
1-2-1 Basement Complex	33
1-2-2 Caraballo Group	33

1-2-3	Mamparang Group	37
1-2-4	Santa Fe Formation	38
1-2-5	Aglipay Formation	39
1-2-6	Matuno Formation	39
1-2-7	Maddela Formation	39
1-2-8	Pantabangan Formation	40
1-2-9	Pliocene to Quaternary Lavas	40
1-2-10	Alluvium	40
1-3	Intrusive Rocks	41
1-3-1	Ultrabasic Rocks	41
1-3-2	Gabbro	41
1-3-3	Dolerite	42
1-3-4	Dacite	43
1-3-5	Dioritic Rocks	43
1-3-5-1	Diorite—Quartz Diorite	43
1-3-5-2	Monzonite	44
1-3-5-3	Granodiorite—Granite	45
1-4	Chemical Compositions of the Dioritic Rocks	45
1-4-1	Analytical Samples	46
1-4-2	Analytical Results	46
1-4-3	Results and Discussions	46
1-5	Ages of Intrusion of Igneous Rocks	53
1-6	Geological Structure and Geological History	53
1-6-1	Geological Structure	53
1-6-2	Geological History	56

2.	Ore Deposits	58
2-1	General Statement	58
2-2	Mineralized Zone	61
2-2-1	Bolo River Mineralized Zone	61
2-2-2	Benneng River Mineralized Zone	61
2-2-3	Mapayao River Mineralization	62
2-2-4	Maasin River Mineralization	62

PART II GEOCHEMICAL SURVEY

1.	General Remarks	64
2.	Sampling and Analyses	65
2-1	Sampling	65
2-2	Analyses	65
2-2-1	Atomic absorption spectrometry	65
2-2-2	Colorimetry	66
3.	Compilation and Interpretation of the Results	67
3-1	Compilation of the Analytical Results	67
3-2	Interpretation of the Results	68

PART III AIRBORNE MAGNETIC SURVEY

1.	General Remarks	72
2.	Outline of Airborne Magnetic Survey	73
2-1	Survey Area	73
2-2	Survey Period	73
2-3	Surveyors	75
2-4	Summary of Field Operations	75
2-5	Survey Instrumentation	76

2-6	Data Processing	86
2-6-1	Flight Path Map	86
2-6-2	Correction of Daily Magnetic Variation	86
2-6-3	Total-Intensity Map	87
2-6-4	Residual Anomaly Map	87
2-7	Analysis Methods	88
2-7-1	Spectrum Analyses	89
2-7-2	Band-pass Filter	91
2-7-3	Pseudo-gravity Filter	94
2-8	Magnetic Measurements of Rock Samples	95
3.	Survey Results	98
3-1	Residual Map	98
3-2	Band-pass Maps	100
3-2-1	Band-pass Map BP-1	102
3-2-2	Band-pass Map BP-2	105
3-2-3	Band-pass Map BP-3	106
3-3	Pseudo-gravity Map	107
3-3-1	Pseudo-gravity Map PG-1	107
3-3-2	Pseudo-gravity Map PG-2	107
3-3-3	Pseudo-gravity Map PG-3	107
3-4	Quantitative Analyses	108
4.	Concluding Remarks	109

LIST OF ILLUSTRATIONS

Fig.	1.	Location map of the survey area	2
	2.	Physiographic provinces of northern Luzon	19
	3.	Location map of the tested samples	23
	I-1	Normative quartz-plagioclase-alkali-feldspar diagram	48
	2	Alkali contents of the dioritic rocks	48
	3	Chemical components plotted against Fe^*/MgO of the dioritic rocks	49
	4	MFA diagram of intrusive rocks	52
	5	Location map of porphyry copper deposits, Philippines	59
	III-1	Location map of Survey area	74
	2	Flight altitude	77
	3	Block diagram of airborne magnetic survey (airborne system)	79
	4	Block diagram of airborne magnetic survey (ground system)	84
	5	Flow Chart of Data Processings and Analyses	90
	6	Index to Survey area	99
	7	Energy Spectrum vs. frequency	101
	8	Characteristics of band-pass filter BP-1	103
	9	Characteristics of band-pass filter BP-2	103
	10	Characteristics of band-pass filter BP-3	103
Table	1.	Period of survey, length of survey route and number of geochemical samples	14
	2.	Characteristics of the dioritic rocks	23
	I-1	Generalized stratigraphic section in the survey area	32
	2	Chemical composition of the dioritic rocks	47
	3	Normative constituents of the dioritic rocks	47
	4	Chemical composition of the granitic rocks	51
	5	Features of the dioritic rocks in the survey area	51
	6	Locality and names, ore reserves in tons, grades in percent copper, and daily production of porphyry copper prospects and mines in the Philippines	60

II-1	Regional mean background and threshold values of stream sediment samples	68
III-1	Suscptibilities of rock samples	96
2	Remanent magnetism of rock samples	97

LIST OF APPENDICES

Table	1. Fossils	A- 1
	2. Potash-Argon ages on some intrusive rocks	A- 3
	3. Microscopic observations	A- 4
	4. Chemical analysis of rock samples	A-23
	5. X-ray diffractive analysis	A-24
	6. Metal content of geochemical samples	A-25

Fig.	1. Histogram of Cu, Zn and Mo	A-32
	2. Cumulative frequency distribution of Cu, Zn and Mo	A-32
	3. Corration diagram Cu-Zn	A-32

Plate I-1.	1. Geological map	1 : 250,000	(1 sheet in pocket)
	2. Geological profile	1 : 250,000	(1 sheet in pocket)
	3. Geological map	1 : 100,000	(3 sheets in pocket)
	4. Geological profile	1 : 100,000	(1 sheet in pocket)
	5. Route and sample map	1 : 100,000	(3 sheets in pocket)
	6. Columnar section of local stratigraphy	1 : 300,000	(1 sheet in pocket)
	7. Tectonic map	1 : 250,000	(1 sheet in pocket)
	8. Tectonic profile	1 : 250,000	(1 sheet in pocket)
	9. Tectonic map	1 : 100,000	(3 sheets in pocket)
	10. Tectonic profile	1 : 100,000	(1 sheet in pocket)

II-1.	1. Geolochemical anomalies of stream sediments	1 : 250,000	(1 sheet in pocket)
	2. Location map of geochemical samples	1 : 100,000	(3 sheets in pocket)

III-1.	1. Residual map	1 : 100,000	(3 sheets in pocket)
	2. Band-pass map BP-1	1 : 250,000	(1 sheet in pocket)
	3. Band-pass map BP-2	1 : 100,000	(3 sheets in pocket)
	4. Band-pass map BP-3	1 : 250,000	(1 sheet in pocket)
	5. Pseudo-gravity map PG-1	1 : 100,000	(3 sheets in pocket)
	6. Pseudo-gravity map PG-2	1 : 250,000	(1 sheet in pocket)
	7. Pseudo-gravity map PG-3	1 : 100,000	(3 sheets in pocket)
		1 : 250,000	(1 sheet in pocket)

8. Interpretation map (Band-pass 1)	1 : 100,000	(3 sheets in pocket)
	1 : 250,000	(1 sheet in pocket)
9. Interpretation map (Band-pass 2)	1 : 100,000	(3 sheets in pocket)
	1 : 250,000	(1 sheet in pocket)
10. Interpretation map (Band-pass 3)	1 : 100,000	(3 sheets in pocket)
	1 : 250,000	(1 sheet in pocket)
11. Interpretation map	1 : 100,000	(3 sheets in pocket)
	1 : 250,000	(1 sheet in pocket)

ABSTRACT

Phase I of the mineral resources survey of Northeastern Luzon, Philippines was carried out to determine promising areas for ore deposits. It consists of geological, geochemical and aeromagnetic surveys.

Based on aeromagnetic survey results the main geological structures of the survey area are NW-SE direction in the west and NE-SW in the east. In the north-western portion of the survey area many lineaments are oriented obliquely to some of the major N-S lineaments controlling the distribution of dioritic rocks which coincide with magnetic anomalies.

The metavolcanics and metasediments classed as the Cretaceous to Paleogene system (KPg & UV) were divided into three formations by geological survey, and their characteristics and geological structures became clear. The time intervals of the diorite intrusion were also established. That is, the Sierra Madre — Eocene and the central part and the Cordillera Central — Close to the Oligocene. The western diorite is younger than the east. These time intervals seem to have caused the differences of rock series, i. e., the Sierra Madre — calc-alkalic series, and the central part and the Cordillera Central — alkali-olivine basalt or tholeiitic series. Therefore, the same age and some type of mineralization as the porphyry copper deposits related to the Agno-batholith is probably limited in the central and the western portion of the survey area.

Geochemical survey disclosed some anomalies of copper, zinc and molybdenum. The anomalies in the north are widely distributed and are more promising than those in the south. The former seems to have a genetic relation to the diorite intrusion of alkali-olivine basalt series.

The results of geological, geochemical and aeromagnetic survey in the north-western parts of the survey area is considered to have high potential for mineral resources. In Phase II, therefore, it is recommended to carry out the detailed geological, geophysical (EM and/or IP method) and geochemical surveys in this area to determine the nature of mineralization.

GENERAL INFORMATION

1. Introduction

1-1 Purpose of Survey

The purpose of the survey for the Phase I in the Northeastern Luzon Project, Philippines was to delineate promising area of about 30 percent which has potential for mineral resources.

1-2 Outline of Survey

In Phase I, aeromagnetic survey was conducted to define the distribution of acidic igneous rocks and to detect magnetic anomalies where ore deposits could be associated and later on checked by ground survey.

The aeromagnetic survey was conducted by using a Japanese aircraft YS-11. The team was composed of three parties of eleven staff; (a) observation party consisting of one Filipino and five Japanese, including pilot, (b) compilation party consisting of one Filipino and two Japanese geophysicists, and (c) ground station party consisting of one Filipino and one Japanese.

A base station for diurnal observation of geomagnetism was set up in Bayombong, the provincial capital of Nueva Viscaya, located near the north end of the project area. It has the largest population (about 25,000) in the survey area. Telecommunication system can be used in the daytime from this town to Manila.

Prior to the geological field works, a preparatory tour was made for one month to gather information on peace and order conditions and accessibility of the project area, especially within the mountain ranges.

Chartered light plane, helicopter and jeep were utilized during the course of the tour.

From the aerial observations, many logging roads are visible, so that, at the start, geological survey by jeep was expected on some area.

Ground check, showed that some of the logging roads were imposible due to poor maintenance and landslides. In addition steep valley walls and rugged topogra- phy prevented the survey members to penetrate the interior parts of the area. Peace and order situation was not feasible, thus, the portion of the northern area extending from the Philippine Sea to the Sierra Madre Range covering approximately 1, 700 km² has been eliminated.

The geological survey team arrived in the field when the aeromagnetic survey had been almost completed. The survey area was divided into four parts. Each part was covered by one party consisting of one Filipino and one Japanese geologist. A base camp was established in Bambang, Nueva Viscaya, for preparation of geo- chemical samples sent by geological parties and for better communication.

Consequently, after the joint survey, additional geological and geochemical surveys were undertaken by the Bureau of Mines geologist on some of the uncovered area. In this report the additional data are also discussed.

Airphotographs over 5, 000 sheets were interpreted by one B. M. photogeologist during and after the field work.

The period of stay in the Philippines, the total length of the survey routes, and the number of geochemical samples are shown in Table 1.

The writers are indebted to Professor Yoshio Ueda, Tohoku University on chronologizing the intrusive rocks and Dr. Kunitaru Matsumaru of Saitama Univer- sity on identifying of fossils. Drs. Hiroo Kagami and Kenji Shuto provided instructive comments on chemical compositions of dioritic rocks. Their kind advice and sugges- tion are highly acknowledged.

Table 1 Period of survey, length of survey route and number of geochemical samples

	Stay in the Philippines	Actual field work	Length of survey route	Number of geochemical samples
Geophysical team	Jan. 4 ~ Mar. 19 1975 75 days	Jan. 21 ~ Mar. 3 42 days	11,244 km	1,001 pcs
Geological team	Feb. 4 ~ Apr. 5 1975 61 days	Mar. 2 ~ Mar. 26 25 days	1,080 km Foot 620 Car 430 Boat 30	

1-3 List of Members

The list of members engaged in the survey are as follows.

(Management)

FEDERICO E. MIRANDA	Bureau of Mines Philippines	HIROSHI FUCHIMOTO	Metal Mining Agency of Japan
		SHINSEI TERASHIMA	do
CONSTANTE BELANDRES	do	MASAHARU SAKANO	do
		SATORU KOHIYAMA	Japan International Cooperation Agency

(Geological team)

ARNULFO V. CABANTOG	do	HIROSHI FUCHIMOTO	M. M. A. J.
JOSE N. ALMASCO	do	TAKEOMI MIYOSHI	do
ORLANDO M. PINEDA	do	IKUHIRO HAYASHI	do
ANDRE P. VICTORIANO	do	SADAHARU IWANE	do
BENJAMIN S. CADAWAN	do		

(Geophysical team)

CAROL S. SAMONTE		MASAO YOSHIZAWA	do
ROMEO L. ALMEDA	do	IKUO TAKAHASHI	do

URBANO PALAGANAS	do	SABURO TACHIKAWA	do
		(Aircraft Crew)	
		MOTOJI ICHIKAWA	do
		MITSURU SAKAZAKI	do
		SHOZO KIMURA	do
		TAMOTSU FUJIKAWA	do
		TAKASHI YAMANAKA	do

(Photo-interpretation)

PANFILO O. MONTERO	do
--------------------	----

1-4 Reference

- | | | |
|------------------------|------|--|
| Allen C. R. | 1962 | Circum-Pacific faulting in the Philippines-Taiwan Region. Jour, Geophys. Res., V. 67 p 4795-4812 |
| Almogera D. H. | 1974 | Philippine porphyry coppers. World Mia. V. 27 No. 13 p 28-33 |
| Aramaki S. et al. | 1972 | Chemical composition of Japanese granites, Pt. 2, Variation trends and average composition. Geol. Soc. Japan V. 78 p 38-49 |
| Becker F. C. | 1899 | Brief memorandum on the geology of the Philippine Islands. U. S. Geol. Surv. 20th Ann. Rept. p 3-7 |
| Bryner L. | 1969 | Ore deposits of the Philippines - An introduction to their geology. Econ. Geol. V. 64 p 644-666 |
| Coby G. W. et al. | 1951 | Geology and oil possibilities of the Philippines. Dept. Agricul and Nat. Resour. Tech. Bull No. 21 |
| Durkee E. F. et al. | 1961 | Geology of northern Luzon, Philippines. Bull. Am Ass. Petr. Geol. V. 45 No. 2 p 137-168 |
| Fernandez J. C. et al. | 1967 | Preliminary report on the reconnaissance geology of the northwestern Luzon, Philippines. Geol. Soc. Phil. V. I p 35-45 |
| Gervasa F. C. | 1966 | The age and nature of orogenesis of the Philippines. Phil. Geol. V. 20 p 121-140 |
| — | 1966 | A study of the tectonics of the Philippine archipelago. Phil. Geol. V. 20 p 51-74 |

- Gervasio F. C. et al. 1967 Concept in the preparation of a metallogenic Map of the Philippines. Phil. Geol. V. 22 p 117-126
- 1967 Age and nature of metallization of the Philippines. First Symp. on Geol of Min. Resour. Geol. Soc. Phil. V. I p 52-75
- Gorai M. 1975 Magmatism (in Japanese) Kyoritu Press.
- Hashimoto W. 1968 A contribution to the study of geologic structure of the Philippines. (in Japanese)
(Part I) Geol. Soc. Japan V. 77 p 78-116
- 1969 do. (Part II) Geol. Soc. Japan V. 78 p 235-270
- 1970 do. (Part III) Geol. Soc. Japan V. 79 p 1-27
- Hess H. H. 1955 Serpentes, orogeny and epeirogeny
Geol. Soc. Am. special paper 62 p 391-408
- Ishihara S 1970 Porphyry copper deposits (in Japanese)
Maruzen Press.
- I. U. G. S. Subcommission
1973 Plutonic rocks, classification and nomenclature recommended by the I. U. G. S. Subcommission on the systematics of igneous rocks. Geotimes V. 18 p 28-30
- Kinkel J. A. R. et al. 1956 Copper deposits of the Philippines. Dept. Agriculture and Nat. Resources. Spec. project series No. 16
- Kintanar E. R. L. 1967 Petroleum geology of the Philippines. First Symp. on Geol. of Min. Resour. Geol. Soc. Phil. VII. p 401-432
- Lepeltier C. 1969 A simplified statistical treatment of geochemical data by graphical representation. Econ. Geol. V. 64 p 538-550
- Miyashiro A. et al 1975 Petrology (II) (in Japanese) Kyoritsu Press
- O. T. C. A. & Phil. Bur. of Mines 1974 Report on geological survey of eastern Mindanao.
- Pena R. 1970 Brief geology of a portion of the Baguio mineral district
Geol. Soc. Phil. V. 24 No. 4 p 41-42
- Phil. Bur. of Mines 1963 Geological map of the Philippines (1:1,000,000)
- 1964 Mineral distribution map of Philippines (1:2,500,000)

- 1975 Mineral prospects in the area proposed for the joint
BM-Japanese project in the northeastern part of Luzon
(unpublished)
- Santos-Ynigo L. M. 1966 Island arc features of the Philippine Archipelago.
Phil. Geol. V. 20 p 79-92
- Titly S. R. et al. 1966 Geology of the prophyry copper deposits. Southwestern
North America. University of Arizona Press
- Wolf J. A. 1970 Interpretations of potassium-argon (K/Ar) dating in
the Philippines. Geol. Soc. Phil. V. 24 p 9

2. General Information

2-1 Location and Accessibility

The project area is located in the northeastern part of Luzon. It covers an area of about 11,000 km² bounded by the following lines: (See Fig. 1)

- in the north : the latitude 16° 30' North
- in the south : the foothills, from lower Agno River
to Dingalan Bay, bearing S45° E
- in the east : the eastern coast line
- in the west : the longitude 120° 45' East

The area covers the provinces of Nueva Viscaya, Quirino, Benguet, Pangasinan, Nueva Ecija and subprovince of Aurora Quezon.

Philippine Air Lines maintain the regular flights, 3 times a week, between Manila and Bagabag which is about 20 km from Bayombong.

The accessibility in the area is very poor owing to rugged topography. The national roads running through the area are Route No. 5 leading to Bayombong with its two branches; one is going to Baguio and the other to Baler.

The wide upper basin of the Cagayan River, the central part of the area, there are few roads and trails, so that this basin has been left behind as an undeveloped area.

Light airplanes are commonly used in the eastern, coastal region where roads are almost absent. Small private airstrips are laid in Dilasag, Mutuyong, Baler and Dilalongan etc. Along the Cagayan River, some runways are also constructed by missionaries.

2-2 Topography

The topographic features of Northern Luzon can be divided into several subdivisions

as shown in Fig. 2. From the east to the west; (1) Sierra Madre; (2) Cagayan Valley; (3) Cordillera Central; and (4) Coastal folded belt. Both (1) and (3) are uplift zones and show generally very steep topography. On the contrary, (2) and (4) are subsided zones showing plain or relatively flat topography. South of the Cagayan Valley is the Caraballo Mountains which surrounds the Cagayan Basin with the two uplifted zones stated above. These mountains are cut in the south by the large structural line (Philippine Fault) which traverses the Philippine archipelago and they are in contact with the Luzon Central Plain.

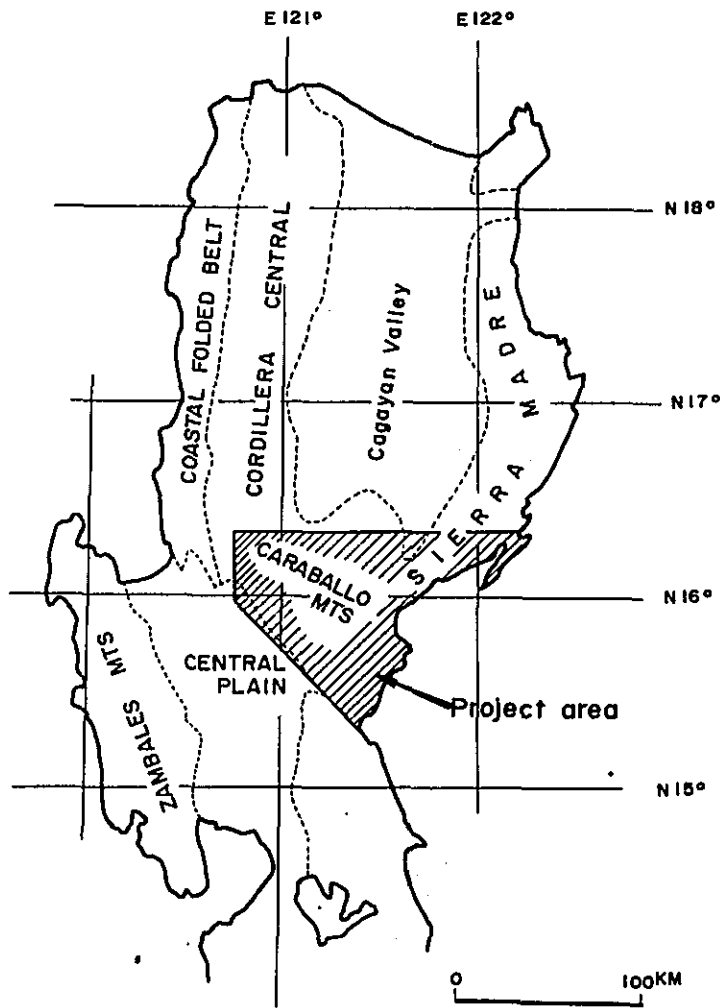


Fig. 2 Physiographic provinces of northern Luzon

The survey area includes the Sierra Madre, the Caraballo, the Cordillera Central and the Mamparang mountains consisting of relatively younger volcanics and limestone.

The Sierra Madre Mountain Range has an average elevation of 800 to 1,200 m with some of the peaks reach over 1,800 m. It is very rugged with steep and high walls of cliffs tower at places. In the southern part, crystalline schist is exposed and the V-shape dendritic valleys are well developed.

The Caraballo Mountain Range extends in the northwest direction with an elevation of 800 to 1600 m. From the airphoto-interpretation, the ridges are composed of volcanic rocks and it looks very hard to traverse the range on foot like the Sierra Madre.

The Cordillera Central consists generally of high mountains with many ridges of more than 1,200 m above the sea level. The highest peak in the survey area is found in this range. It is Mt Ugu which reaches an elevation of 2,150 m. Many faultline vallays trending NNW-SSE (which is parallel to the Philippine Fault) are developed in the area.

Most of the drainage systems in the whole area belong to the Cagayan, the Agno and the Pampanga Rivers. The Cagayan River is the largest river in the Philippines and flows down northward in the Cagayan Plain up to Aparri about 400 km for. It has a large discharge all the year round. In the area, it shows an annular pattern controlled by the geological structures.

Both the Agno and the Pampanga Rivers are important water sources for the Central Luzon Plain and many irrigation dams were constructed along the courses. There is one existing dam at Pamtabangan in the upper reaches of the Pampanga River. Now a new project to lead water by a tunnel from the upper stream of the Cagayan to the Pampanga is in progress.

2-3 Climate and Vegetation

The climate of the area can be divided into 3 types. They correspond roughly to the physiographic subdivisions.

In the Sierra Madre Mountains in the east there is no pronounced dry or rainy season and rain falls throughout year.

Most of the typhoons originated near the Philippines Sea causing damage to this area.

In the Cordillera Central Mountains in the west there are the pronounced dry and rainy seasons. The dry season lasts for 6 months from November to April and the rest is wet.

The Cagayan Valley in the central portion, the climate is intermediate between the above mentioned area, dry or rainy season is not so pronounced, but it is rather dry from November to April.

As stated above, the rainfall in the area is generally heavy, but vegetation is relatively thin owing to typhoons and steep topography. Especially in the mountain ranges west of Route 5, few trees can be found because of few reforestation.

3. General Discussion

The Phase I survey team have collected new data which may concern the future programme for ore-research. In this chapter these problems will be chiefly discussed.

3-1 Natures of dioritic rocks

In north eastern Luzon, there are two up lifted zones ie., the Cordillera Central and the Sierra Madre, where large scale dioritic rocks have been intruded. Most of the porphyry copper type of ore deposits are concentrated in the Cordillera Central. Megascopically, the dioritic rocks of the Sierra Madre are coarse grained and leucocratic. Although some vein-type of copper mineralizations grain and leucocratic. Although some vein-type of copper mineralizations can be recognized, no disseminations have been reported. In 1967, F.C. Gervasio estimated the intruding ages of quartz diorite as two periods, ie., Oligocene in the Sierra Madre and close to the middle Miocene in the Cordillera Central, mainly based on the study of the distribution of various rock units with their structures and nature of deformation.

Remembering these facts, rock samples were collected from the places, as shown in Fig 3, and analyzed them by means of petrographic observation, chemical analysis and K/Ar dating, to correlate a relationship between the porphyry copper type ore deposits and the dioritic rocks.

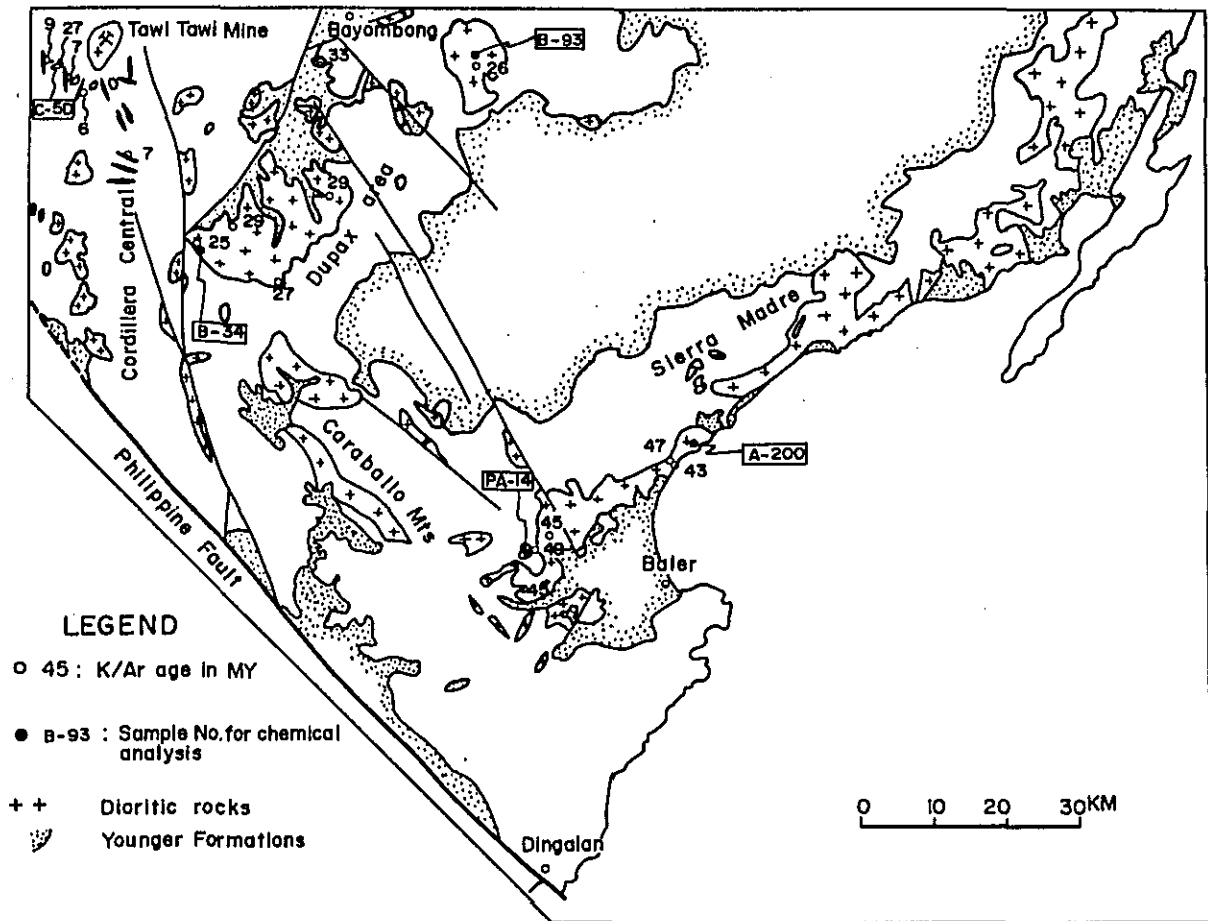


Fig. 3 Location map of the tested samples

Table 2 Characteristics of the dioritic rocks

Features Sampling sites	Rocks	Rock series	K/Ar ages MY	Geochemical anomalies
Sierra Madre	Granite	Calc-alkalic	43~49 (5)	Weak, limited Cu,Zn,Mo
Dupax	Diorite	Tholeiite (?)	25~29 (4)	Weak, limited Cu,
	Monzonite	Alkali-olivine -basalt	26~33 (3)	Strong, aerial Cu,Mo
Cordillera Central	Diorite	Alkali-olivine -basalt	27 (1)	Strong, aerial Cu,Zn,Mo
	Dacite	?	6~9 (5)	None

Remarks : MY — Million Years (5) — Number of observations

The results are summarized in Table 2.

The following are clearly evident from the table.

1. Intrusive rocks in the Sierra Madre are granitic and belong to the calc-alkali rock series. They were intruded in the early Eocene (the earliest activity).
2. In Dupax area, there are two rock series, ie., the tholeiite and the alkali-olivine series. Both of them intruded in almost the same age of the late Oligocene.
3. Diorite of the Cordillera Central belongs to the same rock series of monzonite in Dupax area, and intruded in the same age.
4. Numerous dacite dykes in the Cordillera Central intruded close to the Miocene (the latest activity). As they were not analyzed, their series are unclear.

The above-mentioned features include the following questions because of few data on chemical composition.

1. The Dupax batholith is microscopically dioritic. As fresh samples could not be collected from the center of the batholith because of intense weathering. A fresh rock sample taken from the margin was chosen for chemical analysis in spite of having gabbroic facies. Therefore, it may be unsafe to say that the sample has not been contaminated by the wall rock.

It might be too hasty to conclude that the batholith belongs to the tholeiitic by using one sample from the margin for the whole body.

2. The diorite of the Tawi Tawi ore deposits are characterized by strong mineralization. The sample for chemical analysis was taken from a small isolated stock located in the outermost mineralized zone. The K/Ar age of the diorite which seems to be related to the mineralization was upper Oligocene. It differs from J. A. Wolf's age of the Agno Batholith (close to the Miocene*). Although the Tawi-Tawi ore deposits are located at the east side of the Batholith, they resemble the porphyry

* The age of dacite dykes intruded in this area is Miocene. It is close to Wolf's age.

copper ore deposits distributed close to its margin at the west side. As it is natural to consider that the mineralizations at both sides occurred at the same time, it is necessary to study this problem from a regional standpoint.

As stated above, it may be concluded that there are differences on dioritic rocks not only in intruding ages but also physical characteristics in rock series. For example, the dioritic rocks have the lowest magnetic susceptibility in the Sierra Madre ($100 - 1200 \times 10^{-6}$ emu/cc), the highest in the Caraballo and the Dupax areas ($1900 - 11700 \times 10^{-6}$ emu/cc) and intermediate in the Cordillera Central (1100×10^{-6} emu/cc). In the Dupax batholith, some changes of rock facies can be noted. The magnetic susceptibility shows the highest value ($7000 - 11700 \times 10^{-6}$ emu/cc) for grano-dioritic facies occupying the northeast part of the batholith or stock and relatively low values ranging $1900 - 3000 \times 10^{-6}$ emu/cc in dioritic to gabbroic facies of the central to southwest part of the batholith.

3-2 Geochemical survey results

The geochemical survey for determination of Cu, Mo and Zn disclosed the geochemical anomalies as shown in PLII-1. Unlike limited distributions in the other areas, geochemical anomalies in the northern parts of the Cordillera and Dupax have areal extensions where ore deposits can be highly expected. This zone including the Tawi Tawi mineralized zone is characterized by intrusive rocks of alkali-olivine-basalt series, suggesting the existence of a close relationship between the copper mineralization and the rock series.

The geochemical anomalies in the Tawi Tawi mineralized zone is distinguished by a typical pattern of high values of Cu, Mo and Zn. On the other hand, the anomalies in the Kong-Kong Valley have high Cu contents with low Mo and Zn. The highest Cu values concentrate in about 200 ppm with few fluctuations. As the Cu anomalous

zone almost concentration is about 200 ppm with few fluctuations. As the Cu anomalous the difference of lithologic characters. The anomaly in the Sulong basin is characterized by high values of Mo with relatively low in Cu and Zn. Generally, Mo in porphyry copper type ore deposits is said to precipitate in the later stage of mineralization. That is, in a cycle of igneous activity in certain area, few minerals are accompanied with quartz diorite of the first stage, then Cu, after a granodiorite stage, and finally Mo is concentrated in the most felsic stage. An igneous rock related to Mo in the Sulong basin seems to be a monzonite. Therefore, Mo and monzonite might occur in the last stage of the Dupax batholith.

3-3 Aeromagnetic survey results

A synthetic interpretation of the magnetic chart obtained by the aeromagnetic survey are shown in PLIII-11. The following are evident:

- a. The distribution of strong magnetism probably caused by basalt and andesite lavas trends NE-SW in the east shore-line and NW-SE in the Caraballo Mountains. In the south of the lava exposures weak anomalies corresponding to the basement rocks are distributed showing the same hook shaped. Moreover, the younger volcanic rocks in the central area have the same trend. So it may be considered that the main structure of the area is characterized by the uplift U-shaped.
- b. Many magnetic-tectonic lines parallel to the main structure can be inferred. They correspond well with those of photogeological interpretation.
- c. In the northwest part of the survey area, many magnetic-tectonic lines branched away from the Philippine Fault. In addition to the major structure trending NNW-SSE direction, there are possibly few lines trending ENE-WSW which could not be interpreted by aerial photograph. Although the magnetic-

tectonic line cutting the I-7 magnetic body is distinct, it is hard to discuss its nature because of few geological data.

d. Dioritic rocks are widely distributed in the northwest area. There are concentrated near or along the magnetic tectonic line. This fact indicates that this area is the most important for exploration of porphyry copper type ore deposits.

e. In the schist zone near Dingalan, it is considered that dioritic rocks are absent or they are in a small scale. In spite of the existence of some mineral indications this area can be omitted from the detailed survey of Phase II because of poor occurrence of dioritic rocks.

f. No magnetic anomalies corresponding to diorite bodies were detected in the Tawi-Tawi mineralized zone. The main reason is that the diorites have relatively low magnetism ($1,100 \times 10^{-6}$ emu/cc), compared to the surrounding basalt lavas which obliterate the dioritic effect. This time, geological survey was not carried out inside the mineralized zone, so the exact shape of the diorite body is not clear.

g. In the northwest part of the survey area, any thick and strong magnetic bodies are hardly expected from the surface to about 2,000 m depth. This fact indicates that the subsurface rock consists of pyroclastics or schists of the Basement Complex. For lack of strong magnetic bodies, the nature of "Fracture zone" is hard to presume.

3-4 Summary

Focusing on the Sierra Madre and the other area, the facts mentioned above will be summarized as follows.

A. Rock series and ore deposits

	Rock series	Type of Ore Deposits
Sierra Madre	calc-alkali series	vein type
Others	tholeiite alkali-olivine	basalt series
(North America)	calc-alkali series	do

B. Ages and ore deposits

	K/Ar age	Type of Ore Deposits
Sierra Madre	43-49 my	vein type
Others	25-39	distinct geochemical anomalies, Tawi-Tawi ore deposits (?)
	10-15	porphyry copper deposits near Ago batholith
	-60	porphyry copper deposits in Toledo, Cebu
(North America)	54-72	porphyry copper deposits in Arizona

C. Geochemical anomalies

	Anomalies
Sierra Madre	isolated
Others	areally distributed

D. Igneous rocks and magnetic susceptibilities

	Rock	Susceptibility
Sierra Madre	granitic	100 - 1,200 x 10 ⁻⁶ emu/cc
Others	dioritic	1,900 - 11,700 x 10 ⁻⁶ emu/cc

For reference, data on typical porphyry copper deposits in the Philippines and the north America were added in the above summary. Although in spite of insufficient data, the above comparisons on some items bring two areas, the Sierra Madre and the other area, into focus with deep interest.

4. Conclusions and Future Problems

Geological, geochemical and aeromagnetic surveys were carried out for delineating the area of high potential for mineral resources. From the studies based on these surveys, the conclusions are as follows;

1. The main structure prevailing over the survey area is U-shaped uplifted zone which occurred during the Eocene and close to the Oligocene periods.
2. The Caraballo group of the Cretaceous system (so-called KPg & UV), which is widely distributed in the area was divided into three formations and their geological features became clear.
3. Large-scale dioritic rocks have been intruded into the group and recognized that they are of different ages of intrusion and chemical compositions. That is, (a) the Sierra Madre—Eocene—calc-alkali rock series (b) the southern part of the central area—close to Oligocene—tholeiite series (c) the northern part of the central area and the Cordillera Central—close to Oligocene—alkali-olivine-basalt series.
4. The porphyry copper deposits and the distinct geochemical anomalies are considered to be genetically related to the said alkali-olivine-basalt series.
5. Aeromagnetic survey disclosed that many magnetic tectonic lines are proved to exist in the northwestern part of the survey area and that some small-scale magnetic bodies probably corresponding to dioritic rocks distributed along these lines.
6. Judging from the synthetic studies made on the natures of igneous bodies, geochemical anomalies and geologic structures etc., the western area is considered to be more promising for mineral resources than the eastern side, therefore, the detailed survey is needed to conduct in former area.

7. The best way is to carry out a detailed geological and geochemical surveys for delimiting the initial area, and thereafter airborne or surface-electromagnetic and/or IP methods should be applied on the selected area.

8. It is clear from the geological survey results of Phase I that there are some rock types of dioritic composition. But detailed discussions could not be made because of insufficient data. This point becomes a very important problem on ore research, therefore, further study is necessary in Phase II.

PART I GEOLOGICAL SURVEY

1 Geology

1-1 Previous Works

Northern Luzon is characterized by two district zones, namely: the Sierra Madre and the Cordillera Central. The survey area is located at the junction of these two zones, whence, it has a complicated geological structures. A large-scale granitic to dioritic rocks have closely occurred in these areas and many porphyry copper type of ore deposits are related to these intrusions.

In 1951, a reconnaissance survey was carried out in Cagayan Valley by G. W. Corby et al, for oil exploration and the stratigraphic correlation. E. E. Durkee et al (1961) and J. C. Fernandez et al (1967) also conducted regional surveys on northern and northwestern Luzon and they described the stratigraphy and geological structures of these areas. However, their reports are confined on the northern side of the survey area and have few descriptions on the altered rocks of Cretaceous to Paleogene (so-called KPg or UV) which are widely distributed in the survey area.

In 1962, C. R. Allen discussed the nature of circum-Pacific faulting in the Philippines-Taiwan region and concluded that the relative movement of the Philippine Fault has been left-lateral. He pointed out the consistent stream offsets of the Digdig River as a good example of the field evidences.

As mentioned above, there are few published reports on the geology or geological structure of the area. The comprehensive conception on the geology of the Philippine Island can be obtain from the Geological Map of the Philippines in scale of 1:1,000,000 (published by Bureau of Mines, 1963) and F. C. Gervasio's papers (1966, 1967).

It is well known since the old time that many ore deposits are located within Baguio District west of the project area. They show zonal distributions, that is, from the center around Baguio to the outside, gold-silver zone and copper zone. Recently this area has been spotlighted by successive developments of porphyry copper type ore deposits. In 1970, J. A. Wolf interpreted the intrusion age of diorites closely related with these deposits as 9.7 to 14.8 million years (uppermost of Middle Miocene to lowermost of Upper Miocene).

1-2 Stratigraphy

The stratigraphy of this area was mainly based on the photogeologic interpretation map newly made by Bureau of Mines for this project, correction will be made from the local data to be obtained by the geological survey later on.

A generalized stratigraphic section in this area is shown in Table 1-1.

Table I-1 Generalized stratigraphic section in the survey area

Geological age		Group or Formation	Columnar section	Rock facies	Structural movement	Igneous activity	Mineralization	
Quaternary	Recent							
	Pleistocene	Pantabangan F. 1,000m+		Conglomerate with Clastics. Andesite Lava				
Tertiary	Pliocene							
		Maddela F. 2,000m+		Clastics				
	Miocene	Upper	Matuno F. 1,200m+		Conglomerate			
		Middle	Aglipay F. 200m		Limestone and Clastics			
		Lower	Sta Fe F. 200m+		Limestone and Clastics			
	Oligocene	Mamparang G. 1,000-2,000m		Basalt and Andesite Lavas with thick Limestone at the top				
Eocene								
Cretaceous		Caraballo G. 2,000-3,000m(II)		Basaltic Pyroclastics with Basalt Lavas				
		(II) 2,000~3,000m		Andesite Lavas with Basalt Lavas, Pyroclastics and Clastics				
		(I) 1,500~1,800m		Andesitic Pyroclastics with minor Clastics				
Paleozoic		Basement Complex		Green Schlts.				

Orogenic movement

Philippine Fault

Structural movement

Epilrogenetic movement

Basic rocks

Peridotite

Basalt

Andesite

Dioritic rocks

Porphyry copper

1-2-1 Basement Complex

The Basement Complex is widely distributed around Dingalan and crops out at several places in the eastern area near the Philippine Fault having the shape of small-scale windows. Their exposures are also expected in the folding zone where the Caraballo Mountains joined with the Sierra Madre Mountains, and in the northern area of Casiguran. The Complex consists of weakly metamorphosed schists. They are quartz-plagioclase-augite-hornblende schist, quartz-plagioclase-garnet-hornblende schist, quartz-plagioclase-epidote-two mica schist, muscovite bearing quartz-plagioclase-hematite-calcite schist, quartz-plagioclase-epidote schist and saccaroidal calcareous schist. The original rocks are supposed to be mostly basic to intermediate igneous rocks with calcareous ones.

The general strike trends NE-SW in the east shore but NE-SE system prevails along the Philippine Fault. Sometimes they show linear structures but the observations are too small to clarify their trend.

The schists are unconformably overlain by the following Caraballo Group and possibly formed during the Pre-Jurassic time.

1-2-2 Caraballo Group

The Caraballo group is distributed in the greater part of the survey area. Its areal distribution almost corresponds to the area of KPg (undifferentiated sedimentary with pyroclastics rocks of probably Cretaceous — Paleogene) and UV (undifferentiated volcanics of the same age) in the 1 : 1,000,000 Geologic Map of the Philippines. It consists of intermediate to basic volcanic rocks and their pyroclastics with minor clastics. For a few field data, it is hard to subdivide the Caraballo groups in detail. It was roughly divided into three formations.

Formation I-----This formation is distributed in the east shore line, from Dingalan to Baler, the area from the middle of the Calaanan River to Villa Aurora, and the east side of the Digidig River unconformably overlying the Basement Complex. This formation is characterized by extensive accumulation of andesitic to basaltic pyroclastics associated with lavas and thick clastics at the top.

The pyroclastics are composed of tuff, tuff breccia and lapilli tuff with greenish gray to reddish gray in color. To sum up, the coarse-grained tuff tends to crop out in the east side (coastal line) and a fine-grained one in the west side (Digidig River). Microscopically, rock fragments (2-3 mm in size) of andesite or basalt and chips of plagioclase, quartz and pyroxene are cemented by mostly chloritized tuffaceous materials and in most cases, the particles are strongly affected by silicification, chloritization or carbonitization.

The clastics are mainly composed of gray colored, fine to medium grained graywacke and are locally associated with phyllite, slate and chert.

The general strike trends NE-SW— E-W in the east shore line, and E-W in the Digidig basin. The thickness of this formation probably attains 1,500 - 1,800 m.

Since no fossils can be found, the age of the Formation I is not clear. In this report, however, it is tentatively placed as Cretaceous based on the similarities of the volcanic products among the Formation I, II and III. But it probably corresponds to Cretaceous (K) in the 1 : 1,000,000 Geological map of the Philippines.

Formation II-----This formation is distributed in the river basins of the Magat and the Cagayan, and in the west side of the Sierra Madre. It has the widest area of distribution compared to the other formations of the Caraballo group.

It mainly consists of andesitic lavas and pyroclastics. Roughly speaking, the andesitic lavas are predominant in the west area and the pyroclastics in the Sierra Madre. A small amount of basaltic lavas interbed with sandstone or shale are

intercalated in this formation. They might be the key beds to subdivide the Formation II.

The andesite in the formation consists of two rock types, viz: porphyritic and aphyric. Both of them are massive rocks whose color ranges from dark gray to dark blue. The porphyritic rock is augite andesite which is microscopically composed of idiomorphic to hypidiomorphic plagioclase and augite scattering in the matrix with an intersertal texture. The matrix consists of albite-twinned, prismatic to acicular plagioclase, granular augite, magnetite, and glass. Some andesites, like the one exposed in the upper reaches of the Casignan River, contains a few hornblende crystals. The aphyric andesite is mostly basaltic and commonly shows an amygdaloidal texture. It has no or a few phenocrysts. Under the microscope, phenocrysts consists of small augite and rarely olivine in a pilotaxitic matrix of plagioclase laths, augite and chlorite etc. Although both of them commonly suffered chloritization, carbonitization and albitization are noticeable locally. However the intensity of alteration are generally weak. A few basalt lavas with pillow structure are intercalated in this formation.

The pyroclastics are also andesitic and show dark gray to pale green coloration. Rock fragments, ranging in diameter from 50 cm of volcanic conglomerate to few millimeters of tuff, resemble each other in kind like crystal chips. The rock fragments of the above-mentioned two type of andesites and crystal chips of augite, plagioclase, hornblende and iron ore etc. are cemented by chlorite and tuffaceous materials. They are poorly sorted and stratified. The existence of chlorite, calcite, albite and laumontite etc. indicates burial metamorphism corresponding to high temperature part of zeolite facies. A few thin beds of dacitic pumiceous tuff with pale green color are intercalated in the pyroclastics.

The clastics are composed of mudstone, sandstone and conglomerate. Oftentimes they are interfingering with the tuff. The mudstone are dark gray to black or pale blue in color and has a siliceous composition. The mudstone or sandstone with intercalated tuff is at the top of this formation. The formation II bordered the Formation III by those clastics.

The general strike of this formation trends NE-SW with steep dip toward N in the west side of the Santa Cruz River, NW-SE with gentle dip toward N or S in the central parts of the Caraballo Mountains and NE-SW with gentle dip toward N in the Sierra Madre.

This formation conformably overlain by the Formation I and attains about 3,000 meters in thickness. By lack of fossils, the age is not clear like the Formation I.

Formation III---This formation is narrowly distributed in Kasibu area and in the west side of the Philippine Fault. It consists of basaltic tuff to tuff breccia associated with minor basaltic lavas characterized by pillow structure.

The tuff exposed along the Imugan River where the Philippine Fault pass through, is the low horizon of the Formation III. It is a fine to coarse-grained rock with dark green in color and alternates with reddish brown basic tuff or muddy tuff. The strike trends N-S dipping toward N or S, but as a whole, the west portion is supposed to be the upper section. Tuff breccia and volcanic breccia are widely distributed along the Pampanga River which are parallel to Imugan River at a distance of 5 km west. However, fine grained tuff beds are rather few unlike along the Imugan River. In this vicinity, a strike of E-W is predominant and small-scale folding structures with folding axes of the same direction, are repeatedly observed. This feature is discordant with the major structure of the whole area (the Cordillera Central), therefore, it can be assumed that the structure of E-W direction is not

reflected by the lower section but presents a very shallow feature. (There is no trend in the distribution of magnetic anomalies.)

The formation occurring in Kasibu area, consists of pale blue tuff and tuff breccia, and occupies an inner part of large synclinal structure with folding axis trending in the NW-SE direction. The tuff is andesitic in composition unlike one exposed in Imugan River. They are probably contemporaneous heterotopic facies in relations with the Formation II.

Formation III conformably overlain by the Formation II and unconformably by the Mamparang Group. The thickness of this formation is more than 3,000 m.

As described above, the Caraballo Group is divided into three formation (I, II and III) and each feature of volcanic rocks is roughly described. Roughly speaking, a calm andesitic volcanic activity occurred in the first stage followed by the sedimentation of tuff, sandstone and mudstone. In the second stage, volcanic activity was vigorous and mass of andesitic lava and tuff were accumulated. The third stage was characterized by thick deposition of pyroclastics and igneous rock whose composition varied from andesitic to basaltic. The existence of pillow lavas in this formation suggests they were deposited in a neritic environment.

1-2-3 Mamparang Group

This is widely exposed from the central part of the Mamparang Mountains to the upper part of the Cagayan River. It is also typically exposed in the middle course of the Diduyon River and along the upper part of the Cagayan River in the vicinity of Sitio Wasig. It is chiefly composed of basaltic volcanics and pyroclastics with a thick limestone at the top. It unconformably overlies the Caraballo Formation II. The exposed sequence of this group can be observed in the upper reaches of the Cagayan River. It is a series of andesite lava — basaltic tuff — basalt lava — andesite lava — andesitic volcanic conglomerate — calcareous mudstone with limestone brec-

cia — limestone.

The alternation of this group is weaker than the Caraballo group so it is easy to distinguish the former from the latter in the field. Both andesite and basalt lavas are compact and massive rocks with dark gray to black in hues. The lava are 5 - 10 m in thickness. Sometimes pillow structures are indistinctly observed.

In addition to augite, hyperthene is characteristically present in the andesite. Under the microscope, somewhat abundant phenocrysts of zoned plagioclase (<1mm in size), augite (<0.5mm) and hyperthene (<0.3mm) occur in a hyalopilitic matrix of plagioclase laths, augite and glass. No secondary minerals are recognized. Even a glass is not altered at all. The mineral components of the basalt are similar to those of the andesite. Phenocrysts of plagioclase, augite and hyperthene are in a matrix of the same constituent minerals. Pseudomorphs of something like olivine can be observed in the matrix.

Rhyolitic lava and tuff exposed along the middle course of the Diduyon River are tentatively included in this group because of few alteration. They are probably the lowest section and are distributed in the limited area which does not extend to the Cagayan River.

General strike of the Mamparang group trends NE-SW along the Cagayan River and dips 10—20° toward N in spite of presence of many local disturbances. Although data are not adequate, the trend in the Diduyon basin seems to be the same as the Cagayan's. The thickness of the formation is supposed to be over 1,000 m. The age of the limestone beds occupying the upper part of the formation is upper Oligocene based from fossils identification.

1-2-4 Santa Fe Formation

Unconformably overlying the Caraballo Group is the Santa Fe Formation which crops out around Dalton Pass where the provincial boundary between Nueva Vizcaya

and Nueva Ecija lies. It consists of limestone with white-grayish or white-pale pink in color and attains over 200 m in thickness. By the study of larger foraminifera, the age of the formation was determined to be lower Miocene.

1-2-5 Aglipay Formation

The Aglipay Formation is exposed near the town of Aglipay in the lower reaches of the Addalam River. It consists of pinkish white limestone unconformably overlying the Caraballo Group. Apparently it resembles the Santa Fe Limestone but it is more clearly stratified. Owing to folding, its strike and dip have no definite trends.

The limestone, exposed along the Matuno River, is probably correlated with the Aglipay's limestone from its appearance. It covers the Caraballo Group unconformably. Its upper portion is composed of alternated beds (20—30 m in thickness) of black siltstone and sandstone.

The thickness of this formation is about 200 m and its age is middle Miocene. It is correlative, therefore, with the Kennon Limestone (G. W. Corby 1951)

1-2-6 Matuno Formation

The Matuno Formation is distributed only in the small area of the Matuno upper stream. It consists of alternating beds of sandstone and conglomerate, reaching a thickness of over 1,200 m. The conglomerate consists of andesite, dioritic, calcareous and muddy, rock pebbles and cobbles, ranging in diameter from 1 to 10 cm.

The formation overlies the Aglipay limestone with an unconformable contact, it has a strike of E-W and dipping 30—15°N. It is correlated with the Klondyke conglomerate (G. W. Corby) of upper Miocene.

1-2-7 Maddela Formation

The Maddela Formation includes the whole younger clastics; yellowish brown

to gray sandstone, mudstone and their fine equivalent which are distributed on the hilly regions around Maddela area, it is generally trending NN-SE but dips 10° — 20° toward N or S owing to gentle synclinal folding structure. The formation unconformably overlies the Mamparang group with parallel contact. Its age is ranging from upper Miocene to lower Pleistocene. It is probably correlated with the Rosario formation of G. W. Corby. The thickness of this formation is more than 2,000 m.

1-2-8 Pantabangan Formation

The Pantabangan Formation, overlies the Basement Complex and the Caraballo group. It is widely distributed in Pantabangan and Carranglan regions in the upper stream of the Pantabangan River, stretching in N-S direction. It is molasse deposits and chiefly consists of loosely consolidated pebble with gray to brownish gray in color. It interbeds with thin beds of shale, mudstone and sandstone. The fragments are basalt, andesite and tuff of the Caraballo group, and dioritic rocks. They are rounded and most of them can be classified as "subrounded" in the Roundness Scale. Having no fixed strike, the formation is supposed to have been formed by turbidity currents. No intrusions of igneous rocks can be observed in this formation. The Pantabangan formation was probably accumulated in the N-S stretching sedimentary basin formed in the upper Pliocene time. Its thickness is approximately 1,000 m.

1-2-9 Pliocene to Quaternary Lavas

Isolated peaks are located along the Magat and Carranglan Rivers. They were not surveyed at this time but they are believed to be pyroxene andesites formed during the Pliocene to Quaternary volcanic activities from 1 : 1,000,000 Geological Map of the Philippines.

1-2-10 Alluvium

Alluvium is extensively distributed along the Cagayan, the Magat and the Pampanga Rivers and at the mouths of some big rivers near Baler and Casiguran on

the east coast. It consists of unconsolidated sands and gravels.

1-3 Intrusive Rocks

1-3-1 Ultrabasic Rocks

The Ultrabasic rocks are exposed in the mountain region south of Baler. In the northern Luzon, it is well known that the big structural line passes along the east coast and ultrabasic rocks have been intruded along the line. The ultrabasic rocks distributed in this area is the southern extension of the intrusive body.

From observation along the Matayat River the ultrabasic rocks are composed chiefly of pyroxenite and small peridotite dykes. Both of them are compact rocks with pale greenish gray in color (which changes to yellowish brown after weathering). Under the microscope, the pyroxenite has a hypidiomorphic-granular texture. It consist of predominant clino-pyroxene (diopside) and interstitial olivine. A few serpentine and calcite are secondarily produced. The peridotite has also an hypidiomorphic-granular texture. It consists of clino- and ortho-pyroxenes, and olivine. Among the three, the clino-pyroxene is quantitatively predominant. Serpentine commonly shows pseudomorph after olivine.

From the air-photograph interpretation, these rocks are in contact with the Basement Complex by thrust faults.

1-3-2 Gabbro

The gabbro intrudes into the Caraballo group at places. It is fine-to medium-grained, holocrystalline rock, with dark gray in color. It is exposed as a small scale stock or dyke. Microscopically the gabbro can be divided into two types; one with clino-pyroxene and the other with two-pyroxenes. The latter type tends to occur always around dioritic rocks. It may, therefore, be considered that there are some genetic relations between the two.

Under the microscope, the former type has a hypidiomorphic-granular texture.

Main constituents are hypidiomorphic plagioclase and xenomorphic clino-pyroxene with accessories of magnetite and/or quartz and/or hornblende as accessory minerals. Uralite, epidote and calcite occur as secondary minerals.

Two-pyroxene gabbro contains hypidiomorphic to xenomorphic ortho-pyroxene with idiomorphic to hypidiomorphic plagioclase and xenomorphic clino-pyroxene.

A few magnetite and rarely biotite are also included in this type.

1-3-3 Dolerite

The dolerite intrudes the Caraballo group and dioritic rocks at many places, trending NW-SE. The dolerite rocks exposed along the Tabayon River, one of the branch of the Cagayan River, are fine-grained ones. It also intrudes the Caraballo group as parallel dykes with 1—10 m in width. The constituent minerals and alteration of these facies are similar to those of basalts in the Mamparang group. So it is probable that they are genetically related to each other.

Most of the pale greenish gray dolerite dykes which intrude the western part of the survey area, are strongly altered. Microscopically, idiomorphic plagioclase and xenomorphic augite show an ophitic or porphyritic texture. They are sometimes accompanied by olivine. Uralite, epidote, chlorite, prehnite and kaolinite are secondarily produced by saussuritization and uralitization.

The dyke exposed in the lower reaches of the Benneng River, one of the branch of the Agno River, is somewhat coarse-grained and massive rock contained minor hornblende. Under the microscope, saussuritized plagioclase, clino-pyroxene, relatively abundant intersertal quartz and a few accessories of hornblende and magnetite are observed. This rock differs from other gabbro or dolerite in having quartz and hornblende primarily. This fact indicates it is probably related to the diorite exposed in the neighborhood.

1-3-4 Dacite

The dacite occurs in the Caraballo group's tuff in the western part as small scale dykes with about 10 m in width. It is pale greenish gray and porphyritic. Microscopically, phenocrysts of zoned plagioclase, greenish brown to green hornblende, quartz and biotite are in a cryptocrystalline matrix. A minor apatite and clino-pyroxene are sometimes included. Chlorite, calcite, zeolite and greenish brown clay minerals can be recognized as alteration minerals.

The dacite exposed between Santa Fe and Dalton Pass intrudes diorite as a stock. It is reddish gray in color and shows an indistinct flow structure. The Santa Fe limestone was thermally metamorphosed by this dacite.

1-3-5 Dioritic Rocks

The dioritic rocks are widely exposed as batholiths, stocks and dykes in the whole survey area except in the central part where the Mamparang group is distributed. They range from granite to gabbro in chemical compositions. Microscopically, they can be roughly divided into the following.

1-3-5-1 Diorite—Quartz Diorite

The diorite—quartz diorite, intruding the Caraballo group, and distributed at places in the Caraballo and the Cordillera Central Mountains. Most of them are less than 10 km² in size but exceptionally, a big mass is exposed over 200 km² like the Dupax body. There are some changes in rock facies such as granodiorite diorite gabbro towards west from east. Generally, the diorite tends to crop out in the northwest area and become acidic (quartz-dioritic) toward the Sierra Madre.

They are medium- to coarse-grained rocks, gray in color and show a granular texture. The main constituents are plagioclase, common hornblende, biotite and quartz accompanied by accessory minerals such as magnetite, sphene and apatite. Epidote, chlorite, uralite, kaolinite and prehnite are produced as secondary minerals.

The plagioclases are idiomorphic to hypidiomorphic. Albite twins and composite twins of Albite-Carlsbad type are commonly observed. Zonal structures are also developed. The plagioclase is mostly andesine in composition.

The common hornblende are hypidiomorphic tabular with fair pleochroism green to pale brown and well twinned. The biotite flakes are chloritized and minor in quantity. A small amount of K-feldspar is interstitially included. Quartz is not recognizable in the diorite.

1-3-5-2 Monzonite

The monzonite of about 80 Km² in area is located in the upper reaches of the Solong River. It is pinkish gray holocrystalline and contains characteristically many large crystals of pinkish K-feldspar. Microscopically, the texture is hypidiomorphic-granular. K-feldspar and plagioclase (K-feldspar plagioclase in volume) are accompanied by mafic minerals such as hornblende, biotite and pyroxene. The accessory minerals are magnetite, apatite and sphene. Secondary chlorite, sericite and kaolinite are also observed.

The plagioclase, with idiomorphic to hypidiomorphic in shape, is well albite-twinned and is strongly altered to epidote and sericite. The K-feldspar is hypidiomorphic to xenomorphic in shape and dull colored due to presence of kaolinite dots scattered all over like ash. Small mafic minerals are poikilitically enclosed in the K-feldspar. The common hornblende is brown to greenish brown in color and it is hypidiomorphic and tubular (max. 2 mm in length). The biotite occurred as flakes about 0.3—0.5 mm in size and is partially altered to chlorite as well as hornblende. Both clino-pyroxene and ortho-pyroxene are found in this type of rock. The former, with a weak pleochroism, is pale brown in color and rarely shows an intergrowth with biotite. The latter clino-pyroxene with pale green color is prismatic. Besides, large crystals of maximum 2 mm in length are characteristically contained in this

rock.

The syenite porphyry may be included in the monzonite group. This rock was found in a small creek near Dingalan as boulder and considered to be a small scale dyke. It is more fine-grained than the Monzonite and has a porphyritic texture.

The matrix is pink and as a whole the rock shows pinkish gray in color. Under the microscope, somewhat abundant phenocrysts of plagioclase (< 5 mm in length) and clino-pyroxene (< 2 mm) occur in a matrix of alkali-feldspar, clino-pyroxene, magnetite, ilmenite, biotite and apatite. From the composition of mineral assemblages, this rock is more basic than the monzonite.

1-3-5-3 Granodiorite—Granite

The granodiorite—granite are distributed in the Sierra Madre Mountains as a large scale dyke. They are characterized by grayish white in color, medium - coarse grain, granular texture and more quartz than the dioritic rocks stated above. The main constituents are quartz, K-feldspar, plagioclase and hornblende, accompanied by magnetite, chlorite, epidote and calcite etc.

The plagioclases, idiomorphic—hypidiomorphic in shape, are well albite-twinning and zoned, and are mostly oligoclases which are altered to muscovite, Kaolinite, calcite and epidote. The K-feldspar, hypidiomorphic to xenomorphic in shape, shows perthite texture. Alteration minerals such as kaolinite and muscovite occur dustily in the K-feldspar as well as in the monzonite's. This rock contains about 25 % of xenomorphic quartz. Mafic mineral is only hornblende which occupies less than 10 % of the whole rock and is altered to chlorite and epidote etc.

1-4 Chemical Compositions of the Dioritic Rocks

As stated in the foregoing paragraph, the dioritic rocks in the survey area can be microscopically divided into three types. Five typical rock samples were analyzed to study the chemical compositions. Discussions will be made using these

five results and one analytical datum of Eastern Mindanao Survey (1973).

1-4-1 Analytical Samples

The analytical samples are: one (1) from the Cordillera Central, two (2) from the Caraballo and two (2) from the Sierra Madre. All of them are fresh rocks.

Brief description of these rocks is as follows:

C-5D----Microdiorite in the Benneng River. This intrusive body is considered to be closely relation with the Tawi-Tawi ore deposits.

B-34 ----Gabbroic facies at the southeast margin of the Dupax batholith. The batholith ranging from granodioritic to gabbroic facies, is dioritic in the mean mineral compositions.

B-93 ----Monzonite in the upper reaches of the Solong River. Gold deposits are known near the monzonite contact. Geochemical anomalies of Mo, as mentioned in the latter part of the report were detected in the rock body.

PA-14----Quartz diorite intruded in the orogenic belt at the intersection of the Sierra Madre and the Caraballo Mountains.

A-200----Granite. This is the one of typical granite which forms the Sierra Madre Mountains. In the Northern Luzon, no large scale ore deposits of porphyry copper type are known in this mountain unlike in the Cordillera Central.

D-5-52----Quartz diorite distributed in Bislig region, eastern Mindanao. The rock is accompanied by porphyry copper type mineralization. The sample was chosen at 52 m depth of DDH-No 5. Alteration is negligibly weak.

1-4-2 Analytical Results

The analytical results of 6 samples are shown in Table I-2, and the normative mineral (wt %) calculated from this table, in Table I-3.

1-4-3 Results and Discussions

As shown in Table I-1, normative constituents of each sample are plotted in

Table I-2 Chemical composition of the dioritic rocks

Sample No.	C-5D	B-34	B-93	PA-14	A-200	D-5-52
SiO ₂	49.03	51.46	51.64	54.98	75.15	64.34
TiO ₂	0.55	0.85	0.92	0.71	0.58	0.50
Al ₂ O ₃	19.56	18.72	19.10	16.89	11.72	15.71
Fe ₂ O ₃	1.95	3.87	2.04	5.07	1.68	1.88
FeO	4.44	5.83	2.70	2.66	1.12	3.34
MnO	0.15	0.18	0.03	0.01	0.02	0.07
CaO	11.62	11.11	7.93	9.23	4.30	3.92
Na ₂ O	3.23	1.98	3.40	3.86	3.51	3.91
K ₂ O	1.09	0.53	3.97	0.94	0.50	1.09
P ₂ O ₅	0.07	0.07	0.03	0.05	0.02	0.18
H ₂ O(+)	2.25	0.23	2.92	0.69	0.60	2.24
H ₂ O(-)	0.34	0.11	0.80	0.20	0.27	0.14
Total	99.92	100.61	99.33	100.55	100.47	99.90
FeO*	6.19	9.31	4.54	7.22	2.63	5.03
FeO*/MoO	1.10	1.64	1.18	1.37	2.63	1.95
Na ₂ O+K ₂ O	4.32	2.51	7.36	4.80	4.01	5.00

Table I-3 Normative constituents of the dioritic rocks

Sample No.	C-5D	B-34	B-93	PA-14	A-200	D-5-52
Quartz	-	5.71	-	5.65	43.48	23.60
Corundum	-	-	-	-	-	0.92
Orthoclase	6.68	3.34	23.37	5.57	2.78	6.68
Albite	19.92	16.78	24.64	32.51	29.89	33.03
Anorthite	35.60	40.32	25.03	26.14	14.74	19.47
Nepheline	3.98	-	2.27	-	-	-
Diopside	17.70	9.96	10.44	15.37	5.20	-
Hypersthene	-	15.00	-	-	-	9.60
Forsterite	5.63	-	3.52	-	-	-
Fayalite	2.65	-	0.81	-	-	-
Magnetite	2.78	5.56	3.01	6.28	2.08	2.78
Ilmenite	1.06	1.67	1.82	1.37	1.06	0.91
Hematite	-	-	-	0.64	0.32	-
Quartz	-	8.63	-	8.09	47.84	28.51
Alkali-feldspar	42.77	30.42	65.73	54.50	35.94	47.97
Plagioclase	57.23	60.95	34.27	37.41	16.22	23.52

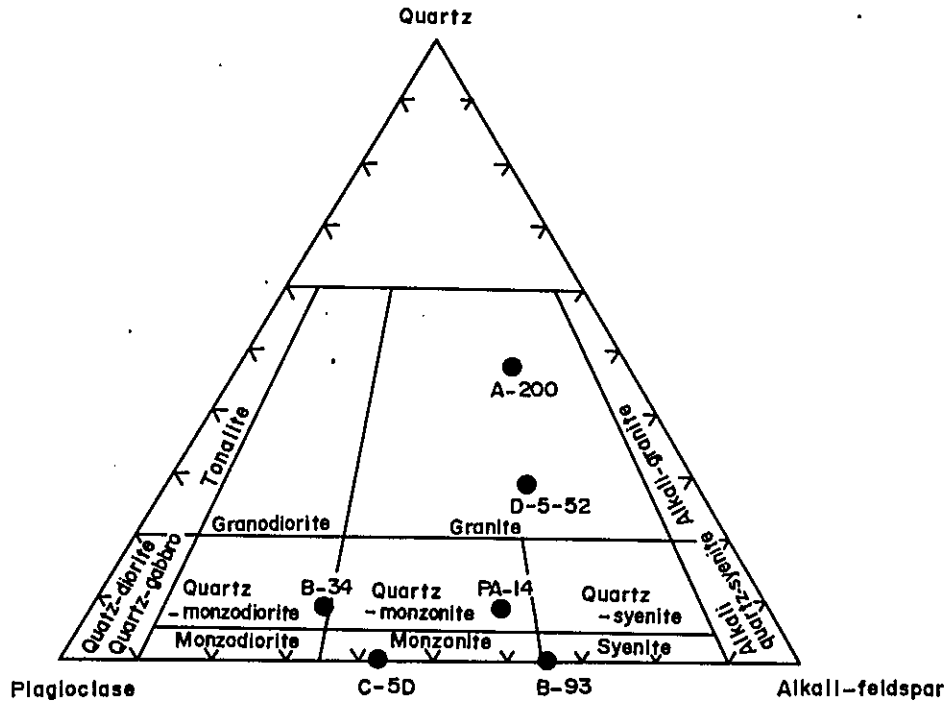


Fig. I-1 Normative quartz-plagioclase-alkali-feldspar diagram

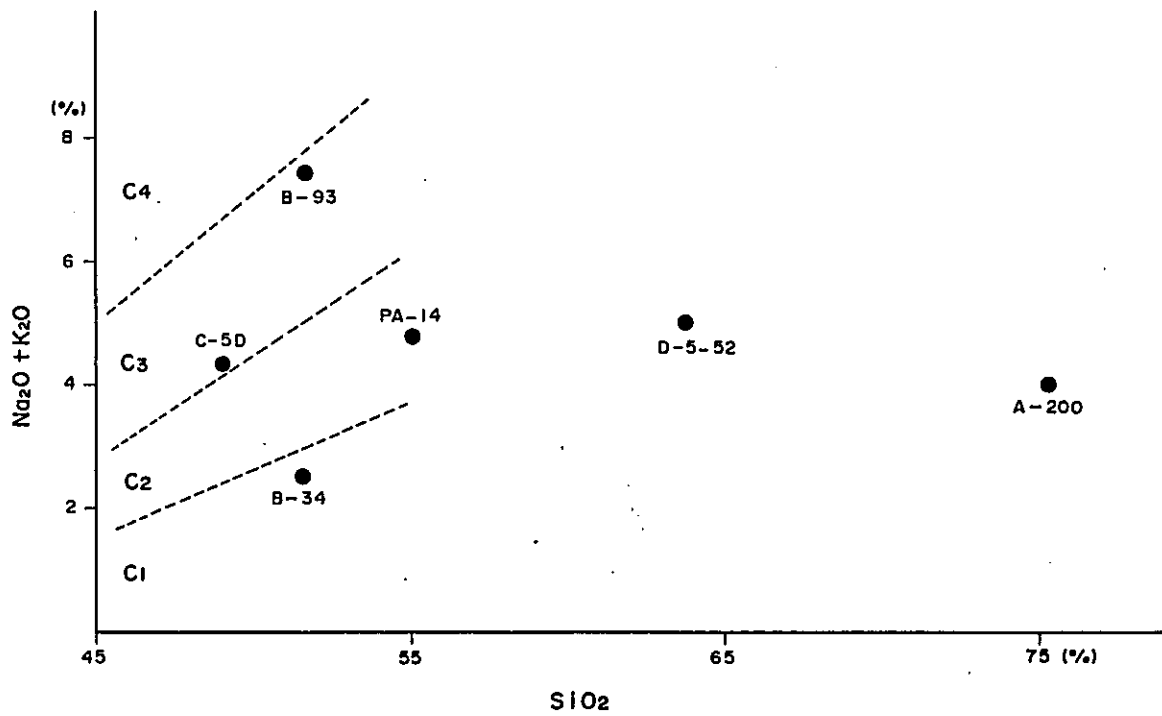


Fig. I-2 Alkali contents of the dioritic rocks

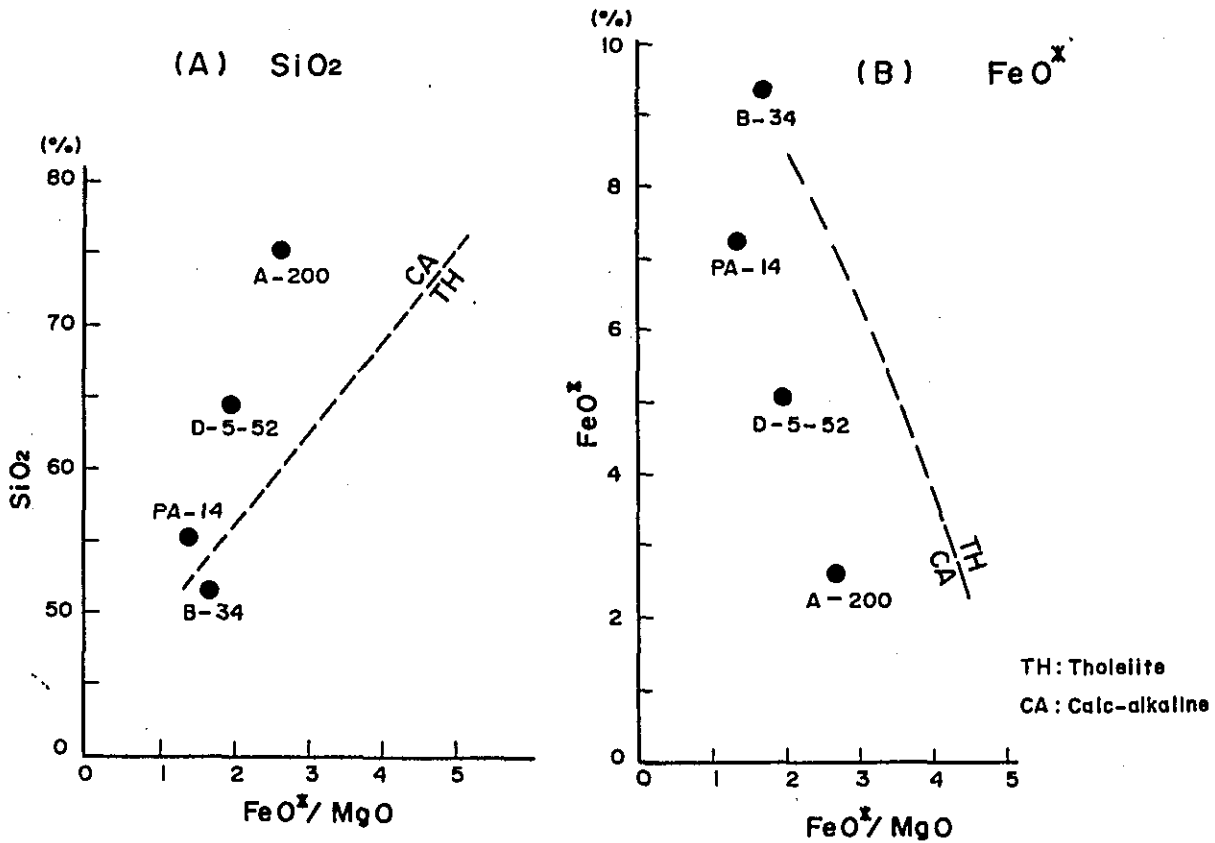


Fig. I-3 Chemical components plotted against Fe^*/MgO of the dioritic rocks

the Qz-Pl-Kf diagram proposed by IUGS Subcommittee 1973. The relationship between alkali and SiO_2 is shown in Fig. I-2 and the relationships between FeO^*/MgO and SiO_2 or FeO^* , in Figs. I-3A and 3B respectively.

The following are evident from these table and figures.

C-5D-----The SiO_2 content is basic (SiO_2 45 % - 52 %). This is plotted near the boundary between C2 (high alkali tholeiite in the Island arc-Continental arc zone) and C3 (alkali basalt in the same zone). As it contains olivine and a few nepheline in the norm, it can be considered that C-5D belongs to the alkali-olivine-basalt magma type. This is plotted in the monzonite field of Fig. I-1.

B-34 -----The SiO_2 content belongs to intermediate (SiO_2 52 - 66 %). It is

* Ferrous oxide calculated from total Fe content.

plotted in tholeiite field of Figs. I-3A and 3B, and C1 (low alkali tholeiite) of Fig. I-2. In the Qz-PL-Kf diagram, it falls in the quartz-monzonite field.

B-93 ----The SiO₂ content indicates that this rock is rather basic than intermediate. It is plotted near the boundary between C3 and C4 (high alkali basic rock) of Fig. I-2. As it contains olivine and a few nepheline in the norm constituents like C-5D, it belongs to the alkali-olivine basalt magma type. This is plotted near the boundary between monzonite and syenite fields of Fig. I-1.

PA-14----The SiO₂ content is intermediate. It falls in the calc-alkalic fields of Figs. I-3A and 3B, and in the C2 of Fig. I-2. This rock is quartz monzonite after IUGS' classification (Fig. I-1).

A-200----The SiO₂ content is clearly acidic (SiO₂ 76.6 %). It is characterized by very low K₂O content compared with SiO₂ content. The mean chemical compositions of Japanese granite having the nearly same SiO₂ content as A-200 (Aramaki et al. 1972) and those of 546 granite occurred in the world (Daly 1914) are shown in Table I-4.

Comparing A-200 with other samples, the following is evident.

1. A-200 contains slightly lower Al₂O₃ content than those of the others.
2. It has higher CaO but lower K₂O content.

These features indicate that A-200 is the granite with a trondhjemitic mineral assemblage.

D-5-52----The SiO₂ content is rather intermediate than acidic. This is summarized in Table I-5.

As described above, each feature on chemical compositions was roughly stated. Although there are few data, the following trends may be pointed out. *

* As the number of sample is insufficient, additional data are needed for further discussion in Phase II.

Table I-4 Chemical composition of the granitic rocks

Sample No.	A-200	Aramaki	Aramaki	Aramaki	Daly
SiO ₂	75.48	77.24	75.45	73.55	70.91
TiO ₂	0.58	0.06	0.14	0.23	0.39
Al ₂ O ₃	11.77	13.10	13.66	14.20	14.62
Fe ₂ O ₃	1.69	0.42	0.59	0.76	1.59
FeO	1.12	0.44	0.93	1.42	1.80
MnO	0.02	0.03	0.04	0.05	0.12
MgO	1.00	0.00	0.20	0.55	0.89
CaO	4.32	0.52	1.18	1.84	2.01
Na ₂ O	3.52	4.00	3.91	3.82	3.52
K ₂ O	0.50	4.21	3.90	3.59	4.15
Total	100.00	100.00	100.00	100.00	100.00

Table I-5 Features of the dioritic rocks in the survey area

Sample No.	Name after I.U.G.S.	Rock series	K/Ar age	Remarks
C-5D	Monzonite	Alkali-olivine basaltic	27 ^{MY}	
B-93	Syenite	do.	26	
B-34	Quartz-monzodiorite	Tholeiitic	25	
PA-14	Quartz-monzonite	Calc-alkalic	49	
A-200	Granite	do.	43	
D-5-52	Granite	do.	149	

1. There are three series of dioritic rocks occurred in the area: a) alkali-olivine-basaltic series, b) tholeiitic series and c) calc-alkalic series. They are distributed in the Cordillera Central and northern part of the Caraballo (monzonite - syenite type), the Caraballo (quartz-monzodiorite - quartz-monzonite type) and the Sierra Madre (granite type).

2. The Tawi-Tawi ore deposits of porphyry copper type are presently under exploration and the remarkable geochemical anomalies of Mo along the Solong River are closely related to a)-series.
3. The fact that large scale ore deposits of porphyry copper type are not located in the Sierra Madre but concentrated only in the Cordillera Central (cf. Fig. I-6), may be due the above-mentioned difference of the series.

In the Philippines, there are few studies on the chemical compositions of the intrusive rocks closely related to the ore deposits of the same type. But many studies have the intrusive rocks related to the ore deposits belong to the calc-alkalic series, except Bingham, Utah. (Fig. I-4). This feature does not corresponds to any one of the dioritic rocks exposed in the survey area. This is very important problem on the primary magma which may influence the principle of the future ore-exploration. It is, therefore, desirable to study this problem in detail on and after Phase II.

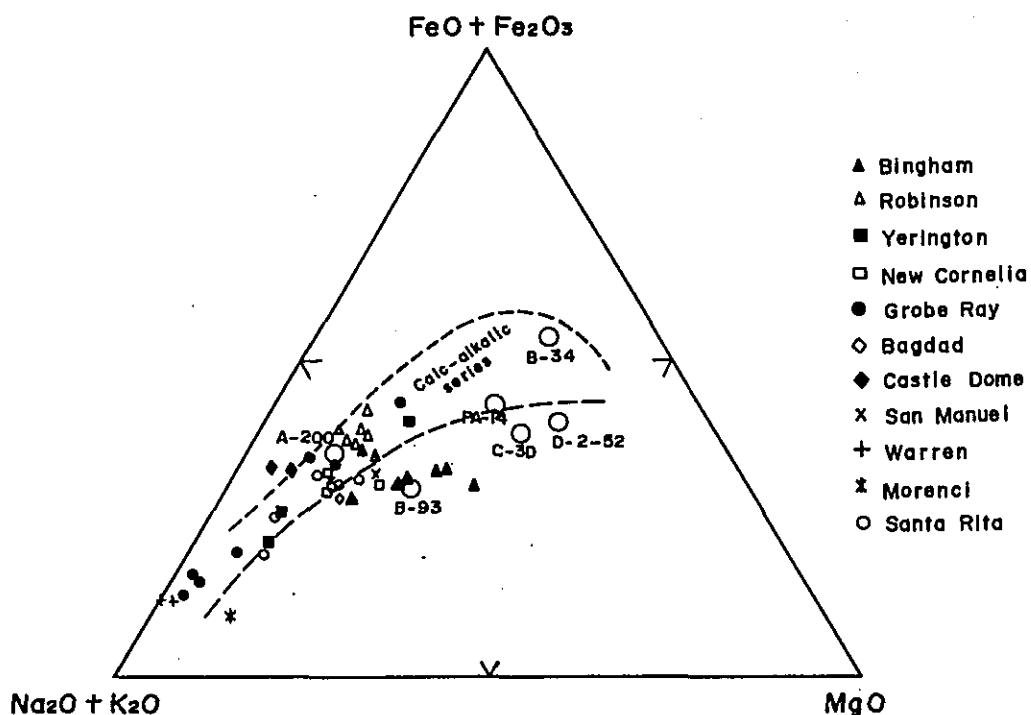


Fig.I-4 MFA diagram of intrusive rocks

1-5 Ages of Intrusion of Igneous Rocks

As shown in Table 2 in appendices, K/Ar ages of dioritic rocks into three groups: the first group ranges from 43 to 49 million years (Eocene); the second from 25 to 33 million years (Oligocene); and the last, from 6 to 10 million years (close to Miocene).

As shown in Fig. 3, the first group are granitic rocks exposed east of Sierra Madre; the second group are dioritic rocks distributed at Dupax area to Sulong River and the last group are dacite dykes west of the survey area. It is that K/Ar dating of igneous rocks tends to become younger from east to west.

It is already stated that the age of Agno Batholith is 9.7 % to 14.8 million years (Wolf 1970). They are close to the third group's age. Igneous activity in the same period as the Agno Batholith was probably limited in the Cordillera Central and cannot be correlated with the Caraballo Mountain ranges due to lack of data.

1-6 Geological Structure and Geological History

1-6-1 Geological Structure

The topography of northern Luzon is characterized by wide Cagayan Valley trending N-S bordered by two mountain ranges rising in both sides of the valley, viz., the Sierra Madre in the east and the Cordillera Central in the west. These two ranges are connected by NW-SE trending Caraballo Mountains. Such topographic features clearly reflect geological structures.

Plate I-8 shows the schematic geological structures by means of classifying the rocks distributed in the area into three groups.

The uplifted zone consist of basement and ultrabasic rocks. It extends narrowly from Dingalan at the south end of the survey area to Divilacan Bay, and continues along the east coast to the north.

The other basement rocks not associated with ultrabasic rocks are exposed sporadically along the Philippine Fault. As a whole it is considered that the uplifted zone trending NNW-SSE along the fault contributed in forming a U-shape feature. The sedimentary basin of Cagayan Valley is bounded by the U-shaped uplift zone. Based on the aeromagnetic survey its depth increases toward the north and attains more than 1,000 m. Small scaled basement rocks are assumed to occur in the upper reaches of the Balintogon about 25 Km west-northwest of Baler.

The Caraballo group unconformably overlies the basement rocks. However their geological structures seem to be conformable by having NE-SW strike with gentle dips (20° — 30° ?) toward the N in Sierra Madre and NW-SE strike in the Caraballo Mountains, Dupax and Bambang areas. The bending point of the strike is not clear due to thick cover of younger sediments which have probably the same U-shape structure as the basement rocks. Some information on the structures of the basement rocks and the Caraballo group were obtained by the aeromagnetic survey results. PL III- 3 is a magnetic chart which is reduced to about 1,000 m below sea level. Accordingly, the magnetic anomalous zone coincided with the mountain ranges extending NE-SW direction in Sierra Madre and NW-SE direction over the area from the Caraballo Mountains to Dupax and Bambang suggesting the same U-shape feature. The weak magnetism in the central part of the plate shows perhaps the sedimentary basin of the Cagayan Valley.

In the northwest portion of the area a NNE-SSW trending fault runs along the Santa Fe River. This NE-SW system is discordant in relationship with a NW-SE system in the area. The discordancy was caused by faulting as well as folding which is plunging toward the north. The western extension of this fault is cut by a large-scale splay of a NNW-SSE trending Philippine Fault. On the west side of the fault, the structure is not clear except a small-scale dome structure near the Tawi-

Tawi ore deposits. The general structure in this area is considered to be trending N-S, assuming the E-W strike direction of the Pampanga River is local.

As a whole, the geological structure in the area including the Cordillera Central is characterized by U-shape feature. Distribution of quaternary volcanic cones or plugs are probably controlled by this structure. They are mostly pyroxene-andesites in the Santa Fe River, in Carranglan and in the upper reaches of the Ditali River. Luis Santos-Ynigo (1966) pointed out that the inner volcanic arc in northern Luzon are distributed along the east side of acidic intermediate plutonic belt forming the Cordillera Central and the Caraballo Mountains, and along the west side of the Sierra Madre.

The major structural lines in the Philippines were discussed by Smith and Masao (1927), Alcaraz (1947), Irving (1951), Teves (1955) and Gervasio (1966) etc. They believed that the Lingayan-Dingalan Line traversing the base of Luzon and the North Luzon Offset Line running through the northern Luzon are related to the structure in the survey area. The location of the latter is well manifested from the sudden change of depth of the sea.

The large structural line passing Dingalan with a NW-SE direction separates into two lines near Rizal. One of them maintained the same direction to Lingayen and the other changes direction to NNW and goes north along the Cordillera Central.

The former is characterized by the distinct topography characteristics separating the mountain ranges from a plain. On the other hand, the latter is a group of parallel or echelon faults with few topographic features. Phase I surveys could not get any geological or magnetic evidences showing a large displacement of this fault. Therefore, this structural line is not considered to be a part of the Philippine Fault but as a fracture zone accompanied by little "lateral displacement". The extension of the Philippine Fault, as Hashimoto & Sato (1970) pointed out is

considered to be the Lingayen-Dingalan Line like the initial idea proposed when the fault was first recognized.

Accordingly based on airphoto-interpretation, many structural lines are recognized in addition to the two large lines. The structural lines crossing the main structure in the area tend to continue for a short distance from the intersection and those parallel to the main are long. In other words, the structural lines, being concordant with the U-shape structure are characterized by the NE-SW system in the east side and the NW-SE system from the central part to the western area. The block between two NW-SE faults which appears to intersect each other at San Luis seems to be down faulted for about 2,000 m, this is based on the aeromagnetic interpretation. A magnetic body like dioritic rocks was detected at about 1,500 m depth in the plain, south of the Philippines Fault. The throw of the Philippine Fault seems to be about 2,000 m assuming that the depth showed the ground level before its displacement.

1-6-2 Geological History

The basement rocks of Paleozoic in the area chiefly consist of green schist derived from original basic flows. According to Gervasio (1967), it has been produced by the tectonic movement during Permian from ophiolite or flysch type sediments deposited in the Paleozoic geosyncline. Landmass during Paleozoic possibly existed east of Luzon within the present Philippine Sea.

Later on, the survey area becomes a platform and no sedimentation has taken place till the end of Triassic. In Cretaceous period, marine transgression began and strong basaltic to andesitic volcanic activities chiefly occurred. Consequently the Caraballo group, over 8,000 m in thickness accumulated in the subsiding zone formed west of the said landmass, with a N-S extension. From the distribution of lava flows or pyroclastics, the center of the volcanic activities are considered to

be located west of the Cordillera Central. After the deposition of Caraballo group probably during the Cretaceous, ultra-basic rocks were intruded in the eastern area possibly controlled by an arcuate thrust fault. In northern Cordillera Central, the existence of thick piles of Paleocene to Eocene coarse (boulder) conglomerate beds suggests local uplift. At the same time, gradual uplift of Sierra Madre, has occurred along the Paleozoic belt and intrusion of calc-alkali granitic rocks have taken place.

During the Oligocene time volcanic activities were vigorous. The Mamparang group with about 1,000 m in thickness were deposited in the sedimentary basin formed by the upliftment of Sierra Madre. The sedimentary environment at that time is presumably continental or neritic. At the last stage, thick limestone beds were deposited. A gentle uplifting occurred in the neighborhood west of Dupax and subsequent intrusion of dioritic to monzonitic rocks of alkali-olivine basalt or tholeiite series took place. The Tawi-Tawi ore deposits (porphyry copper type) is considered to have a genetic relation with the dioritic rock of this stage.

After these events, marine transgression continued through Miocene over the whole area so that a few sedimentation and local deposition of limestone were recognized. Middle Miocene period is characterized by vigorous uplift and fracturing trending N-S. The Philippine Fault is said to be an active fault formed during the Tertiary (King et al 1949). Its movement in late Miocene brought about the intrusion of Agno batholith and some dacitic dykes. Molasse deposits of Matuno River were probably deposited during uplift.

The whole area continued uplifting, but mudstone, sandstone and their alternating beds are locally deposited in a neritic sedimentary basin near Maddela.

During Pliocene to Quaternary period local movements and volcanics activities occurred. Consequently the Pantabangan molasse and conical volcanoes within the U-shaped structure were formed.

2. Ore Deposits

2-1 General Statement

As described above earlier, the Cordillera Central in the western part of the survey area has a geoanticlinal structure formed during the Neogene orogeny. Miocene dioritic igneous rocks intruded the central part of this orogenic belt. There are eight producing porphyry copper mines including Toledo in the Philippines. Four out of the eight mines are located in the Cordillera Central and a few mines are expected to be in production in the near future.

The four mines (ie. , Boneng, Santo Niño, Black Mountain and Philex) are distributed close to the western margins of the Agno Batholith (Schafer, 1956). The Agno batholith is relatively coarse-grained and essentially biotite to hornblende quartz-diorite in composition. Mineralized areas are characterized by intensely crumbled host rocks and possess at least three mappable alteration haloes, namely: (1) an outer argillic alteration zone; (2) a middle, narrow, partly silicified, and partly argillic-pyritic alteration zone; and (3) an inner biotitized-chloritized-silicified zone where most of the copper value are concentrated (Gervasio, 1964).

The main ore minerals of the porphyry copper types are chalcopyrite and pyrite accompanied by local bornite, chalcocite, covellite, molybdenite and magnetite.

Many gold mines are known within Baguio District since older times even before the porphyry copper deposits were discovered.

Many large scale porphyry copper and gold ore deposits are clustered along the west side of the Agno batholith, and since the east side of the batholith is within the project area new ore deposits might be found.

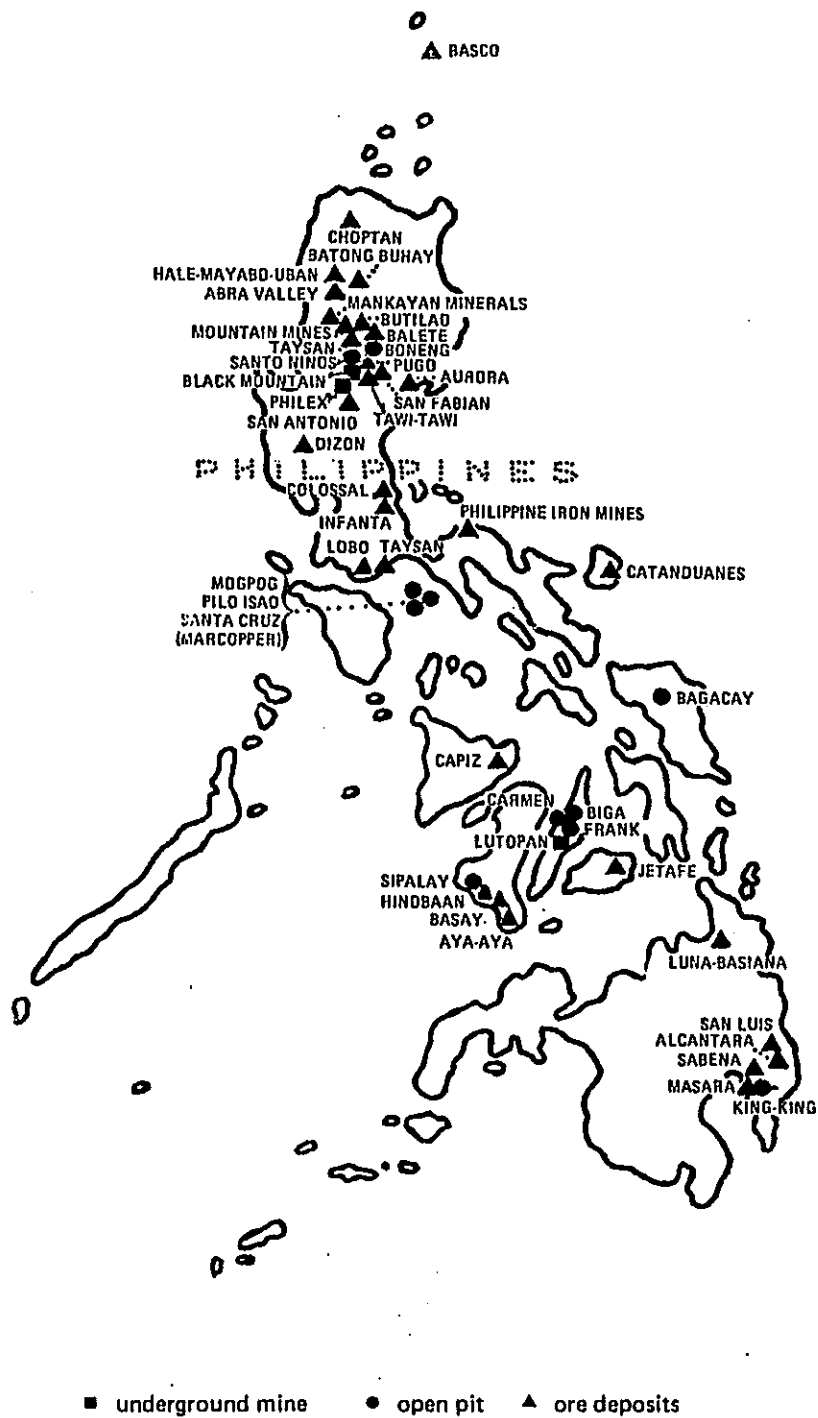


Fig. I-5 Location map of porphyry copper deposits, Philippines
after D.H. Almogera (1974)

Table I-6 Locality and names, ore reserves in tons, grades in percent copper, and daily production of porphyry copper prospects and mines in the Philippines

Locality	Name of Mines or Prospects	Reserves, Tons	Copper, Percent	Tons per Day Milled or Remarks
NORTHERN LUZON				
Central Cordillera				
Benguet	Boneng-Lobo	98,305,605	0.48	10,000
Benguet	Sta. Nino	53,119,915	0.35	4,500
Benguet	Black Mountain	26,917,550	0.47	2,700
Benguet	Philix Mines	121,079,544	0.468	16,000
Kalinga-Apayao	Batong Buhay	50,129,000	0.702	Explored Deposit
Benguet	San Antonio	28,100,000	0.50	Under Exploration
Ilocos Sur-Abra	Hala-Mayabo	45,350,000	0.50	Under Exploration
Isabela	Cordon	50,000,000	0.35-1.70	Under Exploration
Abra	Abra	Unknown	---	Under Exploration
Kalinga-Apayao	Butilao	30,000,000	0.60	Under Exploration
Kalinga-Apayao	Mountain Mines	Unknown	---	Under Exploration
Benguet	Pugo Mines	Unknown	---	Under Exploration
Benguet	Tawi-Tawi	176,000,000	0.393	Under Exploration
Total Proven and Probable Ore Reserves		678,992,614		
CENTRAL LUZON				
Zambales Range				
Zambales	Dizon	56,667,800	0.45	Explored Deposit
SOUTHERN LUZON				
Batangas area				
Batangas	Taysan	60,000,000	0.38	Explored Deposit
Paracale-Quezon District				
Camarines Norte	Philippine Iron Mines	17,000,000	0.56	Under Exploration
Quezon	Colossal	100,000,000	0.42	Under Exploration
MARINDUQUE				
Marinduque				
Marinduque	Marcopper Mining Corporation	101,500,000 ¹	0.64	21,000
		8,000,000 ²	0.53	
Marinduque	Ino-Capayang	75,187,861	0.61	Explored Deposit
Total Proven and Probable Ore Reserves		359,687,861		
CENTRAL PHILIPPINES				
Cebu District				
Toledo, Cebu	Atlas Consolidated Mining & Development Corp.	697,528,000	0.47	70,000
Toledo, Cebu	Carmen ore body of Atlas	267,000,000	0.44	Explored Deposit
Negros Island				
Negros Occidental	Sipalay Mines of Marinduque Mining and Indus. Corp.	342,021,000	0.521	12,000
Negros Occidental	Hinobaan	98,000,000	0.6	Explored Deposit
Negros Oriental	CDCP Mining Corp.	64,000,000	0.56	Explored Deposit
Negros Oriental	Sipalay Mining and Exploration Co.	30,000,000	0.6	Under Exploration
Total Proven and Probable Ore Reserves		1,480,549,000		
MINDANAO				
Davao				
Davao del Norte	Apex Exploration & Mining Co.	27,500,000	0.39-0.53	2,500
Davao del Norte	King-King	45,000,000	0.5	Explored Deposit
Tagapura, Davao del Norte	Sabena Mining Corporation	8,377,356	0.632	Under Exploration
Kalamatan, Davao del Norte	Sabena Mining Corporation	12,700,000	0.383	Under Exploration
Davao del Norte	Alcantara	Unknown	---	Under Exploration
Davao del Norte	San Luis Mining	Unknown	---	Under Exploration
Davao	Samar Mining Corporation	44,230,000	0.445	Under Exploration
Cabadbaran, Agusan	Luna-Baslana Mining Company	80,707,780	0.293	Explored Deposit
Total Proven and Probable Ore Reserves		218,515,456		

¹ Sulphide. ² Oxide

2-2 Mineralized Zone

The known mines and prospects in the survey area are summarized in a unpublished report by Bureau of Mines. The mineral indications encountered are as follows:

2-2-1 Bolo River Mineralized Zone

This mineralized zone can be observed along Bolo River, one of the branch of the Agno River. The mineralized outcrop is 80 m in width. It is overlain by Quaternary sand and gravel. The original rock may be diorite—monzonite, although it is hard to assume due to strong sericitization and silicification. Ore minerals are chalcopyrite and pyrite, occurring as disseminations or veinlets in the silicified rock.

Secondary copper minerals such as malachite and chalcantite are observed. A chemical analysis of the representative part of the outcrop is as follows:

Sample	Width	Grade
Cp-py dissemination	5 m	1. 5g/tAu, 20g/tAg, 0.17%Cu, 0.02%Mo, 2. 50%S

The mineralized zone is possibly the northern extension of the Tawi-Tawi porphyry copper deposit.

2-2-2 Benneng River Mineralized Zone

The micro-diorite stocks intrudes the basaltic lavas in the Benneng River, the southern margin of the Tawi-Tawi mineralized zone. The mineralization in the area is not so intense as the Bolo mineralized zone.

An intense silicification is remarkable in the uppermost part of the mineralized zone, where diorite porphyry dykes intrude into autobrecciated andesite lavas trending N20E. The silicified zone measures about 700 m across but it is almost

barren with only minor pyrite dissemination. Near the contacts of porphyry dikes and host rocks, irregular quartz stringers, with 5 cm in width are noticeable. A small amount of fine-grained chalcopyrite, sphalerite and pyrite are occasionally observed. In the middle course and lower reaches of the Benneng River, epidote-quartz or clay minerals veinlets are developed with dissemination of chalcopyrite showing 0.10% Cu and 5.20% S. In area where the host rock is generally fresh, the copper mineralization becomes weak.

2-2-3 Mapayao River Mineralization

A small scale intensely silicified stock of medium-grained diorite crops out in the upper reaches of the Mapayao River. Minor amount of malachite and azurite stain along fractures were observed with an assay value of 0.6g/tAu, 0.64% Cu and 0.05% S.

On the eastern extension of the mineralized zone, another prospect was reportedly explored by drilling and it contains about 8 million tons of 0.4% copper. Both of them appear to be a porphyry copper type.

2-2-4 Maasin River Mineralization

Along the Sulong River monzonite body is widely distributed. Mineralized porphyritic andesite and andesitic volcanic breccia crop out at the western margin of this monzonite in the upper reaches of the Maasin River. Fine grained pyrite disseminations or veinlets accompanied by a small amount of chalcopyrite are observed in a 5 m in width outcrop. In addition to silicification, sericitization and kaolinitization are also noted. Assay values are 0.2G/tAu, 0.13% Cu and 2.01% S.

The gold deposits of the Sulong River are explored by drilling by a private company. According to a local information, the gold deposits are found in the pyroclastics near the monzonite body. It occurs as disseminations rather than in vein along fissures.

In other showings, some pyrite disseminations are found in the following places:

1. Pyrite-chalcopyrite dissemination ($< 0.1\%$ Cu) with silicification were observed in a diorite dyke and neighbouring andesite lava in the upper reaches of the Baan River.
2. Pyrite dissemination with silicification were observed in mudstone and coarse-grained tuff in the middle course of the Mapayao River.
3. Pyrite dissemination occurred in a granodiorite body about 7 Km south-east from Dupax.
4. Pyrite dissemination (0.01% Cu, 3.12% S) in porphyritic andesite in the Campote River. An intrusion of a diorite porphyry dyke brought about alterations such as silicification, chloritization and sericitization.
5. Pyrite dissemination (0.3g/tAu, 0.01% Cu, 6.49% S) occurred in porphyritic andesite in the lower reaches of the Sulong River.

Host rock suffered intense argilization (sericitization) and silicification.

The mineralization and alterations stated above can be summarized as follows:

1. Mineralization observed here are pyrite impregnation with chalcopyrite which are closely related to the intrusions of dioritic rocks. They occur at the margin of the intrusive body and intruded rocks near the contact.
2. Minor mineralization could also be found at the core of large igneous mass ie. Dupax batholith. Known large scale ore deposits are located in places where dioritic rocks have been intruded in the form of dyke or stock.
3. Rock alterations in the area are silicification, chloritization and sericitization. Most of them are very limited, except the extensive alteration of Tawi-Tawi ore deposit.

PART II. GEOCHEMICAL SURVEY

1. General Remarks

The geochemical reconnaissance stream sediment survey of this phase was carried out together with geological survey. Main roads and rivers were taken as the geological survey routes and geochemical samples are confined mainly around them. The four parties could not cover all drainage systems within one month so an additional survey was conducted over some of the uncovered area after the joint survey. In this report the additional 167 samples collected were also discussed.

The most potential ore deposit in the area is a porphyry copper type so all collected samples were analyzed quantitatively for Cu, Zn and Mo.

1. Eight (8) geochemical anomalies of Cu, Zn or Mo were disclosed in the survey area. All of them occur in places where dioritic rocks are intruded or expected.
2. The anomalous zone of Cu, Zn and Mo are located in some mine prospects and in area where drilling operation were abandoned.
3. The anomalies of Cu or Zn in the Kongkong Valley and the Sulong River are distributed widely unlike other anomalies. Although they are considered to depend upon the difference of rock facies, it is necessary, to conduct a detailed a detailed survey to clarify their causes.
4. The Zn anomalies obtained from each branches of the Cagayan River, are not accompanied by Cu and Mo anomalies. Since they are limited within the Mamparang group, it is possible that they are caused by different rock facies.

2. Sampling and Analyses

2-1 Sampling

Generally silty sediments (under 80-mesh fraction) deposited in the active channels of streams were collected. Tributaries were chosen as the sampling sites instead of main rivers because the source of mineralization can be easily reflected. Stream sediments were also collected at the center of dry river channel or underground drainage system.

Care was taken to avoid contamination with organic materials and bank sediments to minimize sampling errors. PH values of water in main streams were measured using PH test paper.

About 10 to 20 grams of sediments were collected and placed in vinyl bags. They were sent to the base camp for drying.

To avoid confusions, each party used different letters, viz., A, B, C and D, and the sample numbered respectively. The letter J was assigned to the additional samples collected by Bureau of Mines' geologists after the joint survey.

2-2 Analyses

All samples collected in the field were analyzed in Japan by atomic absorption spectrometry for Cu and Zn, and colorimetry for Mo.

The Analytical Procedure is mentioned as follows.

2-2-1 Atomic absorption spectrometry

The analytical method used by the Geological Survey was adopted in sample decomposition of Cu and Zn.

1 gram of sample was taken and digested with 5 ml of concentrated HNO₃ and 3 ml of HClO₄ in a sandbath until white vapor appeared. After cooling, dissolution

was accomplished by addition of 5 ml of HNO_3 (1 : 2). The solution was made up to exactly 20 ml mark with distilled water. The sample solution was filtered and filtrate was analyzed by atomic-absorption spectrophotometry using a wave lengths of 3247A° for Cu and 2139A° for Zn.

2-2-2 Colorimetry

Mo was determined by a handy procedure of I. L. Elliotts zinc-dithiol method. A 0.25 gram of sample was digested with 2 ml of aqua regia, 1 ml of HClO_4 and 2 ml of H_2SO_4 (1+1) on a sandbath until white vapor appeared. After cooling, the cake was dissolved by dilute H_2SO_4 and heated again. The solution was transferred to a test tube and adjusted to 10 ml mark with the addition of 2-3 ml of NH_4OH and distilled water. A 2 ml of the clear solution was pipetted into a test-tube and a solution was pipetted into a test-tube and a 2 ml of hydroxylamine hydrochloride solution (2.5%) was added and shaken gently. A 0.5 ml of zinc-dithiol solution (1%) was added to solution. After thorough shaking, the color of the organic layer was compared with a standard series previously prepared.

3. Compilation and Interpretation of the Results

3-1 Compilation of the Analytical Results

The analytical data of geochemical survey are usually treated statistically. But, for this purpose, a uniform sampling density is always needed. In this phase, the sampling locations were shown in PLII . They were mostly concentrated in the relatively accessible area and were very few in the Central and the Sierra Madre Mountain Ranges. Therefore, it is still doubtful to treat the collected 1,168 analytical data statistically, though they may apparently represent a lognormal distribution pattern. The survey area consists of granitic to dioritic rocks and sedimentary rocks that can be divided into several groups. There are small variations of mean background values of metal content for different rock type (ex. Dupax' diorite; Cu 38ppm; Kasibu' granodiorite, Cu 72ppm; sedimentary rocks, Cu 47ppm). Consequently, 2.5%-value (t) of total data from the highest was simply taken as the threshold or the upper limit of normal background values. The results are shown in PLII-1. The general trend of geochemical anomalies become complicated when the anomalies are isolated, so that the value (t') corresponding to 10%-value of total observations from the highest, and $2t$ (for giving an impression of very high value) are more or less schematically represented on the same map.

The mean background and the threshold values of 3 elements, Cu, Zn, and Mo, are shown in Table II-1.

Table II-1 Regional mean background and threshold values of stream sediment samples

	b	t'	t	2t	Remarks
Cu	50	112	175	350	Number of observations : 1,168
Zn	97	225	450	900	do
Mo	<2	2	5	10	do

b : mean background value
t' : 10%-value of total observations from the highest
t : threshold value

3-2 Interpretation of the Results

From PLII-1, several geochemical anomalies of stream sediment analysis were obtained in the survey area. Some anomalies are apparently related with the known ore deposits while the others have no relationship. The main anomalies are described below in detail.

Anomaly 1, Cu, Zn, Mo

The anomaly is situated in the south side of Bolo creek. It extends over 2 km in width. Stream sediment results show very high values ranging 188- 1,184ppm Cu (number of anomalous value : 4), 1,018— 1,446ppm Zn(2) and 7-20ppm Mo (4). The anomaly is located at the north end of the Tawi-Tawi Project where new ore deposits have been explored. Along the creek, disseminations and veinlets of chalcopyrite and malachite were observed in the diorite body which suffered a strong quartz-sericite alteration. Although a configuration of the anomaly is not clear because of omission of the survey on the central part of the mineralization this area has the most remarkable anomaly detected.

Anomaly 2, Cu

The anomaly is situated in the upper reaches of the Mapayao River. It is related to the diorite stock intruded into the basaltic andesite. Copper disseminations with a strong silicification were noted in prospect explored by drilling.

Relatively high Cu contents, ranging from 245ppm to 610ppm (3) were obtained. However, Zn and Mo contents do not exceed the threshold values but they are higher than the mean background values.

Anomaly 3, Cu, Zn

The anomaly is situated in the west branch of the lower reaches of the Imugan River and extends about 2km up the junction of the Santa Cruz. Anomalous values of copper and zinc are 1,819ppm and 994ppm respectively, while Mo is generally absent. The exposed rock in the area is coarse grained basalt which is locally serpentinized. No mineralized floats can be found and no other geochemical anomalies occur in the adjacent branches, the anomaly is considered to be very local.

At the midway between Anomalies 2 and 3 on the east bank of the Santa Cruz River, small amount of disseminated chalcopyrite and pyrite were observed in the dark gray basalt, so Cu and Mo values in the stream sediments become high (130 – 205ppm Cu and 4 – 7ppm Mo (2)). This anomaly seems to be the extension of Anomaly 3, thus further studies will be needed.

Anomaly 4, Cu

Anomalous copper value (405ppm) was obtained from the small branch near San Francisco, mid-course of the Marang River and at the center of Dupax Batholith. Because of limited exposures, their details are not clear. No other significant results were found in the adjacent branches, the anomalous zone is more or less than 0.3 km² in area.

Some claims were reported between Dupax and San Francisco where pyrite impregnations and veinlets with a few chalcopyrite are found near contact between diorite and altered basalt. The anomaly is probably due to the same mineralization mentioned above and possibly with a limited sialic.

Anomaly 5, Cu

A wide Cu anomaly was found in the Kongkong Valley in the upper reaches of the Kasibu River. Most of the samples collected from all branches have higher Cu contents than the threshold value. Copper contents range from 175 to 245ppm (12), with the mean value of 191ppm. Mo and Zn are generally absent.

The anomalous area covers about 30 km². It seems to have close relationship with the diorite body trending in a NE-SE direction along the Kongkong Valley. A low geochemical contrast (max/t=1.4) were noted along the anomalous zone with the diorite body. The small variations of Cu values suggests that the anomaly depends partly on the different rock facies. Hence it is necessary to conduct a detailed survey to determine the cause of widely dispersed anomalous zone.

Other Cu anomalies were also found at 6 km and 12 km points southeast of Kasibu. They are 175—195ppm (3) and 185—210ppm (3) respectively.

Anomaly 6, Mo

The anomaly occurs in the eastern part of monzonite stock in the upper reaches of the Sulong River that flows down parallel to the Kongkong Valley. Anomalous Mo content ranges from 5ppm to 16ppm (22) with the mean value of 9.7ppm. The estimated anomalous area is about 20 to 25 km².

As mentioned before, a gold deposit is known in the pyroclastics near the monzonite in the upper reaches of the Sulong River. According to the unpublished report, its location must be in the Mo anomalous zone disclosed by this reconnaissance. Genetical relationships between gold and molybdenum are not clear because details of the gold deposits are not known. However, the Mo anomaly is probably related to the porphyry copper type of mineralization since molybdenite-pyrite stringers are reportedly found in the diorite body near Dupax. Although remarkable anomalies of Cu and Zn were not detected in this area, the Mo anomaly is so significant that a

follow-up survey work will be necessary.

Anomaly 7, Zn

A zinc anomaly occurred along the Cagayan River extending from Bo. Wasig to 20 km upstream. The anomalous value ranges from 486 to 793ppm (8) exceeding t' (225ppm). This area is underlain by basaltic lava flows and pyroclastics of the Oligocene age belonging to Mamparang group. The rapid decrease of Zn contents from 324ppm to 188ppm in the Caraballo group suggests that the Zn anomaly was caused by the differences in rock facies.

Anomaly 8, Cu, Zn, Mo

The anomaly is in the upper reaches of the Diarabasin River. The values of Cu, Zn and Mo are 186, 870 and 6ppm respectively exceeding the threshold values. In spite of the existence of remarkable Zn anomalies (491—1,000ppm) in adjacent branches, Cu and Mo values are lower than the mean back ground values.

This area is characterized by pyrite disseminations with weak argillization especially where pyroxene andesite lavas or pyroclastics are exposed. Dioritic rocks is generally absent. According to the local information, quartz diorite intrusion accompanied by copper mineralization are known a few kilometers north of this place near the coast.

PART III AIRBORNE MAGNETIC SURVEY

1. General Remarks

The Airborne Magnetic Survey conducted over Northeastern Luzon, Philippines, covering about 14,500 Km², forms part of Phase I Mineral Resources Survey of Northeastern Luzon, Philippines, designed to delineate potential areas for mineral resources.

This report describes the procedures used for data acquisition and the interpretation of the data obtained.

Taking into account the available information on the geology of the area, the report discusses the major structures and lineament directions revealed by the present survey. It delimits the zones in the northwestern part of the survey area more promising for the ore deposits and suggests that detailed geological, geochemical and geophysical surveys be conducted over these zones.

2. Outline of Airborne Magnetic Survey

2-1 Survey Area

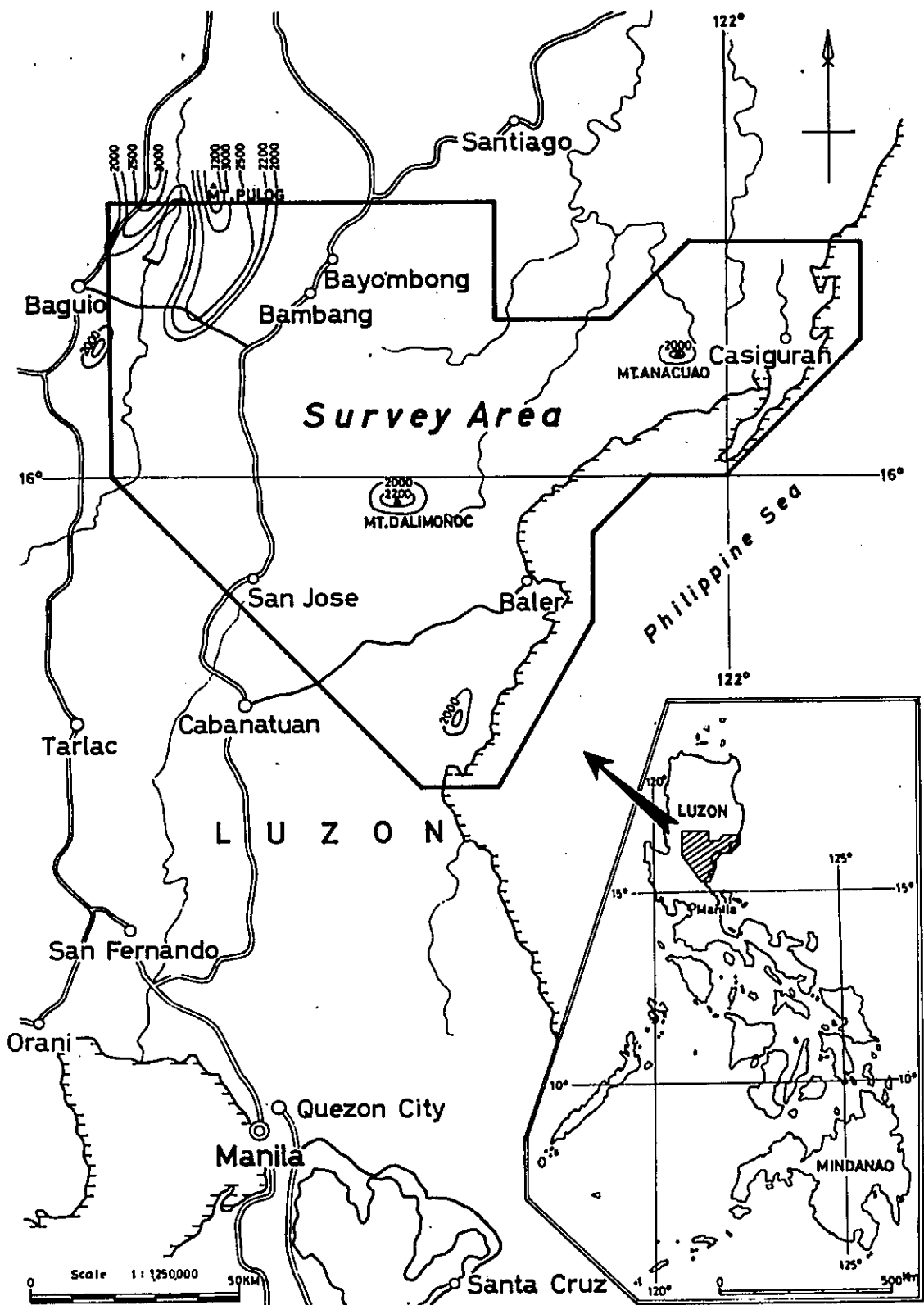
The airborne magnetic survey described in this report was conducted in the northeastern part of Luzon as shown in Fig. III-1. The survey area forms a polygon whose apexes are as listed below.

	latitude N	longitude E
A	16°35'	120°40'
B	16°35'	121°30'
C	16°20'	121°30'
D	16°20'	121°45'
E	16°30'	121°55'
F	16°30'	122°17.5'
G	16°17.5'	122°17.5'
H	16°00'	122°00'
I	16°00'	121°50'
J	15°52.5'	121°42.5'
K	15°41.3'	121°42.5'
L	15°20'	121°30'
M	15°20'	121°20'
N	16°00'	120°40'

2-2 Survey Period

Field Survey;

Reconnaissance Party was dispatched to the Philippines during the period January 4 through March 20, 1975.



(contours indicate areas exceeding 2000M ASL)

Fig. III-1 Location map of Survey area

The main Party was dispatched during the period January 16 through March 20, 1975.

Data Processings and Analyses were conducted during the period March 20, 1975 through October 31, 1975.

2-3 Surveyors

Field Survey;

MASAO YOSHIZAWA

FEDERICO E. MIRANDA

IKUO TAKAHASHI

CAROL S. SAMONTE

SABURO TACHIKAWA

ARNULFO V. CABANTOG

MOTOJI ICHIKAWA

JOSE N. ALMASC O

MITSURU SAKAZAKI

BENJAMIN CADAWAN

SHOZO KIMURA

ROMEO L. ALMEDA

TAMOTSU FUJIKAWA

URBANO PALAGANAS

TAKASHI NAKAYAMA

Data Processings and Analyses;

YUYA FURUKAWA

FEDERICO E. MIRANDA

YOSHIO TAMURA

ARNULFO V. CABANTOG

ICHIRO HONMA

KENICHI NOMURA

MASAO YOSHIZAWA

JIRO KAMATA

IKUO TAKAHASHI

SABURO TACHIKAWA

2-4 Summary of Field Operations

The present field work was dealt with as follows:

Airbase: Nichols Airbase (Manila International Airport)

Observation Station of Geomagnetic Variation: Bayombong, Nueva Vizcaya

Total Survey Area: 14,500 Km²

Flight Altitude: 2,000 M above sealevel (horizontal navigation, see Fig. III-2)

Separation of Flight Lines: 1.5 Km for the traverse lines and 10 Km for the tie lines.

Flight Direction: N-S and E-W

Effective Lengths of Lines: 9,717.25 Km for N-S direction and 1,526.75 Km for E-W direction i. e. , the total length amounts to 11,244 Km.

Geomagnetic Dip-Angle: 20°

Geomagnetic Declination: 0°

Total Geomagnetic Intensity: 40,000 gammas

2-5 Survey Instrumentation

The instrumentation and navigation system used in the present survey are as follows:

- a) Aircraft
- b) High Sensitivity Airborne Proton Magnetometer
- c) High Sensitivity Optical Pumping Magnetometer
- d) High Precision Digital Clock
- e) Radar Altimeter
- f) Barometric Altimeter
- g) 35 m/m Tracking Camera
- h) Two-channel Analog Recorder
- i) Doppler Radar Navigation System
- j) Digital Data Acquisition System

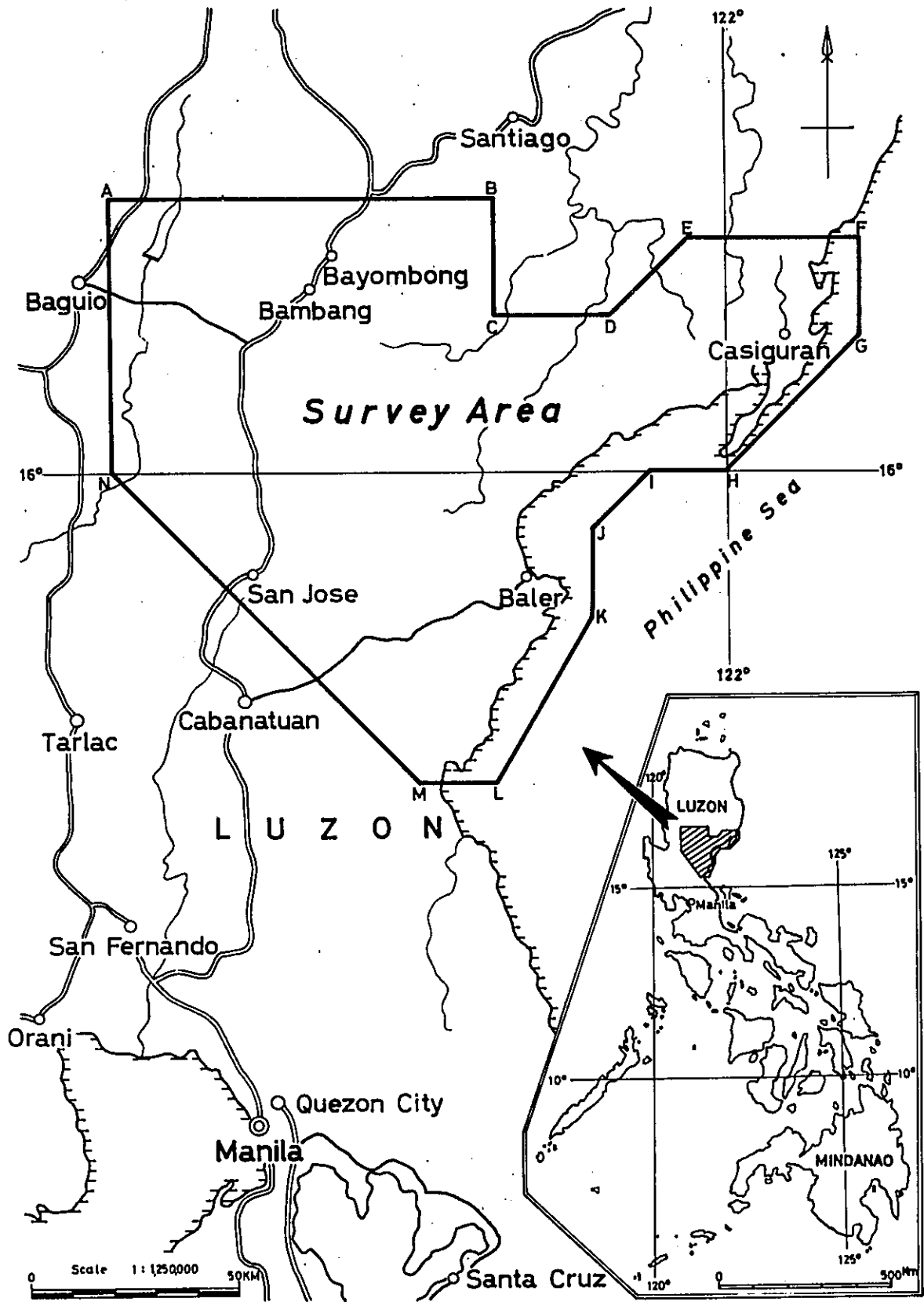


Fig. III-2 Flight altitude

These instruments were synchronized with the signal from a high precision digital crystal clock. Such a synchronization makes it easy to compare the records of one to another's (see Fig. III-3)

The summarized specifications and measuring principles of the above instruments are described as follows:

a) Aircraft

The aircraft used during the survey was a twin-turbine engined a YS-11, Registration JA8612, manufactured by the Nihon Aeroplane Manufacturing Co., Ltd. This aircraft was 60-seated originally, but modified for airborne surveys with ten personnel. The duration of flight was about six hours with a speed of 130 to 200 knots. For the purpose of airborne geomagnetic survey, this aircraft was equipped with a 3 meter-long tail cone (tail stinger), in which a sensor was installed. The remanent magnetism of the aircraft body was compensated by the magnetic field induced with a tri-axial coil.

b) High Sensitivity Airborne Proton Magnetometer

The airborne magnetometer used was a Geometrics High Sensitivity Airborne Proton Magnetometer, Model G-804. This type of magnetometer is highly sensitive and most stabilized of all the proton magnetometers developed until recently. It's performance is given in the following:

- i) High sensitivity and fast sampling rates (0.05 gammas/0.95 sec).
- ii) High precision and small drift (0.5 gamma and 0.1 gammas/month, respectively, in total magnetic intensity).
- iii) A signal-to-noise ratio is at least 400 to 1 achieved by placing the preamplifier tuner close to the sensor. A Larmor signal is so large that the phase lock works efficiently to produce high resolution in reading magnetic values.

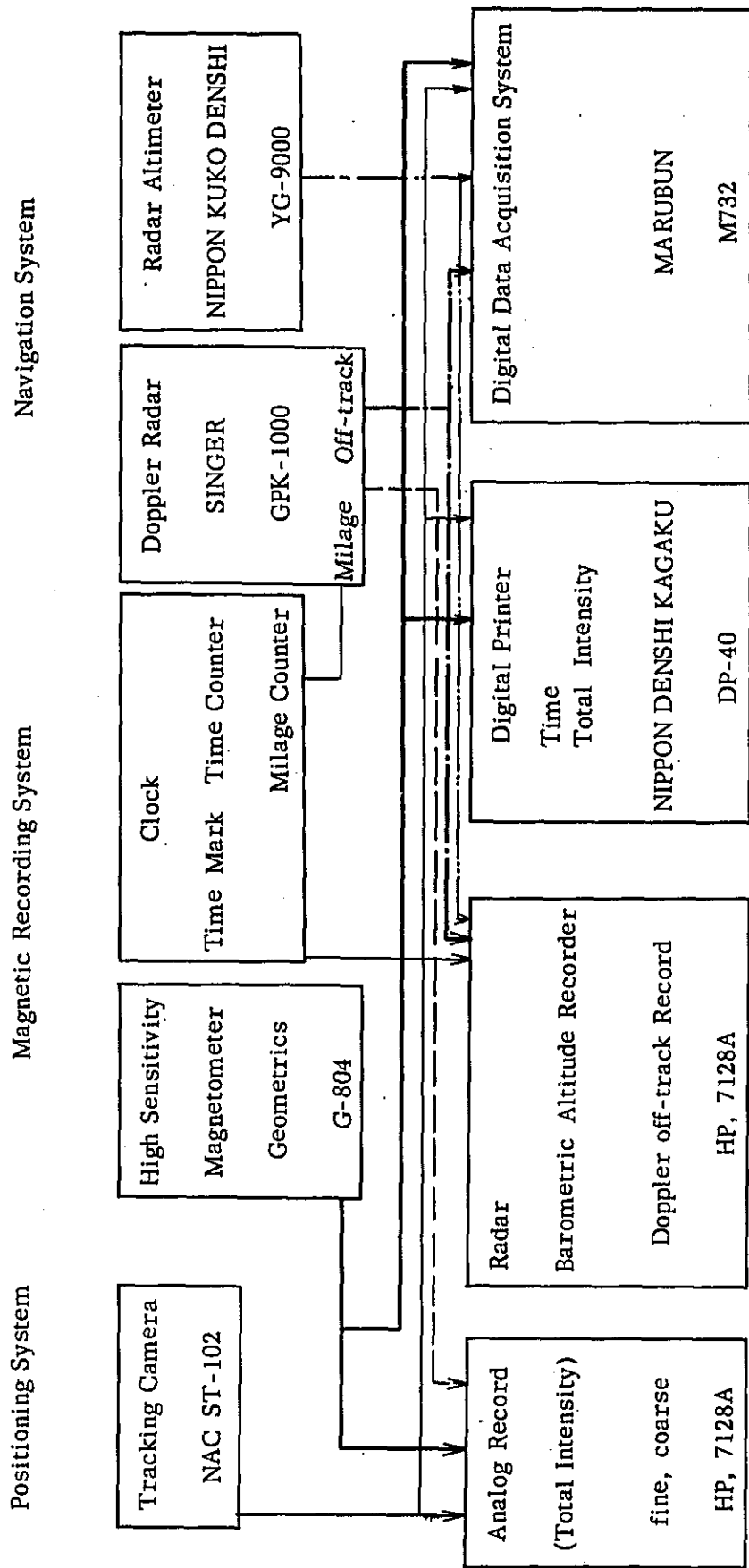


Fig. III-3 Block diagram of airborne magnetic survey (airborne system)

- iv) Analog output together with digital output available in B. C. D. code (1-2-4-8). The digital output enables us to obtain digital data recording and processing.
- v) It is compact, lightweight and highly reliable due to the integrated circuit construction. In case it runs out-of-order, a repair can be easily and readily made by changing the spare card.
- vi) Direct readout in gamma to six significant digits is possible by using the NIXY tubes.
- vii) The Model G-804G has a same-type sensor, preamplifier and additional circuit devices, providing high sensitive measurements in horizontal or vertical gradient of geomagnetic field.
- a) Principle of Measurement by a Proton Precession Magnetometer

The proton precession magnetometer operates on the principle of nuclear magnetic resonance to measure the total intensity of the earth's magnetic field. In the proton magnetometer sensor, a uniform magnetic field is created by passing a few amperes of current through a coil about a small volume of proton-rich hydrocarbon fluid such as water or kerosene. The spinning protons act as small magnetic dipoles and align themselves with the applied field. When the field is removed (i. e. the polarization current is switched off), the protons precess in phase about the direction of the earth's field at a rate proportional to the earth's total magnetic intensity. This rate, which is called Larmor precession frequency, is determined by the value of the gyromagnetic ratio of the proton (23. 4874 gammas/Hz), which is an atomic constant known to an accuracy of 7. 5 parts per million. The precession frequency is independent of the direction of the spins with respect to the

earth's field, but varies with the intensity of the field. The precession signal is maximum when the proton spin axes are perpendicular to the direction of earth's magnetic field, and zero when they are parallel. The Larmor signal is induced by the motion of the precessing protons, and is detected by the same coil used for polarization. The signal is decayed in a few seconds from its peak value of a few tens of micro-volts due to thermal agitation. The frequency of precession signal is approximately 0.04 Hz/gamma, or between 1250 and 3400 Hz, corresponding to a range of 30,000 to 80,000 gammas in the earth's magnetic field.

b) Model G-804 System Description

The specifications of a Model G-804 are described as follows:

Range: 30,000 to 80,000 gammas

Accuracy: ± 0.5 gammas total field

Drift: Less than 0.1 gammas/month

Sensitivity (gammas)	Sampling Rates (per second)	Analog Full-scale Resolutions (gammas)
0.05	1.1	5 , 50
0.10	2.0	10 , 100
0.25	3.5	25 , 250
0.50	5.0	50 , 500
0.20	every 20 sec.	20 , 200

Visual Display: Six digits in gammas

Digital Recording: 1-2-4-8 BCD code

Power Requirements: Standby 85 watts

Maximum 575 watts

Temperature Range: Console: -10°C to 65°C
Analog Recorder: 0°C to 50°C
Sensor: -40°C to 50°C
Relative Humidity: 0 to 90 %

c) High Sensitivity Optical Pumping Magnetometer

The magnetometer used was Cesium Magnetometer Model MDA-7101A manufactured by the MARUBUN. We used the magnetometer for two purposes; i) observation of daily magnetic variations on the ground in order to correct daily variations to the airborne magnetic values obtained, and ii) detecting magnetic storms.

A cesium magnetometer operates on the principle of magnetic resonance absorption due to the optical pumping phenomena of cesium atoms. The outline of the principle is described as follows:

Valence electrons of cesium or rubidium alkali vapor has various energy levels. The Zeeman effect splits the energy levels into various sublevels, whose separations depend upon the Larmor frequency which is proportional to the total intensity of the earth's magnetic field. For the isotope Cs^{133} , the Larmor frequency is $3.498 \text{ Hz/sec/gamma}$. The application of optical-pumping techniques to the isotope gives us an atomic oscillator self-excited with the Larmor frequency. Therefore, the measurements of Larmor frequency enables us to observe continuously the earth's magnetic field. The fact that the Larmor frequency of cesium is about 100 times higher than that of proton implies that the sensitivity of the cesium magnetometer is also 100 times higher than that of proton magnetometer. A Model MDA-7101A Station Magnetometer manufactured by the MARUBUN detects the total intensity of the

earth's magnetic field ranging from 20,000 to 80,000 gammas with an accuracy of 0.1 gammas/0.5 sec at maximum.

A Hewlett Packard Analog Recorder 680 records successively the geomagnetic variations (see Fig. III-4).

d) High Sensitivity Digital Clock

A MARUBUN Digital Clock M733 does not only indicate time but also generates one-second and ten-second interval pulse output. The magnetometer is operated by the trigger pulse of one-second interval, while the ten-second interval signal records time marks both in the analog recorder and in the tracking camera. In processing of data, the analog records are synchronized with the flight-path films and the records of daily magnetic variations by the time marks.

e) Radar Altimeter

A NIPPON KOKU DENSHI Radar Altimeter YG-9000 on board a plane covers an air-to-surface altitude ranging from 0 to 5,000 feet. The flight altitude was checked at all times by the altimeter and recorded by the Hewlett Packard Analog Recorder.

f) Barometric Altimeter

A barometer is used in order to keep a constant barometric altitude for plane navigation. In the present survey, 2,000 M barometric altitude was maintained.

g) 35 m/m Tracking Camera

A NAC 35 m/m Strip Camera ST-102 on board a plane determined the flight-path. It is a lightweight camera with parashock construction, and equipped with the following features:

High Sensitivity Magnetometer

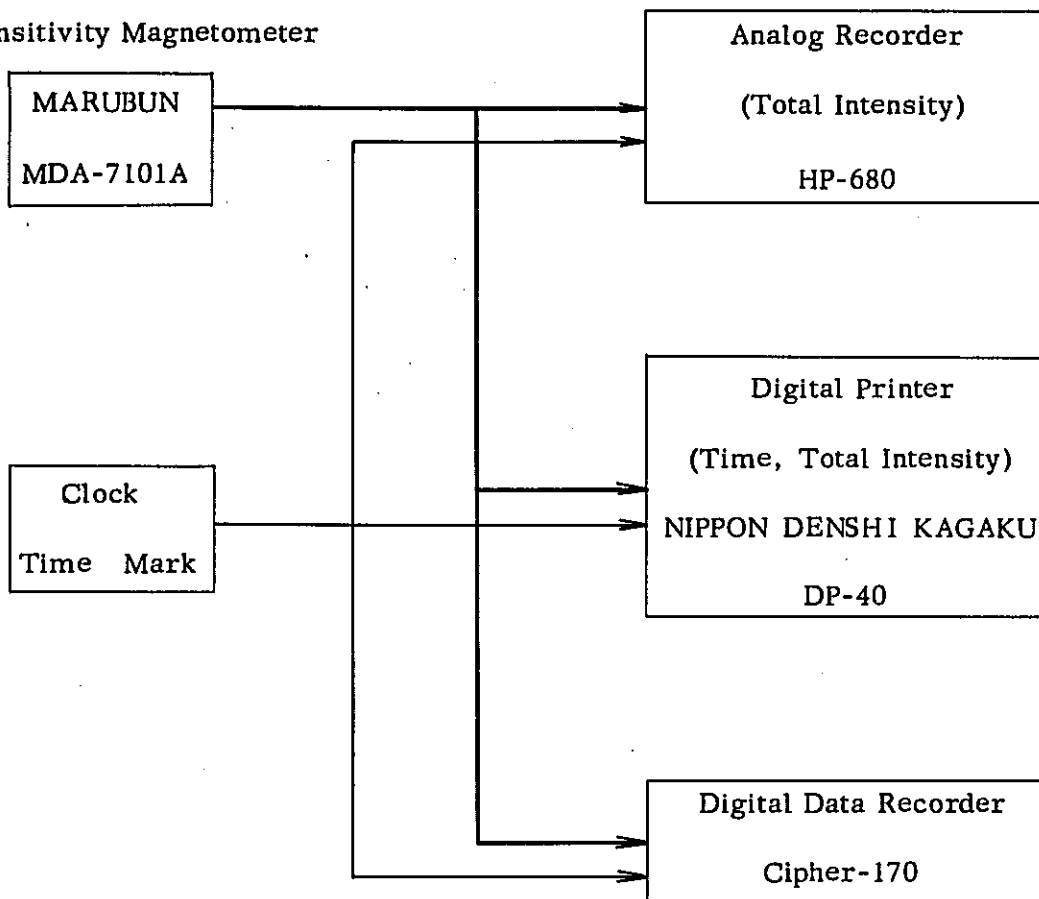


Fig. III-4 Block diagram of airborne magnetic survey (ground system)

- i) Variable film speed
- ii) Remotely operated aperture control
- iii) Film footage counter
- iv) Two independently operated fiducial markers
- v) Film break cut-out switch
- vi) Operates with 400 ft. magazines

This camera was installed under the back-seats of the plane. The film speed varied with Doppler Radar signals to control a constant film footage for the navigation direction. Meanwhile, the film recorded the ten-second time marks.

h) Two-channel Analog Recorder

Two Hewlett Packard 7128A Analog Recorders were used in the present survey. One of them records both 10-gamma and 100-gamma full-scale magnetic values, while the other was used for recording outputs from the Radar Altimeter and off-track data from the Doppler Radar Navigation System. The 10-sec time marks were added to these records for the data synchronization.

i) Doppler Radar Navigation System

The navigation system used in the present survey was the SINGER GPK-1000 and GPQ-601 Doppler Radar Systems. The navigation guidance to flight path was preliminarily programmed in a computer (GPL-GPQ-601) with data of flight-path length, and direction and sampling rate. The deviation between the programmed flight path and the actual one estimated from the Doppler Radar signal was indicated in the cockpit panel. The aircraft was so guided as to lessen the deviation.

j) Digital Data Acquisition System

The digital data acquisition system used was a Model 70 manufactured by Cipher Co. The accumulated data were

- i) Name of flight path and direction of navigation.
- ii) Time.
- iii) Total intensity of the earth's magnetic field.
- iv) Analog records of the Doppler off-track and radar altimeter.

These data were processed by an electronic digital computer in Tokyo.

2-6 Data Processing

2-6-1 Flight Path Map

The determination of flight path was made by using tracking films. In order to reduce the photographs to a scale of 1/50,000, the natural size, the film speed adopted was 4.3 mm/sec on the basis that the flight speed was 165 knots. The flight path charts were completed by the following procedures. The films were developed and dried up every day immediately after flight. Fiducial points plotted on the magnetic data (10-second interval samplings from the magnetic data and the tracking films) were transferred to aerophotographs (scale: ca. 1/40,000) and 1/50,000-scale topographic maps. For such an area as swamp, where it was difficult to find any fiducial point, we took Doppler positionings into account to determine flight paths as exactly as possible. The flight path charts such obtained were also prepared for the following flight projects and further examined whether supplementary surveys were necessary or not.

2-6-2 Correction of Daily Magnetic Variation

Geomagnetic measurements were continuously carried out at Bayombong, Nueva Vizcaya for correction of daily magnetic variations to the airborne magnetic

data and for checking magnetic storms. The amplitude of daily variations ranges from 0.2 to 0.3 gammas/min with no conspicuous disturbance due to magnetic storms during the period of the present survey.

The mean total intensity of the earth's magnetic field amounted to 40,900 gammas at the ground magnetometer station. The correction table of daily variation was made on the basis of the digital and analog records of time variations from the mean total intensity. The airborne magnetic data were corrected in reference to the correction table, and then the final data without any time effect were obtained.

2-6-3 Total-Intensity Map

After the daily-variation corrections, the airborne magnetic data were transcribed on the 10-second interval reference marks plotted on the flight path map. It is sometimes seen that some differences between magnetic values occur at intersection points of traverse-lines and tie-lines. These are caused by such reasons as follows. Possible causes are errors due to positioning, flight altitude and heading of aircraft (heading error is a magnetic change induced by change in flight direction). In case that any magnetic closing-error was found at an intersection point of traverse and tie-lines, we re-examined the positioning and horizontality of the aircraft. The closing errors were minimized in a least-squares sense by an electronic computer by estimating coefficients of 1st order trend of closing-error for each flight line to provide final corrections to magnetic values obtained at all intersection points. Finally, the total intensity map was drawn on the basis of the data given at the grid points.

2-6-4 Residual Anomaly Map

The residual anomaly map was drawn on the basis of the geomagnetic regional variation, which was calculated by subtracting the standard total intensity of the

International Geomagnetic Reference Field (IGRF) from the one interpolated on the grid points.

2-7 Analysis Methods

There are two methods of analyzing airborne magnetic data; they are Qualitative and Quantitative analyses. The former is a qualitative speculation of geological features selectively extracted from geomagnetic residual anomalies by means of some filtering procedures. The filters generally used are given as follows:

- (1) Second vertical derivative filter
 - (2) Band-pass filter
 - (3) Strike filter
 - (4) Pseudo-gravity filter
 - (5) Upward or downward continuation filter
 - (6) Auto-correlation analysis
 - (7) Spectrum analysis
- etc.

On the other hand, the latter analysis aims for estimating depths, shapes and magnetic properties of rock bodies inducing magnetic anomalies. The corresponding methods are as follows:

- (1) Specific point method
- (2) Curve matching method
- (3) Specific curve method
- (4) Analytical method

In the present survey, the energy spectrum analysis by two-dimensional Fourier series was applied to the magnetic data obtained over 40 Km of the survey area including Santa Fe. The wave length characteristics of the magnetic

anomalies divided the magnetic indications into three wave length bands. Then, we obtained three kinds of band-pass filter maps from the residual map. Furthermore, the pseudogravity filter procedure was applied to each of the band-pass filter maps. Thus, we finally obtained seven sheets of maps, including the residual map, as the bases of quantitative analyses.

Qualitative computer analyses, based on the residual map, were also made to 23 magnetic profiles running in the NS direction.

The analytical methods used in the present paper are summarized in the following subsection. The flow chart of data processing and analyses is shown in Fig. III-5.

2-7-1 Spectrum Analyses

The wave length characteristics of magnetic anomalies distributed over the survey area is usefully applied to a magnetic analysis through data processing as well as to an estimate of mean depth to magnetic basement by using the potential theory.

(A) Energy Spectrum

An observed value $F(x, y)$ in the rectangular coordinates is expressed in a two-dimensional Fourier series as

$$F(x, y) = \sum_{m=0}^M \sum_{n=0}^N \left(A_{mn} \cos \frac{2m\pi x}{L_1} \cos \frac{2n\pi y}{L_2} + B_{mn} \cos \frac{2m\pi x}{L_1} \sin \frac{2n\pi y}{L_2} + C_{mn} \sin \frac{2m\pi x}{L_1} \cos \frac{2n\pi y}{L_2} + D_{mn} \sin \frac{2m\pi x}{L_1} \sin \frac{2n\pi y}{L_2} \right) \quad (1)$$

Hence, the Fourier coefficient A_{mn} is given by

$$A_{mn} = \frac{4}{L_1 L_2} \int_0^{L_1} \int_0^{L_2} F(x, y) \cos \frac{2m\pi x}{L_1} \cos \frac{2n\pi y}{L_2} dx dy \quad (2)$$

where the data of F are uniformly distributed over an area of $L_1 \times L_2$.

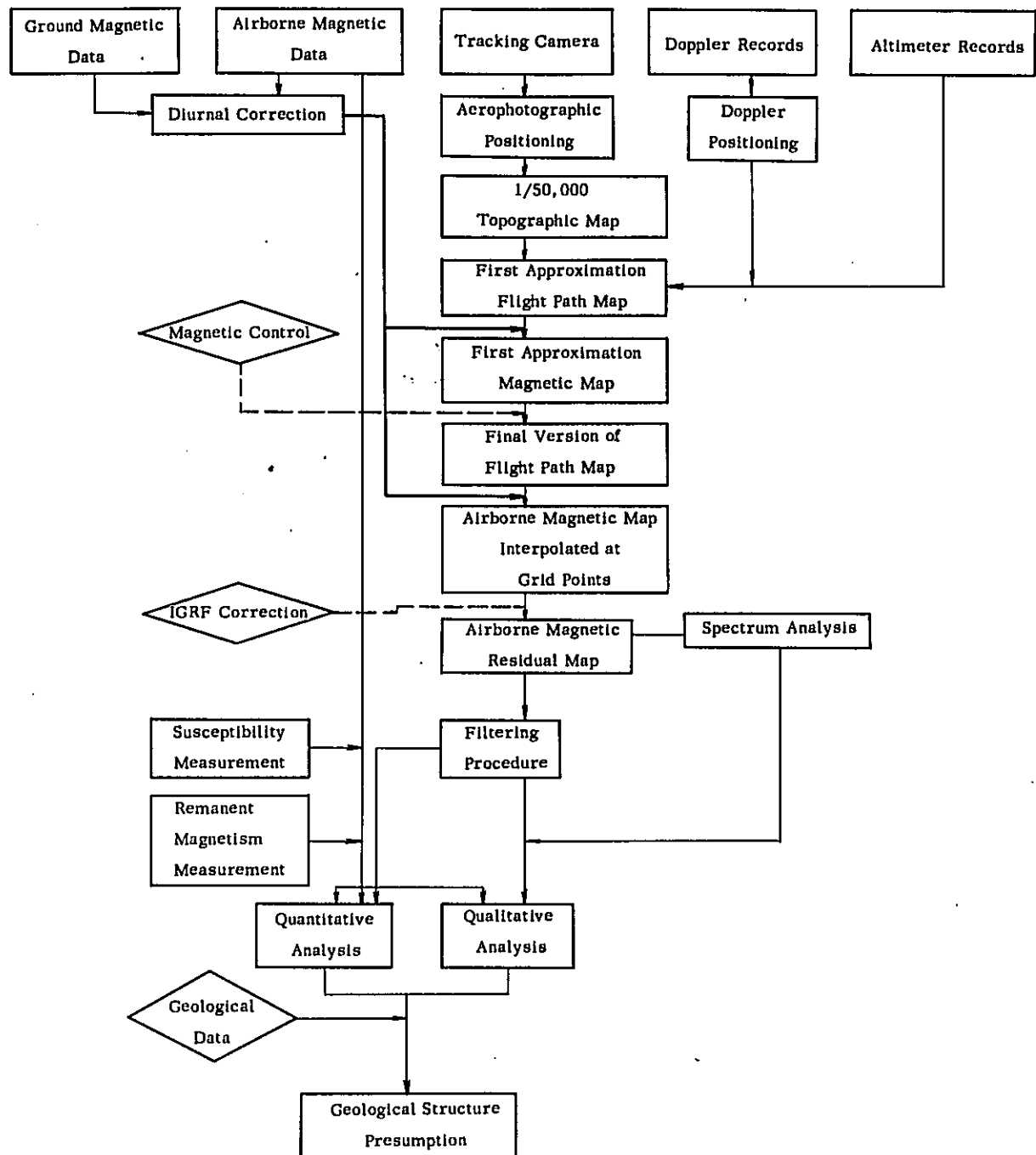


Fig. III-5 Flow Chart of Data Processings and Analyses

Similarly, we can obtain B_{mn} , C_{mn} and D_{mn} . For a computer use, the data of F are given on a rectangular grid with spacings of x and y ; i. e. $F(i, j)$ at the (i, j) th grid point by defining $x = i\Delta x$ and $y = j\Delta y$. Then, Eq. (2) can be rewritten in the form:

$$A_{mn} = \frac{4}{L_1 L_2} \Delta x \Delta y \sum_{i=0}^{L_1/\Delta x} \sum_{j=0}^{L_2/\Delta y} W_{ij} F(i, j) \cos \frac{2m\pi i \Delta x}{L_1} \cos \frac{2n\pi j \Delta y}{L_2} \quad (3)$$

where W_{ij} is the weight function in the two-dimensional trapezoidal rule of numerical integration.

The energy spectrum is then obtained as

$$E_{mn} = A_{mn}^2 + B_{mn}^2 + C_{mn}^2 + D_{mn}^2$$

(B) Estimation of Mean Depth to Magnetic Basement

Suppose that an energy spectrum of magnetic anomalies due to a magnetic layer lying at a depth of H is "white". The potential theory leads the following relation between the energy spectrum E_{mn} of wave numbers (m, n) and H . It is

$$E_{mn} \propto e^{-4\pi H f}$$

where f is a quantity called frequency:

$$f = \sqrt{\left(\frac{m}{L_1}\right)^2 + \left(\frac{n}{L_2}\right)^2}$$

The energy spectrum is plotted in an f vs. $\log E_{mn}$ graph. A straight line is determined by the least square fitting to the plots. Taking Eq. (4) into consideration, H can be estimated from the tangent of the straight line.

2-7-2 Band-pass Filter

The frequency spectrum of a band-pass filter is a deviation between those of two low-pass filters whose cut-off frequencies are different from each other. The frequency spectrum of a low-pass filter with a cut-off frequency of ω_0 is expressed as

$$F(\omega) = \begin{cases} 1 & : |\omega| \leq \omega_0 \\ 0 & : |\omega| > \omega_0 \end{cases} \quad (1)$$

Suppose another low-pass filter with a cut-off frequency of ω'_0 . The difference between these two filters gives the frequency spectrum of a band-pass filter ranging from ω_0 to ω_0 ($\omega_0 \ \omega_0$).

The inverse Fourier transform of a low-pass filter spectrum is

$$\begin{aligned} f(x) &= \frac{1}{2\pi} \int_{-\infty}^{\infty} F(\omega) e^{j\omega x} d\omega \\ &= \frac{1}{2\pi} \int_{-\omega_0}^{\omega_0} F(\omega) e^{j\omega x} d\omega \\ &= \frac{1}{\pi} \int_0^{\omega_0} \cos \omega x d\omega \\ &= \frac{\sin \omega_0 x}{\pi x} \end{aligned} \quad (2)$$

The relation between an input $h(x)$ and the output $g(x)$ is written in a convolution form

$$g(x) = \int_{-\infty}^{\infty} f(x-x') h(x') dx' \quad (3)$$

We assume a filter having a from

$$f(x) = \begin{cases} f(x) & : |x| \leq x_0 \\ 0 & : |x| > x_0 \end{cases} \quad (4)$$

with discrete numbers

$$x = 0, S, 2S, \dots, Ns$$

Eq. (4) is expressed by

$$f_n = f(ns)$$

where s is a spacing of the discrete data.

The Fourier transform of $f(x)$ is then obtained as

$$F(\omega) = \sum_{n=0}^{N-1} \left\{ \int_{ns}^{(n+1)s} f(x) e^{-j\omega x} dx + \int_{-(n+1)s}^{-ns} f(x) e^{-j\omega x} dx \right\}$$

$$= S \sum_{n=0}^N \epsilon_n f_n \cos n \omega s \quad (5)$$

where

$$\epsilon_n = \begin{cases} 1 & n = 0 \text{ or } n = N \\ 2 & n \neq 0, n \neq N \end{cases} \quad (6)$$

The condition of an ideal low-pass filter is to minimize the following integration.

$$I = \int_{-\pi/s}^{\pi/s} \left[\sum_{n=0}^N \epsilon_n f_n \cos n \omega s - \frac{F(\omega)}{S} \right]^2 d\omega \quad (7)$$

By taking derivatives with respect to f_n

$$\frac{\partial I}{\partial f_n} = 0$$

the solution of the above condition is given by

$$f_n = \frac{\sin n \omega_0 s}{n \pi s} \quad (8)$$

For a special case,

$$f_0 = \frac{\omega_0}{\pi} \quad (9)$$

In a two-dimensional case, Eq. (5) is replaced by

$$F(\omega_1, \omega_2) = S^2 \sum_{m=0}^M \sum_{n=0}^N \epsilon_m \epsilon_n f_{mn} \cos m \omega_1 S \cos n \omega_2 S \quad (10)$$

where

$$\epsilon_m = \begin{cases} 1 & : m = 0 \text{ or } m = M \\ 2 & : m \neq 0, m \neq M \end{cases}$$

$$\epsilon_n = \begin{cases} 1 & : n = 0 \text{ or } n = N \\ 2 & : n \neq 0, n \neq N \end{cases} \quad (11)$$

In a fashion similar to (7), we define

$$I = \int_{-\pi/S}^{\pi/S} \int \left\{ \sum_{m=0}^M \sum_{n=0}^N \epsilon_m \epsilon_n f_{mn} \cos m\omega_1 S \cos n\omega_2 S \right\} \frac{F(\omega_1, \omega_2)}{S^2} d\omega_1 d\omega_2 \quad (12)$$

where

$$F(\omega_1, \omega_2) = \begin{cases} 1 & : \quad |\omega_1| \leq \omega_{10}, \quad |\omega_2| \leq \omega_{20} \\ 0 & : \quad |\omega_1| > \omega_{10}, \quad |\omega_2| > \omega_{20} \end{cases} \quad (13)$$

The minimum condition applied to Eq. (12) leads to the following result.

$$\begin{aligned} f_{00} &= \frac{\omega_{10} \omega_{20}}{\pi^2} \\ f_{0n} &= \frac{\omega_{10}}{\pi} \cdot \frac{\sin n \omega_{20} S}{n \pi S} \\ f_{m0} &= \frac{\omega_{20}}{\pi} \cdot \frac{\sin m \omega_{10} S}{m \pi S} \\ f_{nm} &= \frac{\sin m \omega_{10} S}{m \pi S} \cdot \frac{\sin n \omega_{20} S}{n \pi S} \end{aligned} \quad (14)$$

$$f_{mN} = f_{Mn} = f_{MN} = 0$$

For actual computations, we take discrete data h_{mn} , numerically applying h_{mn} and f_{mn} given in Eq. (14) to the convolution Eq. (3). In this case, the frequency spectrum is given by Eq. (10).

The above expressions from (10) to (14) correspond to a two-dimensional low-pass filter. In the case of a two-dimensional band-pass filter, we take another low-pass filter ranging from 0 to M' ($M' < M$) and from 0 to N' ($N' < N$). The difference between the two low-pass filters gives a two-dimensional band-pass filter.

2-7-3 Pseudo-gravity Filter

Magnetic anomaly at the magnetic pole indicates a quantity similar to the first

vertical derivative of gravity. A pseudogravity map shows the magnetic anomaly distribution at a certain dip angle transferred to that at the pole. In a practical computation, $T(x, y)$, anomaly values of the total magnetic intensity are read at a grid point with an interval of 1,000 M in the rectangular coordinates, where the direction of the magnetic north is adopted as the y-axis. Based on the regional tendency $N(x, y)$ calculated by the least squares method from the $T(x, y)$, the residual values at the grid points are obtained as

$$\Delta TR(X, Y) = T(X, Y) - N(X, Y)$$

The pseudogravity values at the rectangular grid points are finally calculated by taking convolution products of $\Delta TR(x, y)$ with weights defined as

$$W^{-1}(x', y') = \frac{1}{2\pi^2 sa} \int_{\frac{1}{N}}^1 \int_{\frac{1}{N}}^1 e^{2\pi h' \sqrt{m^2 + n^2}} \frac{1}{\sqrt{m^2 + n^2}} \cos 2\pi(mx' + ny') dm dn$$

2-8 Magnetic Measurements of Rock Samples

Rock samples, amounting to 57, were sampled from outcrops at the locations as shown in PL. III-1. Magnetic susceptibilities of all the samples were measured by means of a Bison Susceptibility Meter. Remanent magnetisms of 17 samples were also measured by means of a Spinner Magnetometer. The results of these measurements are given in Tables III-1 and III-2.

The mean values of magnetic susceptibility amount to

4629 x 10⁻⁶ cgs emu/cc for 9 andesite samples

4747	"	for 4 basalt	"
2276	"	for 9 diorite	"
539	"	for 11 tuff	"
2080	"	for 4 sandstone	"
378	"	for 3 mudstone	"
13	"	for 3 limestone	"

Table III-1 Susceptibilities of rock samples

Sample No.	Rock	Susceptibility x 10 ⁻⁶ egs emu/cc	Mean Susceptibility x 10 ⁻⁶ egs emu/cc
A - 1	Andesite	4179	
A - 4	Andesite	5790	
A - 6	Andesite	3167	
A - 14	Altered Andesite	3627	
A - 2	Andesite	3356	
A - 15	Andesite	4136	4629
A - 19*	Andesite	52	
B - 4	Andesite	5365	
C - 13*	Andesite	110	
C - 11*	Andesite	26	
D - 5	Altered Andesite	4537	
D - 3	Altered Andesite	7505	
A - 3	Basalt	4736	
A - 5	Dolerite	4544	4747
C - 3	Basalt	2488	
D - 1	Basalt	7221	
A - 13	Granodiorite	1205	
A - 12	Granodiorite	117	
B - 13	Granodiorite	1885	
B - 12	Granodiorite	2965	
B - 14*	Granodiorite	7007	
B - 6	Granodiorite	2334	
C - 2	Granodiorite	1092	2276
D - 2	Quartz Diorite	3135	
B - 8	Diorite	7048	
A - 8*	Diorite Porphyry	1302	
A - 10	Diorite Porphyry	3684	
B - 17*	Diorite Porphyry	11736	
B - 3	Porphyry	2884	

Sample No.	Rock	Susceptibility x 10 ⁻⁶ egs emu/cc	Mean Susceptibility x 10 ⁻⁶ egs emu/cc
C - 1	Dacite	13	
C - 4	Andesitic Tuff	172	
C - 5	Andesitic Tuff	1083	
C - 12	Fine Tuff	293	
C - 10	Fine Tuff	62	
C - 9	Coarse Tuff	8	
C - 6	Tuff Breccia	1768	539
A - 11	Tuff	173	
A - 9	Andesitic Tuff Breccia	215	
A - 17	Andesitic Tuff Breccia	73	
C - 8	Andesitic Tuff Breccia	69	
D - 4	Andesitic Tuff Breccia	2008	
A - 7*	Sandstone	7650	
A - 20	Sandstone	1974	
A - 18*	Sandstone	210	2080
B - 5	Fine Sandstone	1795	
B - 2	Fine Sandstone	2511	
B - 18	Fine Sandstone	2038	
B - 16	Mudstone	636	
B - 15	Mudstone	194	
B - 7	Mudstone	304	378
B - 11	Mudstone	2901	
B - 10	Marl	19	
B - 9	Limestone	14	13
B - 1	Limestone	6	
C - 7	Schist	5340	
D - 7	Schist	34	38
D - 6	Schist	41	
A - 16	Peridotite	1032	

* Excluded from calculation of mean susceptibility

Table III-2 Remanent magnetism of rock samples

Sample No.	Rock	Susceptibility 10 ⁻⁶ cgs emu/cc	Declination deg.	Inclination deg.
A - 8	Diorite Porphyry	1302	9	+ 40
A - 9	Andesitic Tuff Breccia	215	226	- 71
A - 10	Diorite Porphyry	3684	30	- 76
A - 11	Tuff	173	184	+ 15
A - 14	Altered Andesite	3627	186	+ 11
A - 17	Andesitic Tuff Breccia	73	174	- 20
B - 4	Andesite	5365	11	+ 76
B - 6	Granodiorite	2334	30	+ 64
B - 12	Granodiorite	2965	214	+ 72
B - 13	Granodiorite	1885	329	+ 26
B - 14	Granodiorite	7007	306	+ 80
B - 17	Diorite Porphyry	11736	36	+ 71
D - 1	Basalt	7221	232	+ 57
D - 2	Quartz Diorite	3135	1	+ 75
D - 3	Altered Andesite	7505	352	+ 83
D - 5	Altered Andesite	4537	250	- 21
D - 7	Schist	34	nd	nd

5340 x 10⁻⁶cgs emu/cc for 1 schist sample sampled in the northwestern part of the survey area

and 38 " for 2 schist samples sampled in the southern part the survey area.

Taking into account the susceptibility values, the rock samples were classified into Rank A (strongly magnetic rocks), Rank B (intermediately-magnetic rocks), Rank C (weakly magnetic rocks) and Rank D (slightly magnetic rocks). Andesitic and basaltic rocks belong to Rank A, dioritic rocks and sandstone to Rank B, tuffaceous rock and mudstone to Rank C, green-schist and limestone to Rank D.

The porphyry copper type orebodies are presumably associated with the intrusive dioritic rocks in the survey area. The dioritic outcrops are distributed along the geological structural lines. Accordingly, the magnetic survey results may disclose possible geology in association with the structural lines as well as extract areas promising for orebodies from the viewpoint of anomalies in Rank B.

3. Survey Results

The survey area is divided into three parts; Area I, Area II and Area III, as shown in Fig. III-6. For brevity, the magnetic anomalies are classified with these area numbers.

3-1 Residual Map

Judging from the magnetic anomalies shown in the residual map PL. III-1, the magnetic features of the survey area are summarized as follows.

- 1) An outstanding cluster of magnetic anomalies, whose amplitude is larger than 500 gammas with a wave length of about 10 Km, extends for about 40 Km southeastwards from Santa Fe (Area I). The extension changes abruptly its direction into northeast on the province boundary between Nueva Vizcaya and Quezon (Area II), further prolonging the anomalous zone toward the northeast limits of the survey area. It may be presumed that magnetic rocks belonging to Rank A, such as andesitic and basaltic rocks, are extensively distributed over this anomalous zone.
- 2) The northwestern part of the survey area is characterized by an anomaly swarm having amplitudes of 100 to 400 gammas with a wave length of about 3 Km, which possibly indicates scattered, small-scale magnetic sources belonging to Ranks A to C.
- 3) In the northeastern part of Area I, we see a magnetic anomaly having amplitudes of 300 to 700 gammas with a 10 Km wave length. This may be an indication of a magnetic source belonging to Ranks A to B.

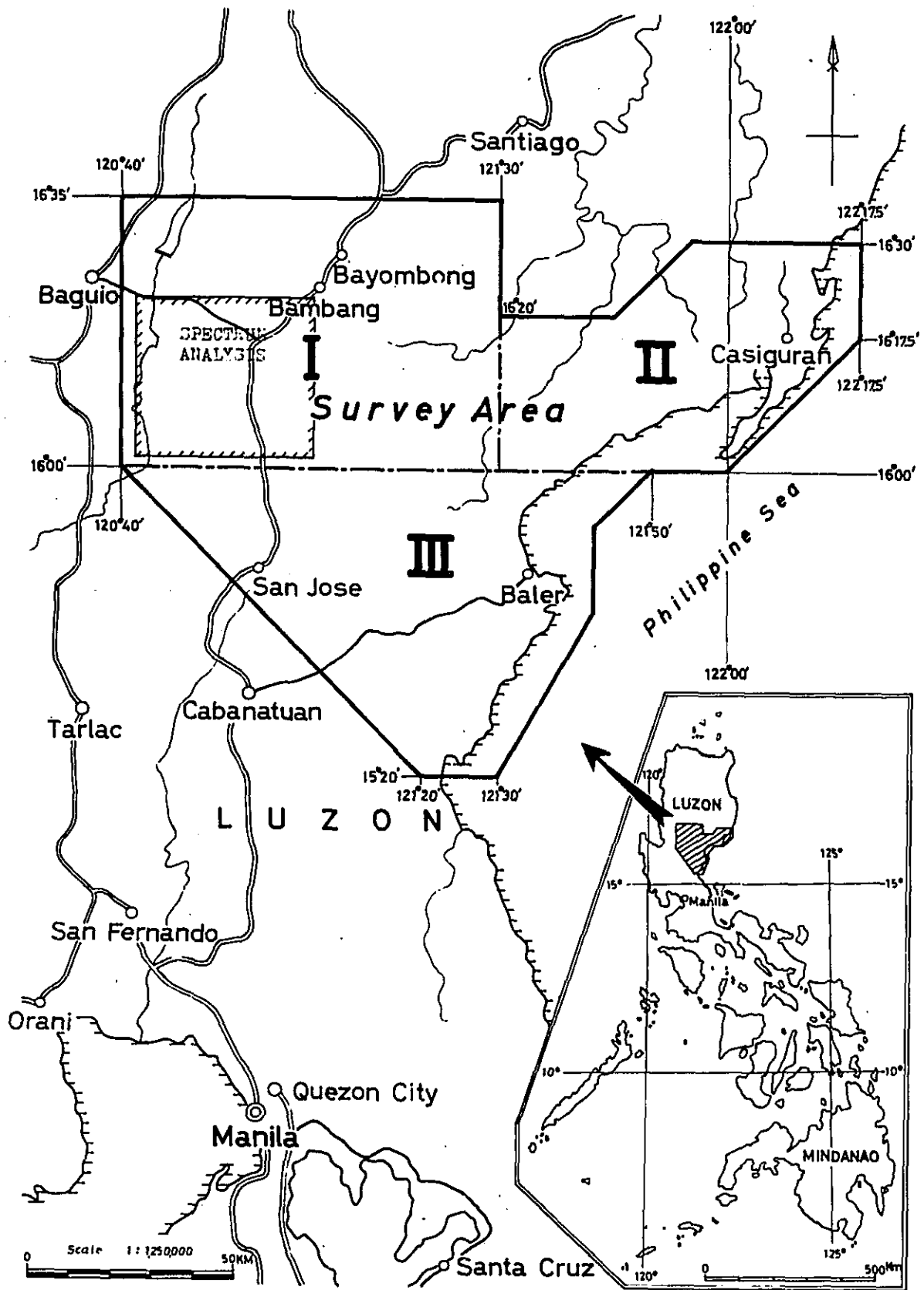


Fig. III-6 Index to survey area

- 4) In the central part of Area I, a gentle-sloped magnetic anomaly having an amplitude of about 300 gammas and a wave length of about 20 Km was recognized and can be represented by an anomalous body ranking among B or C.
- 5) A relatively gently-sloped magnetic anomaly zone with amplitudes of 50 to 150 gammas extends from the southeastern part of Area I to Maddela, the central part of Area II. This zone is presumably an evidence of latent magnetic sources belonging to Rank C and D.
- 6) A magnetic anomaly having an amplitude of about 300 gammas and a wave length of 20 to 30 Km stretches southeastwards along the southwestern margin of Area III. This may indicate a deeply and extensively distributed magnetic source of Rank C or D.
- 7) A positive anomaly zone with amplitude amounting to 600 gammas and a long wave length, (the wave length is about 30 Km), extending northeastwards from Baler Bay to Casiguran Bay, Area III, possibly reflects a deep-seated magnetic source of Ranks B to D.

3-2 Band-pass Maps

Fig. III-7 shows an energy-spectrum analysis result of magnetic anomalies based on the residual map of an area 40 Km NS by 40 Km EW including Santa Fe (Area-I). Judging from the energy-spectrum distribution, the energy-spectrum has a tendency to decrease with an increasing frequency, so that there is no maximum peak in the energy profile. This may imply that the causative magnetic source is almost uniformly distributed from shallow to deep depths.

The frequency domain is divided into four subdomains whose boundary frequencies are 0.5 cycles/Km (i. e. wave length $\lambda = 2$ Km), 0.25 cycles/Km ($\lambda = 4$ Km),

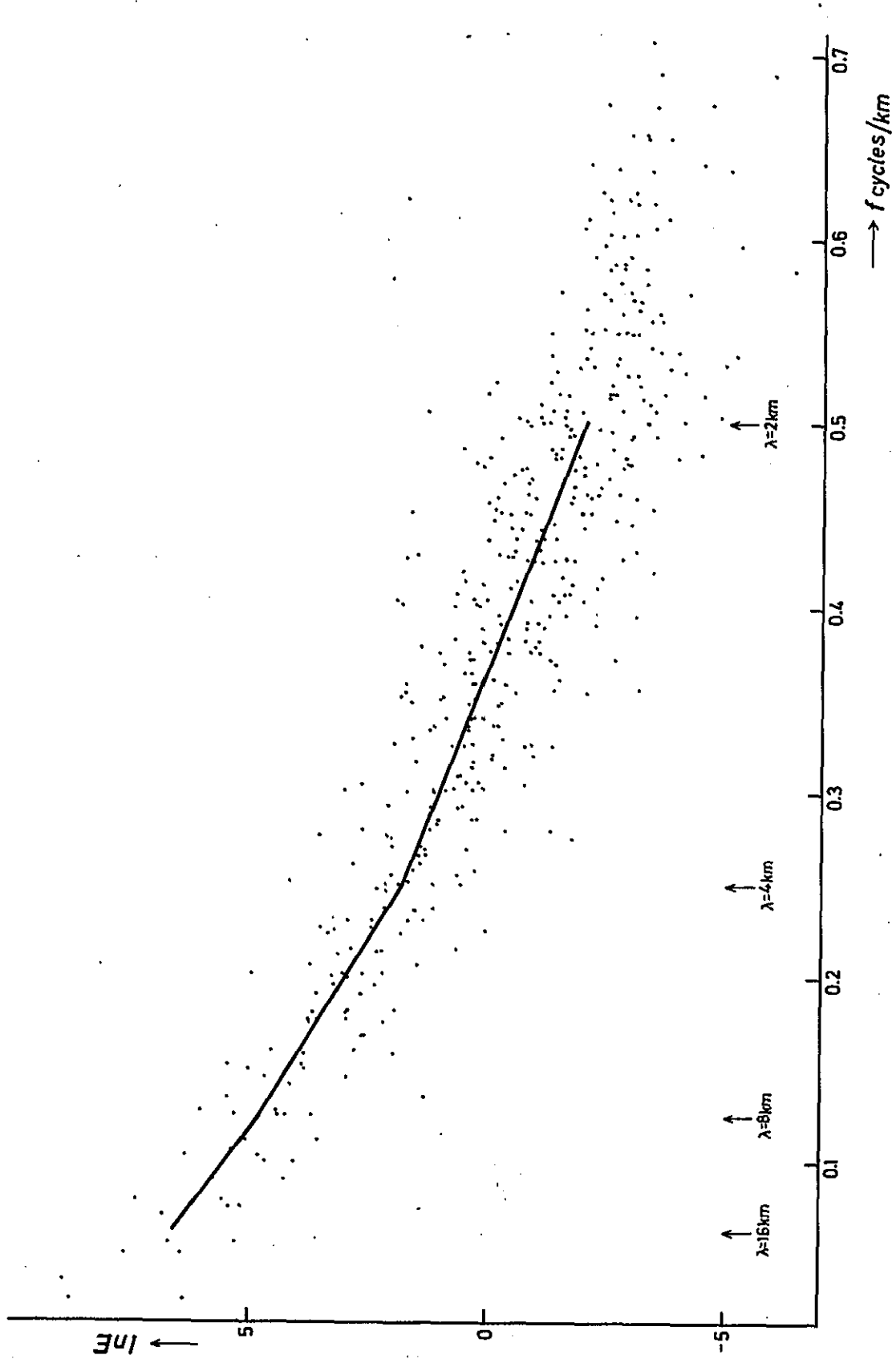


Fig. III-7 Energy spectrum vs. frequency

0.125 cycles/Km ($\lambda = 8$ Km) and 0.0625 cycles/Km ($\lambda = 16$ Km). Straight lines are fitted by the least squares method in each of the subdomains, i. e. 0.5 ~ 0.25 cycles/Km, 0.25 ~ 0.125 cycles/Km and 0.125 ~ 0.0625 cycles/Km. We estimate from the gradients of the straight lines that the depths to the magnetic basement amount to 800 M ASL, 150 M ASL and -400 M ASL, respectively. It is presumed, however, that the frequency domain higher than 0.25 cycles/Km (i. e. wave length shorter than 4 Km) reflects the surface topography, so that the frequency domains lower than 0.25 cycles/Km was adopted to indicate the magnetic basement.

Accordingly, we designed the following three band-pass filters.

- 1) BP-1: Band-pass filter for a frequency domain 0.5 ~ 0.25 cycles/Km (wave length 2 ~ 4 Km).
- 2) BP-2: Band-pass filter for a frequency domain 0.25 ~ 0.125 cycles/Km (wave length 4 ~ 8 Km).
- 3) BP-3: Band-pass filter for a frequency domain 0.125 ~ 0.0625 cycles/Km (wave length 8 ~ 16 Km).

Figs. III-8, III-9 and III-10 show the frequency characteristics of these band-pass filters, which were applied to the residual map to obtain three band-pass maps, BP-1, BP-2 and BP-3.

Judging from the result of energy-spectrum analyses, the band-pass maps, BP-1, BP-2 and BP-3 indicate the magnetic structures between -500 and 500 M, -1000 and 0 M, and -500 and 1,500 M, respectively. Based on these band-pass maps, a qualitative discussion is given below.

3-2-1 Band-pass Map BP-1

Magnetic anomalies with an amplitude of about 200 gammas I-6, III-1, III-3 and III-5 (see PL. III-8) distributed over Santa Fe and Baler are supposed to be due

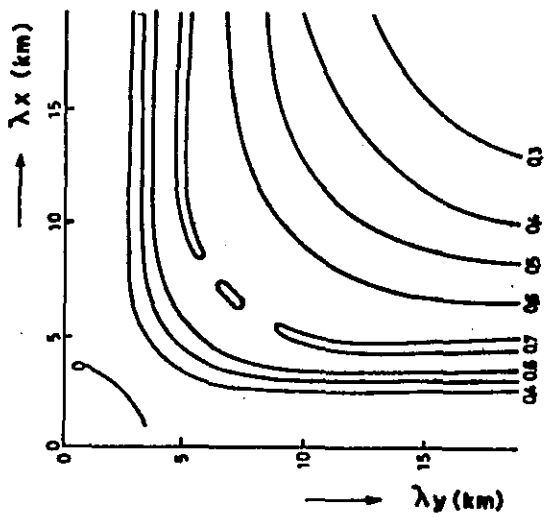


Fig. III-8
Characteristics of
band-pass filter
BP-1

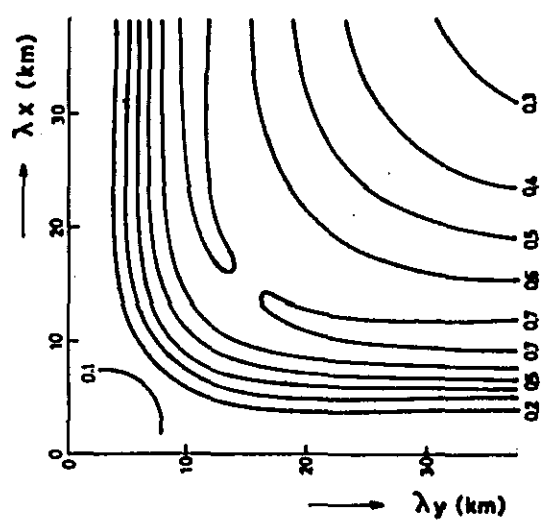


Fig. III-9
Characteristics of
band-pass filter
BP-2

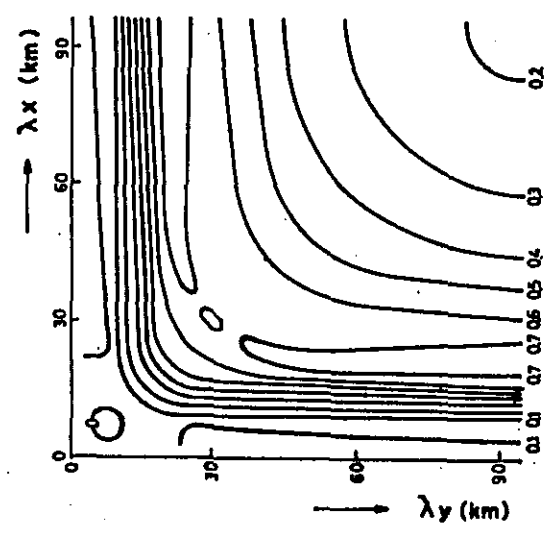


Fig. III-10
Characteristics of
band-pass filter
BP-3

to an extensively large-scale magnetic source of Rank A. In a similar case, there are magnetic anomalies I-11 and I-12 with amplitudes of 300 and 200 gammas, respectively, in the eastern part of Area I.

A group of magnetic anomalies, named "A-Group Magnetic Anomalies," stretches southeastwards up to 75 Km from Santa Fe with a width of about 25 Km including anomalies I-6, III-1, III-3, III-5. "B-Group Magnetic Anomalies" occupy an area of 30 Km by 50 Km including I-11, I-12 and some anomalies northwest of these two anomalies. A group of magnetic anomalies extending with a width of about 20 Km from the southeastern margin of "A-Group Magnetic Anomalies" to the northeastern part of the survey area is called "C-Group Magnetic Anomalies".

The magnetic anomalies belonging to the A, B and C Groups have large amplitudes without exception. It is also recognized that the magnetic anomalies of each group arrange somewhat linearly; the linearity being in the NW-SE direction for A-Group Magnetic Anomalies, mainly in NW-SE direction for B-Group Magnetic Anomalies and in NE-SW direction for C-Group Magnetic Anomalies. The A-C Group contact is at about 20 Km northwest of Baler in the southern part of the survey area.

A narrow zone with a width of about 20 Km, partially located between A and B Groups and partially between B and C Groups, has an amplitude of about 50 gammas and is assumed as a source of Rank C or D.

The magnetic discontinuity as judged from the magnetic anomaly features does not always coincide with geotectonic lines in a geological sense. This is due to the fact that the magnetic discontinuity depends upon susceptibility differences. Taking the above circumstances and the susceptibility measurement results of rock specimens into consideration, a qualitative interpretation is made to the BP-1 Map

as follows.

- 1) A thick deposit of magnetic source of Rank A, composed of andesitic or basaltic rock, is assumed in the area of A-Group Magnetic Anomalies. The main direction of estimated tectonic line is NW-S E.
- 2) In the B-Group area, a deposit of Rank A magnetic source, mainly composed of andesitic or basaltic rock, is presumed. The deposit seems to be thick in the southern part but relatively thin in the northern part. The estimated tectonic line runs in a NW-SE direction.
- 3) In the C Group area, Rank A sources (andesitic or basaltic rock) are distributed over the southern part and northern part of this area. The tectonic line estimated from the magnetic features lies in a NE-SW direction.

3-2-2 Band-pass Map BP-2

A general tendency seen in Map BP-2, as in BP-1, is characterized by large-amplitude magnetic anomalies extending southeastwards from Santa Fe. These correspond to A Group Magnetic Anomalies. In the southern margin of these anomalies, the magnetic linearity changes its direction to northeast, stretching until the northeastern margin of the survey area. The associated anomalies belong to C Group. A magnetic anomaly with an amplitude of 410 gammas is also seen in an area corresponding to B-Group shown in BP-1. Magnetic anomalies I-6, III-1, III-3, III-5 and III-6 having amplitudes larger than 300 gammas are presumed as magnetic sources of Rank A. Magnetic anomalies with amplitudes ranging from 100 to 200 gammas, I-2, I-3, I-4, I-7, I-8, I-9, I-10 and I-12 in Area I, II-2, II-7 and II-9 in Area II, and III-5, III-7, III-9, III-10 and III-11 in Area III, are presumed as magnetic sources of Rank B.

3-2-3 Band-pass Map BP-3

The band-pass procedure corresponding to this map selects preferably a magnetic source deeply embedded between -500 and -1500 M ASL. A NW-SE extension of magnetic anomaly is conspicuously seen in the northwestern part of the survey area, while a NE-SW extension is seen in the eastern part. Being surrounded by these large-scale magnetic anomalies, is seen a gentle-sloped anomaly. The anomaly seems to reflect a basin-like structure. It also seems to continue to the northeastward direction.

The deep geological structure can be speculated on the basis of BP-3 as mentioned below.

- 1) Area I is occupied predominantly by three main structures A, B and B' extending in the direction of NW-SE. As seen in PL. III-10, the structures A and B spread in relation to A- and B-Group Magnetic Anomalies, respectively, which reflect the Rank A sources continuously distributed from shallow to deep down to -1500 M ASL. Magnetic anomalies III-3 and III-5, which are located on the southeastern margin of the A-Group Magnetic Anomalies in BP-1, seem to be stretched from Magnetic Anomaly C in BP-3.
- 2) In the northeastern parts of Area II and Area III, the main structures C and C', which are presumed as Rank A magnetic sources, extend in the NE-SW direction.
- 3) A gentle-sloped magnetic anomaly corresponding to the basin-like structure E, surrounded by the above-mentioned main structures B, B', A, C and C', is located in the central part of the survey area. The magnetic anomaly due to E has an amplitude of 100 gammas or so.

This fact implies that it is unlikely to find any Rank A sources in this region.

3-3 Pseudo-gravity Map

The pseudo-gravity filtering procedures were applied to the above-mentioned band-pass filter maps BP-1, BP-2 and BP-3, to obtain pseudo-gravity maps PG-1 (PL. III-5), PG-2 (PL. III-6) and PG-3 (PL. III-7).

Qualitative interpretations, based on these pseudo-gravity maps, are made as follows.

3-3-1 Pseudo-gravity Map PG-1

This map emphasizes outstanding features of the magnetic sources and lineations of the magnetic-tectonic lines expressed in BP-1. Some lineaments running in a NW-SE direction over the central part of Area I and the western part of Area II, and a similar tendency over the central and western parts of Area III were observed. The direction of the lineaments changes gradually into NS in the north-western part of Area III. NE-SW lineaments appear conspicuously over the eastern part of Area III and the central part of Area II, while a secondary WNW-ESE tendency is predominant over the northeastern part of Area II.

3-3-2 Pseudo-gravity Map PG-2

It is explicitly seen in this map, as shown in BP-1 and BP-2, that one group of magnetic tectonic lines extends in a direction of NW-SE, while another in a direction of NE-SW. The main structure E, which was recognized in BP-3, is also linearly arranged somewhat in a NW-SE direction, which may be indicative of some deep-seated secondary structure.

3-3-3 Pseudo-gravity Map PG-3

There are two mutually-crossing bundles of lineament running NW-SE and

NE-SW in the survey area. A positive pseudo-gravity anomaly coincides with the spread of magnetic source of Rank A as presumed in BP-3. It seems likely that the NW-SE and NE-SW magnetic tectonic lines make the basin-like structure grasped in BP-3.

PL. III-8, III-9 and III-10 show the geological structure qualitatively speculated on the basis of these band-pass and pseudo-gravity maps.

3-4 Quantitative Analyses

We drew 23 NS profiles on the residual map. Depths to magnetic source and its apparent susceptibilities were estimated from data along every profile by two-dimensional automatic computer analyses. In proportion to the obtained susceptibilities, the magnetic intensity of the source is classified into four ranks A, B, C and D, as stated previously in Chapter 2-8.

By means of the quantitative analyses we arrive at the following conclusions:

- 1) Rank A magnetic source is distributed over the central and northeastern parts of Area I and the marginal regions northeast of Area II and Area III.
- 2) Rank B magnetic source is distributed mainly from the central to the western parts of Area I.
- 3) Rank C and D magnetic sources are distributed from the southeastern part of Area I to the southern part of Area III. On the southeastern part of Area I and the northwestern part of Area II, predominant distribution of Rank C magnetic sources are recognized. On the other hand, Rank D source distribution is remarkable over the SW margin of Area I and the southern part of Area III.

PL. III-11 shows the above results synthetically estimated from both the qualitative and the quantitative analyses.

4. Concluding Remarks

Magnetic anomalies in the survey area are classified into four ranks, namely A, B, C and D in proportion to the magnetic intensities of the corresponding courses. In other words, the magnetic anomalies are effects of buried magnetic sources of Rank A (strongly magnetic), Rank B (intermediately magnetic), Rank C (weakly magnetic) and Rank D (slightly magnetic).

According to the susceptibility measurements of rock specimens, andestic and basaltic rocks belong to Rank A, dioritic rock and sandstone to Rank B, tuffaceous rock and mudstone to Rank C, and green-schist and limestone to Rank D.

The results of the survey can be summarized with geological implications as given below.

- 1) Rank D magnetic anomalies are predominantly distributed over the southern part of the survey area, where the ground geological survey recognized the Basement rocks. The Basement Complex outcrops about 40 Km northeast of Baler. According to the qualitative analyses, the magnetic source of Rank A south of Baler has a thickness of 2500 M below the surface (1000 M ASL). The above-mentioned Basement Complex, therefore, becomes deeper to the south, and the depth to the Basement Complex exceeds -1500 M ASL. It tends to crop out again in the southern part of the survey area.
- 2) Rank A magnetic source III-1 is distributed north of Basement Complex outcrops found in the NE part of Baler. The contact between the III-1 and the Basement Complex outcrops coincides with a geotectonic line running in a NW-SE direction. A quantitative analysis estimates that

III-1 has a thickness of about 2,000 M below the ground surface. On the assumption that the bottom of the III-1 makes contact with the Basement Complex, the above geotectonic line is speculated as a dip-slip fault down-thrown 2,000 M in the northeastern side.

- 3) The northwestern extension of the above geotectonic line is interrupted by another line running in an ENE-WSW direction through the northeastern point I-7 of Rank B magnetic source. The former geotectonic line trending in a NW-SE direction extends northwestwards to the west end of magnetic source I-4 along the southwest margin of Rank A magnetic source I-6. According to the quantitative analysis results, the I-6 is estimated to be broadly distributed from the ground surface (1,000 M ASL) down to a depth of 2,000 M; i. e. the depth of the Basement Complex reaches -1,000 M ASL at the I-6 site.
- 4) Geological survey found outcrops of the Basement Complex and tuffaceous rock southwest and south of Rank B magnetic body I-4. We assume that Rank C magnetic source south of I-4 reflects this tuffaceous rock. The Basement-tuffaceous rock contact in the southeast region makes a tectonic line running in an ENE-WSW direction as stated previously. Rank D magnetic source occupies the southeast region of the tectonic line. The quantitative analyses estimate the depth of the magnetic body I-7 as about -1,000 M ASL at its western margin. Assuming that the bottom of the Rank D magnetic body meets with the top of I-7, the thickness of the magnetic body amounts approximately to 1,500 M.

Judging from the above considerations, the depth of the Basement Complex increases southeastwards south of the I-4, and further down to

1,000 M beyond an estimated fault in the NW part of I-7.

- 5) Based on the BP-3, we recognized the main structures A, B, B', C and C' associated with the spatial distribution of deep-seated Rank A magnetic rocks (-500 ~ 1,500 M ASL). It seems likely that these main structures are thick formations of Caraballo Group II mainly consisting of andesitic lava. Among B and B', we recognized Caraballo Group III outcrops, along the synclinal axis which runs in a NW-SE direction.

The main structure E corresponds to the basin-like structure mainly formed of Rank C or D magnetic rocks without Rank A rocks, as presumed in BP-1 and BP-2. It is hardly possible to find a thick Caraballo Group II between the ground surface and -1,500 M ASL.

- 6) In the northwestern part of the survey area, Rank B and C magnetic bodies are predominantly distributed down to -1,500 M ASL. A thick Caraballo Group II may not be distributed there. We see a tectonic line striking NW-SE in the southwestern part of the survey area. The direction of this line changes gradually into NS in the northwestern part. There are many lineaments obliquely crossing the tectonic line at an angle of about 30°.

As a result, the Rank B magnetic sources tend to concentrate into this area concerned. We presume that, the singular distribution of geological lineaments, the Rank B body may consist of dioritic rocks embedded restrictedly by these lineaments.

Based on the above-mentioned considerations, we conclude as follows:

The geological lineation runs in a NW-SE direction in the western part of the survey area but in a NE-SW direction in the eastern part. This tendency is well

consistent with the magnetic lineaments. Many lineaments in the northwestern area are oriented obliquely to some of the NS lineaments. The dioritic formation distribution is limited along these lineaments. Copper porphyry type orebodies are known to be associated with the dioritic intrusions. Therefore, we can conclude that the area limited to Rank B magnetic zones in the northwestern part of the survey area is more promising for the orebodies.

Furthermore, it is suggested that detailed survey including airborne or ground electromagnetic exploration and/or induced polarization prospecting be conducted over the Rank B magnetic zones that have been recognized by the present airborne magnetic survey.

APPENDICES

Table 1. Fossils

Eighteen (18) samples numbered A-12, A-23, A-243, B-13, B-16, B-64, B-70, B-107, B-108, C-72, DF-1, DF-2, DF-3, DF 4, DF-5, DF-6, DF-10 and DF-11 were collected from Caraballo Groups I, II and III. All of them are muddy or sandy rocks but do not contain smaller foraminifera probably due to metamorphism.

Six (6) samples numbered B-102, B-331, C-56, DF-7, DR-20 and DR-77 are coral limestones. No fossils could find in them.

(Larger Foraminifera)

Sample No. A-2

Locality : Cagayan River
 Formation : Mamparang F.
 Species : Eulepidina monstrosa
 E. sp.
 Spiroclypeus leupoldi
 Nephrolepidina parva
 Cycloclypeus sp.
 Operculina sp.
 Gypsina globulus
 G. vesicularis

Geological age : $Te_1 - 4$ (Upper Oligocene)

Sample No. A-3

Locality : Cagayan River
 Formation : Mamparang F.
 Species : Spiroclypeus leupoldi
 Eulepidina monstrosa
 E. sp.
 Borelis philippinensis
 Operculina sp.
 Cycloclypeus sp.
 Heterostegina cf. borneensis

Geological age : $Te_1 - 4$ (Upper Oligocene)

Sample No. A-6

Locality : Cagayan River
 Formation : Mamparang F.
 Species : Eulepidina ehippioides
 Nephrolepidina parva
 Spiroclypeus higginsii
 Cycloclypeus sp.
 Amphistegina radiata

Geological age : $Te_1 - 4$ (Upper Oligocene)

Sample No. A-29

Locality : San Luis River
 Formation : Santa Fe F.
 Species : Flosculinella cf. bontangensis
 Amphistegina radiata
 Austrillina howchini
 Spiroclypeus sp.
 Nephrolepidina sumatrensis

Geological age : Te_5 (Lower Miocene)

Sample No. B-332

Locality : Santa Fe
 Formation : Santa Fe F.
 Species : Amphistegina sp.
 Nephrolepidina sumatrensis
 Flosculinella philippinensis
 Planorbulinella larvata

Geological age : Te_5 (Lower Miocene)

Sample No. B-333

Locality : Santa Fe
 Formation : Santa Fe F.
 Species : Eulepidina sp.
 Cycloclypeus sp.

Geological age : Te_5 (Lower Miocene)

Sample No. B-395

Locality : Aglipay
Formation : Aglipay F.
Species : Operculina sp.
Borelis cf. philippinensis
Nephrolepidina sp.
Gypsina globulus
Geological age : Tf (Middle Miocene)

Sample No. B-401

Locality : Ganano
Formation : Santa Fe F.
Species : Cyclocypeus (Katacylo-
cypeus) annulatus
Miogypsina polymorpha
Amphistegina radiata
Eulepidina sp.
Nephrolepidina sp.
Operculina sp.
Gypsina globulus
Geological age : Te₅ (Lower Miocene)

Sample No. C-57

Locality : Benneng River
Formation : Aglipay F.
Species : Cyclocypeus sp.
Miogypsina polymorpha
Austrotrillina howchini
Amphistegina radiata
Nephrolepidina sp.
Planorbulinella larvata
Gypsina globulus
G. vesicularis
Geological age : Te₅ - Tf (Lower Miocene
-Middle Miocene)

Table 2. Potash-Argon ages on some intrusive rocks

No.	Sample No.	Location	Rock	Mineral	Sample Wt. (g)	k %	$^{40}\text{Ar}/^{40}\text{K}$	Air (%) contamination	Age m.y.
1	A-22	Pacucan R.	Gabbro	hornblende	1.2822	0.07	0.001110	84.78	19
2	A-31	Dibauan R.	Granite	plagioclase	1.4356	0.16	0.002640	79.75	45
3	A-182	Buanad R.	Micro-gabbro	whole rock	1.4760	0.50	0.001740	53.16	30
4	A-200	Ditali R.	Granite	whole rock	1.1140	0.41	0.002527	66.56	43
5	A-201	do.	Gabbro	whole rock	1.2959	0.05	0.002789	85.85	47
6	A-283	Cabatangan R.	Granite	whole rock	1.3034	0.14	0.002643	77.74	45
7	B-35	Smapanuan R.	Gabbro	hornblende	1.1491	0.27	0.001460	62.95	25
8	B-41	Marang R.	Granodiorite	hornblende	1.4007	0.96	0.001600	48.57	27
9	B-93	Sulong R.	Monzonite	biotite	0.5103	5.32	0.001514	23.07	26
10	B-314	Dupax	Granodiorite	hornblende	1.1429	0.59	0.001688	51.76	29
11	B-330	Konkong V.	Granite	biotite	0.5297	4.78	0.001490	16.22	25
12	B-340	Caraballo R.	Diorite	biotite	1.0130	7.10	0.001721	12.70	29
13	B-379	Makati	Porphyrite	whole rock	1.3339	2.57	0.001964	43.96	33
14	C-1D	Pampang R.	Dacite	whole rock	1.1445	1.46	0.000401	77.11	7
15	C-3D	Benneng R.	Diorite aplite	whole rock	1.2468	0.86	0.000529	91.79	9
16	C-4D	do.	Quartz-dolerite	whole rock	1.2224	0.54	0.001597	64.23	27
17	C-6D	do.	Andesite	whole rock	1.4711	0.76	0.000393	81.11	7
18	C-7D	do.	Dacite	whole rock	1.1884	1.26	0.000378	85.04	6
19	D-R7D	Digdig R.	Andesite	hornblende	1.1837	0.50	0.000593	74.23	10
20	PA-14	Dibauan R.	Quartz-diorite	hornblende	1.6269	0.16	0.002909	63.72	49

^{40}Ar R ; radiogenic argon ^{40}Ar ,

$$\lambda_{\epsilon} = 0.585 \times 10^{-10} \text{ yr}^{-1},$$

$$\lambda_{\beta} = 4.72 \times 10^{-10} \text{ yr}^{-1}.$$

$$^{40}\text{K}/\text{K} = 1.19 \times 10^{-2} \text{ atom. \%}$$

Table 3. Microscopic observations

Sample No.	Location	Group or Formation	Rock	Macroscopic features	Microscopic observations	Remarks
Thin Section						
A-1	Cagayan R.	Intrusives	Micro-uraltite gabbro	Fresh, dark gray and compact	Plenocrysts of idiomorphic, zoned and twinned plagioclase (<3mm in length, An 50~An 60, rimmed by albite) and hypidiomorphic clinopyroxene, altered to urtite, occur in a fine grained holocrystalline matrix of the same minerals. Accessories are quartz, magnetite and rutile. A few epidote are also present.	
A-9	do	Mamparang G.	Two-pyroxene basalt	Gray and compact rock with reddish brown patches	Phenocrysts of zoned and twinned plagioclase (0.5~0.1 mm), augite (max 5 mm, mostly 0.5 mm) and hypersthene with reaction rim of clinopyroxene are in a holocrystalline matrix of plagioclase, clinopyroxene, orthopyroxene and magnetite. Calcite replaces augite partially. Iddingsite and yellowish brown clay mineral are secondarily produced.	See PL-III B
A-16	Casignan R.	do	Two-pyroxene basalt	Dark gray, compact	Porphyritic. Idiomorphic plagioclase (<2 mm, An 55), augite (<2 mm) and hypersthene (<2 mm, having sometimes parallel growth with augite) are in a matrix of plagioclath microlites, clinopyroxene, orthopyroxene and magnetite with a pilotaxitic texture. Pale brownish green clay mineral and a few iddingsite are observed.	
A-17	do	do	Two-pyroxene andesite	Dark gray, glassy	Microphenocrysts of zoned plagioclase (<1 mm, An 45), clinopyroxene (<0.5 mm) and orthopyroxene (<0.3 mm, very weak pleochroism) are in a matrix of glass, plagioclase microlites and a few pyroxene with a hyalopilitic texture. No alteration minerals.	
A-18	do	Caraballo G-II	Dacitic pumiceous tuff	Pale green rock with white patch	Pyroclastic texture. Rock fragments of pumice replaced thoroughly by laumontite, and chips of corroded quartz, plagioclase replaced by laumontite and clinopyroxene are in an altered matrix.	
A-19	Tabayong R.	Intrusives	Two-pyroxene dolerite	Dark gray, medium grained, holocrystalline	Holocrystalline. Large plagioclase crystals (2~4 mm) are embedded in a fine grained matrix which is composed of plagioclase (<2 mm, An 50~55), clinopyroxene and orthopyroxene. Magnetite and sphene are also present. Brownish green clay mineral replaces plagioclase and orthopyroxene.	
A-21	do	Caraballo G-II	Augite basalt	Gray, compact and aphyric	A few phenocrysts of plagioclase (<2 mm) and corroded augite (<0.5 mm ZAC = 45°) are observed in a matrix of plagioclase laths (0.1 mm ±), granular clinopyroxene (0.05 mm ±) and magnetite with a basaltic texture. Secondary mineral is chlorite.	

Sample No.	Location	Group or Formation	Rock	Macroscopic features	Microscopic observations	Remarks
A-22A	do	do	Basaltic andesite	Reddish brown, compact, and glassy	Aphyric. Plagioclase laths (0.2 mm \pm in length), prismatic or granular clinopyroxene, magnetite locally altered to hematite and hematite make up a matrix. The texture is trachytic.	
A-22B	do	Intrusives	Two-pyroxene gabbro	Pale gray, medium grained and holocrystalline	Hypidiomorphic-granular texture. The essential minerals are idiomorphic orthopyroxene. A little amount of biotite and reddish brown magnetite are accessories. Uralite, sericite and brownish green clay minerals are produced.	
A-23	Pacuaeo R.	Caraballo G-II	Altered basalt	Dark gray, compact rock with white spots	Phenocrysts of plagioclase, which are less clearly defined by alteration, are enclosed in a matrix of plagioclase laths (0.1~0.2 mm), granular clinopyroxene (0.05 mm \pm) and magnetite with a basaltic texture. Chlorite, prehnite, calcite and epidote are much produced so that the primary texture is not so clear. This rock is similar to A-21 and A-22A.	
A-27	Diteki R.	Caraballo G-II	Altered volcanic rock	Dark green, massive	The rock is composed of epidote, chlorite, mosaic quartz with a undulatory extinction and altered plagioclase. Alteration is too strong to estimate the original rock.	
A-28	do	Intrusives	Gabbro	Greenish gray, holocrystalline	Hypidiomorphic-granular texture. The essential minerals are plagioclase (<5mm) and clinopyroxene which is mostly altered to uraillite. Clinopyroxene and opaque minerals are also produced.	
A-30	San Luis R.	Caraballo G-II	Dacitic tuff	Greenish white	Crystal fragments of corroded quartz, albite, epidote and calcite. From the existence of quartz probably derived from volcanic rocks and the heterogeneous texture, this rock is probably an acidic tuff. There are some parallel laumontite stringers.	
A-31	Bazal R.	Intrusives	Granite	Medium-grained, leucocratic	Hypidiomorphic-granular texture. The essential minerals are hypidiomorphic plagioclase and microcline, and xenomorphic quartz and hornblende. Color index = 10%. A few magnetite and chlorite.	See PL-VA
A-182	Dijanad R.	do	Micro-gabbro	Gray, medium-grained, hard	Similar texture to A-1. Idiomorphic and zoned plagioclase (<3mm, An60 ~An65) and uraillized clinopyroxene are the essential minerals. Magnetite and quartz are accessories. Secondary minerals are uraillite (chiefly tremolite) and calcite.	
A-200	Dibatuman R.	Intrusives	Granite	Medium-grained, leucocratic	Hypidiomorphic-granular texture. The essential minerals are quartz, orthoclase with a perthite texture, zoned plagioclase (<5mm) and hornblende. Chlorite epidote and calcite occur secondarily. C. I. = 10%	
A-201	do	do	Uraillite-gabbro	Medium-grained, melanocratic	Hypidiomorphic-granular texture. Dominant minerals are hypidiomorphic plagioclase (<2mm, An55), clinopyroxene altered to uraillite and magnetite (1~2 mm). A few epidote. C. I. = 50%	

Sample No.	Location	Group or Formation	Rock	Macroscopic features	Microscopic observations	Remarks
A-256A	Matayat R.	do	Pyroxenite	Dark greenish gray, holocrystalline	Olivine, partially serpentinized, is enclosed in interstitial clino-pyroxene (olivine is less than 10%). A little calcite occurs in the rock.	
A-256B	do	do	Peridotite	Brownish black rock with white splashed patterns	The essential minerals are clino-pyroxene, pleochroic ortho-pyroxene and serpentinized olivine. There are some calcite stringers.	See PL-IVA
A-283	Malupa R.	do	Granite	Medium-grained, leucocratic	Mosaic texture consisting heterogeneously of fine - and coarse - grained crystals. The essential minerals are quartz, orthoclase, microcline, plagioclase and hornblende. A little apatite and magnetite. Secondary chlorite, calcite and kaoline are also observed. The constituent minerals are the same as those of A-31 or A-200 but the texture is quite different.	
A-294	do	do	Two-pyroxene gabbro	Coarse-grained, melanocratic	Plagioclase with a lamella twin, uraltitized clino-pyroxene, ortho-pyroxene, with accessory quartz and magnetite, make up this rock.	See PL-IVB
PA-2	Cagayan R.	Manparang G	Basalt	Dark gray, compact rock with tiny, white crystals	Porphyritic. Phenocrysts of zoned and twinned plagioclase and a few clino-pyroxene occur in a holocrystalline matrix of plagioclase laths and clino-pyroxene. A little amount of calcite and pale brownish clay are present.	
PA-7	Casigman R.	Caraballo G-II	Altered andesite	Brownish gray rock with white patches	Phenocrysts of altered plagioclase, quartz and ortho-pyroxene (?) altered thoroughly to clay minerals are in an altered matrix. Pale brownish green clay mineral, sericite and zeolite are observed as secondary minerals.	
PA-9	do	Intrusives	Basalt	Gray, holocrystalline	Porphyritic. Phenocrysts of plagioclase and glomeroporphyritic clino-pyroxene are enclosed in a holocrystalline matrix of plagioclase laths, granular ortho-pyroxene and magnetite. This rock locally shows an ophitic texture. A large part of mafics are altered to chlorite.	See PL-IVC
PA-10	do	Caraballo G-II	Acidic crystal tuff	Greenish gray rock with quartz grains	Clastic texture. Crystal fragments of corroded quartz probably derived from volcanic rock, with angular edges, and prismatic plagioclase are found in an aggregate of felsic minerals. This rock consists of 50% of the crystal fragments with 50% of the matrix.	
PA-14	Bazal R.	Intrusives	Quartz diorite	Medium-grained, holocrystalline C.I. = 35%	The essential minerals are zoned and twinned plagioclase, twinned hornblende and interstitial quartz. Accessories are chloritized biotite and magnetite. A few chlorite and epidote are produced.	See PL-VC
PA-20	Dibutunan R.	Caraballo G-II	Altered andesite	Gray, compact rock with a few pyrite	Phenocrysts of plagioclase (altered partially to calcite and kaoline) quartz and hornblende (altered to chlorite and magnetite) are in a unclearly defined matrix of albitized plagioclase laths, calcite, chlorite and magnetite. There are some vesicles filled with zeolite.	

Sample No.	Location	Group or Formation	Rock	Macroscopic features	Microscopic observations	Remarks
B-4	Casignan R.	Caraballo G-II	Tuffaceous sandstone	Pale green, medium-grained, compact rock with clear bedding	Subrounded particles (0.5 mm ±) are mainly composed of stained quartz with plagioclase, hornblende, augite, hypersthene, sphene and iron ore. Well sorted.	
B-5	do	do	Hornblende-augite andesite	Purplish rock with white and black crystals	Phenocrysts of albitized plagioclase and augite with opacite rims are in a matrix of plagioclase laths, augite, iron ore and apatite with an intersertal texture. A few amount of zeolite.	
B-6	do	do	Altered augite	Dark gray, aphyric and amygdaloidal	A few plagioclase and augite phenocrysts occur in a devitrificated matrix which is composed of albitized plagioclase laths, augite, iron ore and chlorite, with an intergranular texture. There are some amygdaloids filled with chlorite.	See PL-2B
B-9	do	Intrusives	Dolerite	Black, compact	Plagioclase phenocrysts (<4 mm) are enclosed in a holocrystalline matrix of plagioclase laths, augite and greenish brown clay minerals, with an intergranular texture. Some plagioclase in the matrix are rimmed with alkali-feldspar.	
B-14	Munguia R.	Caraballo G-II	Basalt	Black, aphyric	A few phenocrysts of plagioclase (<1 mm, altered to sericite and chlorite) occur in a matrix of plagioclase laths rimmed with alkali-feldspar, augite, iron ore, and brown clay minerals. Texture is intergranular ~ subophitic.	
B-17	do	do	Tuff	Khaki, coarse-grained	Crystal chips of plagioclase pyroxene, opaque mineral and rock fragments of andesite and pumice are cemented by quartz and brown clay mineral. Each particle is 1-2 mm in size.	
B-18	Bendy R.	Intrusives	Granodiorite	Coarse-grained, leucocratic (C.I. = 10)	Subhedral-granular texture. The essential minerals are quartz, K-feldspar and plagioclase are altered to kaoline and sericite. Accessories are apatite, sphene and epidote.	
B-20	do	do	Aplitic granodiorite	Pale orange, microgranitic	The essential minerals are quartz, K-feldspar and plagioclase. A few biotite altered slightly to chlorite and epidote are also observed. The texture is granular and locally graphic.	
B-21	do	do	Augite andesite	Dark blue rock with tinny prismatic crystals	Glomeroporphyritic phenocrysts of augite and plagioclase are in a matrix of plagioclase laths, granular augite, quartz, and chlorite, with an intersertal texture. Some carbonate stringers and laumontite.	
B-23	Diduyon R.	Mamparang G.	Pitchstone	Pale purple rock with pyroxene-needles	Phenocrysts of plagioclase, altered thoroughly to kaoline and zeolite and augite (<2 mm) are in a glassy matrix. Much zeolite are produced.	See PL-III

Sample No.	Location	Group or Formation	Rock	Macroscopic features	Microscopic observations	Remarks
B-27	Campote R.	Intrusives	Diorite porphyry	Dark gray, porphyritic rock	Holocrystalline. Porphyritic texture. Phenocrysts of zoned and twinned plagioclase (<3 mm), hornblende and biotite are in a fine-grained matrix of plagioclase (<0.5 mm) hornblende, biotite and magnetite. A few apatite are present.	
B-29	Malabing R.	Mamparang G.	Acidic tuff	Pale green rock with quartz and plagioclase fragments	Chips of plagioclase, quartz, garnet and spherulite (<4 mm) are cemented by chlorite, magnetite and glassy material. Zeolite and carbonate occur as secondary minerals. Pumice is also present.	
B-30	do	do	Acidic tuff	Pale green, coarse-grained	Chips of plagioclase (replaced by carbonate), glass (<4 mm) and pumice are cemented by less clearly defined glassy material.	
B-32	do	Caraballo G-II	Augite andesite	Gray rock with pyroxene and plagioclase crystals	Phenocrysts of plagioclase (<1.5 mm, altered thoroughly to saussurite) and augite are scattered in a matrix of plagioclase, augite, magnetite, sphene, apatite and glass. A little amount of secondary quartz are also recognized in the matrix.	
B-34	Smapanuan R.	Intrusives	Biotite-hornblende gabbro	Holocrystalline C. I. = 30	The essential minerals are plagioclase, hornblende, augite (cotectic to hornblende), hyperthene, biotite and a few quartz. Accessories are sphene, apatite and magnetite.	See PL-VIA
B-36	do	Basement Complex	Hornblende-augite-schist	Black, schistose	The rock consists of two parts of different mineral assemblage. One is hornblende-quartz-sphene and the other plagioclase-augite-magnetite-quartz. Clear schistosity.	See PL-IA
B-42	Matono R.	Intrusives	Quartz diorite	Leucocratic rock with large hornblende crystals	A Granular texture. The essential minerals are zoned and twinned plagioclase, hornblende and quartz. Accessories are sphene and apatite. A few sericite and chlorite are locally produced.	
B-51	Mapayao R.	Caraballo G-II	Altered andesite	Dark gray rock with amygdals	A few glomeroporphyritic phenocrysts of plagioclase and mafic minerals altered thoroughly to chlorite and calcite occur in a matrix of plagioclase laths, chlorite, epidote, glass and magnetite with an intersertal texture. Most of the plagioclase alter to albite.	
B-53	do	do	Augite andesite	Dark olive, porphyritic	Phenocrysts of twinned plagioclase (andesine) altered to sericite, chlorite and epidote, and augite altered partially to chlorite are in a matrix of plagioclase laths, chlorite, magnetite and brown glass with an intersertal texture. A few sphene are present.	
B-63	do	do	Augite andesite	Dark gray, porous	Some phenocrysts of plagioclase and augite, altered to chlorite and brownish yellow clay are in a hyalopilitic matrix. Plagioclase in the matrix is changed to albite. Accessories are apatite and magnetite.	

Sample No.	Location	Group or Formation	Rock	Macroscopic features	Microscopic observations	Remarks
B-66	Mandaog R.	Intrusives	Hornblende-augite diorite	Dark blue, fine-grained, holocrystalline	A granular texture. The essential minerals are plagioclase (rimmed with alkali-feldspar and partially altered to kaoline), hornblende and augite with accessory apatite, sphene and magnetite. Most of augite are altered to chlorite.	
B-72	do	Caraballo G-III	Dacitic tuff	Pale gray compact rock with pyrite dissemination	Crystal fragments are almost carbonitized or kaolinized. laumontite and sericite occur as the secondary minerals.	
B-75	Mapayao R.	Caraballo G-II	Augite andesite	Dark olive rock with plagioclase phenocrysts	Phenocrysts consist of plagioclase and chloritized augite. They are enclosed by plagioclase microlites, chlorite and brown glass with magnetite. It shows an intersertal texture. A considerable carbonization.	
B-77	do	do	Trachyte	Gray porous rock with pinkish crystals	Phenocrysts of K-feldspar, kaolinized and carbonized plagioclase and few biotite are enclosed in a altered matrix of plagioclase microlite, opaque minerals and glass, with a hyalopilitic texture. Some druses filled with zeolite are present.	
B-82	Sulong R.	Caraballo G-II	Dacitic tuff	Pale green, fine-grained and compact	Very fine-grained quartz, secondary albite, mafic mineral and opaque mineral make up this rock. Most of grains are less than 0.1 mm in size.	
B-93	do	Intrusive	Augite-biotite-hornblende monzonite	Holocrystalline rock with large crystals of hornblende and feldspar	The essential minerals are K-feldspars (more than 60% of the total feldspar), plagioclase, hornblende, biotite and augite. The K-feldspars enclose the rest poikilitically. Accessories are magnetite, apatite and sphene.	See PL-VB
B-96	Dabili R.	Caraballo G-II	Olivine-augite basalt	Black, porphyritic	Phenocrysts of olivine, augite and plagioclase occur in a matrix of plagioclase laths, granular augite, magnetite and brown clay mineral, with an intersertal texture. Augite is idiomorphic ~ hypidiomorphic and is altered to iddingsite with opaque margin. Some druses are filled with brown and fair green clay minerals.	See PL-IC
B-103	Addatan R.	do	Olivine bearing basalt	Black rock with plagioclase crystals	Phenocrysts are plagioclase altered vermicularly and olivine altered thoroughly to green clay minerals. A matrix consists of plagioclase laths, acicular or granular augite, magnetite and chlorite.	
B-105	do	do	Olivine-augite basalt	Dark gray rock with large plagioclase crystals	Phenocrysts of plagioclase (<5 mm An 55 ~ An 60), augite and olivine altered to chlorite are in a matrix of plagioclase laths granular augite, magnetite and brown clay mineral, with an intergranular texture.	
B-311	Casignan R.	do	Andesitic lapilli tuff	Dark green rock with andesitic rock fragments Weak pyrite-dissemination	Rock fragments of porphyritic andesite with an intersertal texture, are cemented with felsic material. Mafic minerals are replaced by chlorite.	

Sample No.	Location	Group or Formation	Rock	Macroscopic features	Microscopic observations	Remarks
B-317	Karuluta R.	Caraballo G-II	Altered basalt	Pale green, aphyric	A few, small phenocrysts of plagioclase and mafic minerals, altered thoroughly to chlorite or calcite, are scattered in a matrix of plagioclase laths and chloritized mafics. Texture is intersertal and locally subophitic.	
B-351	Baan R.	do	Altered andesite	Pale green rock with very weak pyritization	Few tiny phenocrysts of albitized plagioclase are enclosed in a matrix of albitized plagioclase, chlorite, opaque and secondary quartz. Considerably epidotized.	
B-352	do	Intrusive	Diorite	Holocrystalline, medium-grained rock with weak pyrite dissemination	Equigranular texture. The major constituents are twinned, slightly altered andesine, K-feldspar (about 30% of the total feldspar) and hornblende with accessory magnetite and apatite.	
C-1D	Pampang R.	do	Hornblende-biotite dacite	Purplish gray, porphyritic	Phenocrysts of plagioclase with poikilitic hornblende and biotite, corroded quartz, hornblende and biotite occur in a felsic matrix. Mafic minerals are thoroughly replaced by chlorite, calcite or epidote. A little rutile is present.	
C-2D	do	do	Gabbroic dolerite	Greenish gray, medium grained	The essential minerals are plagioclase and unalitized clinopyroxene with an ophitic or granular texture. Uralite, epidote and chlorite are secondarily produced. Ilmenite is also observed.	
C-3D	Benneng R.	do	Diorite-aplite	Gray compact with hornblende needles	A rather even-grained plagioclase and hornblende are associated with a little amount of interstitial quartz and orthoclase. Secondary brownish green clay mineral and calcite are found.	
C-4D	do	do	Gabbroic quartz-dolerite	Greenish gray, fine-grained	Ophitic ~ hyalomorphic granular texture. Sausuritized plagioclase, clinopyroxene with a hourglass texture, interstitial quartz, a little hornblende and magnetite make up this rock. Outer part of clinopyroxene is unalitized. Much chlorite and calcite, and a few epidote are produced.	
C-5D	do	do	Altered micro-diorite	Fine-grained	The main constituent minerals are saussuritized plagioclase, pleochroic hornblende with accessory, chloritized biotite and magnetite. Secondary minerals are much chlorite and uraltite which replaces partially hornblende. Prehnite stringers are developed.	
C-6D	do	do	Augite bearing hornblende-andesite	Gray compact rock with mafic needles	Phenocrysts of hornblende (max = 1 cm in length), plagioclase, and augite are a matrix of plagioclase laths, granular magnetite and altered, interstitial glass, with a hyaloplitic texture. Brown clay mineral and calcite replace the matrix.	
C-7D	Benneng R.	Caraballo G-III	Hornblende-biotite-dacite	Greenish gray, porphyritic	Phenocrysts of twinned and zoned plagioclase, corroded quartz, biotite and altered hornblende are in a fine-grained felsic matrix. Calcite and chlorite mainly replace mafic minerals.	

Sample No.	Location	Group or Formation	Rock	Macroscopic features	Microscopic observations	Remarks
C-1R	Imugan R.	do	Muddy crystal tuff	Dark gray, compact	Rock fragments of mudstone (<2.5 mm) with foraminifera and crystal chips of plagioclase (<0.5 mm), clino-pyroxene, hornblende and quartz are cemented by chlorite and calcite. The texture is well-sorted and clastic.	
C-6R	do	do	Muddy tuff	Gray, compact	Crystal chips of plagioclase, clino-pyroxene and biotite (all of them are 0.1 mm in size) are cemented by chlorite and calcite. This rock is well-sorted and shows a very fine clastic texture.	
C-7R	do	Intrusives	Uralite gabbro	Greenish gray, fine-grained	Hypidiomorphic-granular and locally ophitic. Twinned and zoned plagioclase (<5 mm, An 60) and unalitized clino-pyroxene are the main minerals.	
C-9R	do	Caraballo G-III	Augite (?) basalt	Pale yellowish brown	Variolitic. Phenocrysts of pyroxene, altered thoroughly to yellowish brown clay mineral, occur in a matrix of radiating slender fibers of plagioclase and hematite. Some prehnite, calcite and laumontite stringers are present.	
C-11R	do	do	Glassy andesite	Dark gray, porphyritic	Porphyritic and amygdaloidal texture. Phenocrysts of plagioclase and few clino-pyroxene occur in a matrix of plagioclase microcline and brown glass. There are many amygdaloids filled with prehnite, pumpellyite, calcite and chlorite. A few epidote.	
C-15R	do	Intrusives	Altered dolerite	Yellowish green, banded compact	Strongly epidotized so that the original texture is not clear (probably ophitic). The essential minerals are plagioclase and altered mafic minerals. Much epidote, a few chlorite and fibrous actinolite occur all over this section.	
C-17R	do	Caraballo G-II	Basalt	Dark gray aphyric	A few phenocrysts of plagioclase and unalitized clino-pyroxene are in a matrix of plagioclase, magnetite and chlorite. Some quartz-prehnite stringers are observed.	
C-20R	Panpang R.	Caraballo G-III	Biotite-hornblende-dacite	Pale gray, porphyritic	Porphyritic. Phenocrysts of plagioclase, hornblende, quartz, altered biotite and clino-pyroxene are enclosed in a cryptocrystalline matrix. Apatite, greenish brown clay mineral which replace biotite, and zeolite are present.	
C-22R	do	Intrusives	Dolerite	Greenish gray, compact	The essential minerals are idiomorphic plagioclase and ophitic augite with a few sphene. Chlorite, prehnite and kaolinite are secondarily produced.	
C-24R	Panpang R.	Caraballo G-III	Basalt	Reddish gray, porphyritic	Phenocrysts of plagioclase, replaced vermicularly by kaolinite, are in a matrix of plagioclase laths, granular clino-pyroxene and opaque mineral, with an intergranular texture. There are many amygdaloids which are filled with calcite, prehnite and laumontite. The matrix is partially replaced by chlorite. Hematite is seen along cracks in the plagioclase phenocryst.	

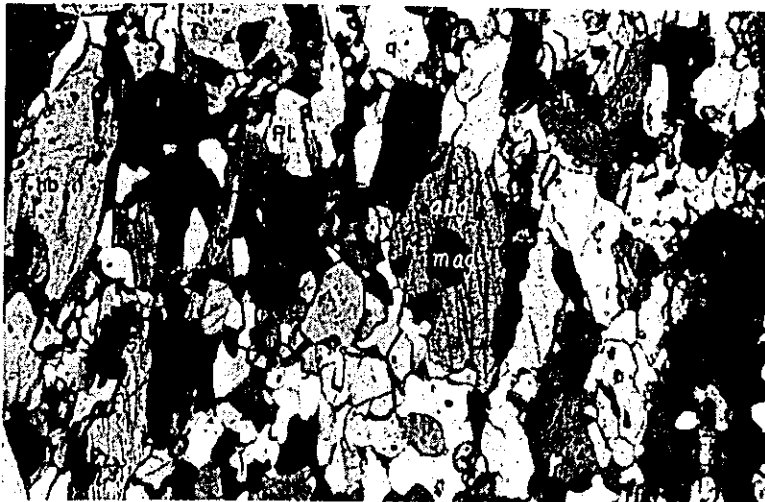
Sample No.	Location	Group or Formation	Rock	Macroscopic features	Microscopic observations	Remarks
C-25R	do	do	Andesitic tuff	Dark greenish gray, compact	This rock is composed of 50% of lithic fragments and 50% of crystal fragments with few matrix, and shows a clastic texture. Lithics : andesite & basalt (both <0.5 mm). Crystals : plagioclase & clinopyroxene (both <0.3 mm). The matrix is replaced by chlorite and plagioclase by kaolinite.	See PL-III A
C-29R	Noso Cr.	do	Basalt	Dark gray, porphyritic	Phenocrysts of plagioclase (<1.5 mm) and clinopyroxene (<0.3 mm) occur in a matrix of plagioclase laths, clinopyroxene and opaque minerals, with an intergranular texture. Secondary minerals are hematite and chlorite.	
C-30R	do	do	Basalt	Dark gray, compact	Saussuritized plagioclase and unalitized clinopyroxene phenocrysts are distributed in a fine matrix of plagioclase laths, acicular clinopyroxene and opaque minerals. Pumpellyite, quartz and albite occur in amygdules. Chlorite is also observed. This rock resembles C-17R in texture.	
C-31R	do	do	Basalt	Gray, porphyritic	Phenocrysts of not so well-defined plagioclase and unalitized clinopyroxene are found in a matrix of plagioclase laths and clinopyroxene. Epidote and laumontite chiefly occur in amygdules. Kaolinite replaces the plagioclase phenocrysts vermicularly. Some chlorite are also present.	
C-34R	Panpang R.	Intrusives	Biotite-hornblende quartz-diorite	Medium grained	Hypidiomorphic-granular texture. The essential minerals are plagioclase (<3mm), hornblende (<1 mm), chloritized biotite and quartz. Plagioclase is partially replaced by kaolinite. A little amount of epidote.	
C-46R	Benneng R.	do	Olivine-dolerite	Black, compact	Large crystals of olivine (<5 mm) occur in a holocrystalline matrix of plagioclase (<2mm) and ophitic clinopyroxene. Clinopyroxene is thoroughly replaced by urtite. Hematite is found along cracks of olivine. Some chlorite.	
C-47R	do	Caraballo G-III	Basalt	Gray, compact	A few smaller phenocrysts of unalitized clinopyroxene are in a matrix of plagioclase laths, clinopyroxene and opaque mineral, with an intergranular texture. Calcite, epidote, prehnite, laumontite and pumpellyite occur in stringers. A little chlorite.	
C-49R	do	do	Muddy tuff	do	Lithic fragments of mudstone and andesite, and cristall chips of plagioclase, quartz, and calcite are cemented by chlorite and calcite. The matrix is very few.	
C-68R	do	do	Basalt	Purplish gray, compact	A few smaller phenocrysts of saussuritized plagioclase (<1 mm) are embedded in a matrix of plagioclase laths (<0.2 mm), carbonized pyroxene and opaque minerals, with an intergranular texture. Chlorite and hematite are also produced. Amygdules are filled with calcite and chlorite.	

Sample No.	Location	Group or Formation	Rock	Macroscopic features	Microscopic observations	Remarks
C-70R	Bolo R.	Caraballo G-III	Muddy tuff	Dark gray, compact	Lithic fragments of mudstone, and crystal chips of plagioclase and quartz are cemented by chlorite, calcite and muddy material. Resemble C-59R.	
C-71R	do	Caraballo G-II	Hornblende-bearing phroxene andesite	Greenish gray, compact	Phenocrysts of saussuritized plagioclase, clino-pyroxene and hornblende are in a matrix of altered glass with plagioclase laths. It shows a hyalopilitic texture. Calcite and chlorite are much procuded. Prehnite is also present in amygdules.	
DR-2	Dingalan	Intrusives	Dolerite	Dark gray, compact	Phenocrysts of twinned plagioclase (less than 3mm in length) and augite (less than 0.7 mm) are in a matrix of twinned plagioclase laths (0.3 mm), granular augite (0.3 mm) partially altered to chlorite, intersertal chlorite and magnetite. The matrix shows an intergranular texture.	
DR-6	East shore	do	Syenite porphyry	Fine grained, pinkish gray	Phenocrysts of euhedral, twinned plagioclase rimmed with alkali-feldspar (less than 5 mm), prismatic augite (C/AZ = 43°, less than 2 mm) and biotite occur in a matrix of alkali-feldspar (less than 2 mm), augite (less than 1 mm) and magnetite. Alkali-feldspar in the matrix is prismatic and shows carlsbad twinning. A few titanite, biotite and apatite are also present.	
DR-7	do	Caraballo G-I	Lapilli tuff	Dark gray tuff with tiny rock fragments	Rock fragments of basalt, andesite, pumice and carbonate are cemented by tuffaceous materials. Basalt is composed of phenocrysts of plagioclase and augite and a matrix of plagioclase laths, granular pyroxene, magnetite and chlorite which fills the amygdules. Andesite is aphyric. There are something like fossil in a carbonate rock.	
DR-8	do	do	Quartz-plagioclase augite-hornblende schist	Dark green, schistose rock with white stripes	HolocrySTALLINE. This rock is composed of quartz, plagioclase, hornblende, augite and sphene and has a schistose texture. Quartz : < 4 mm, irregular form. Plagioclase : altered thoroughly to sericite and chlorite. Hornblende : < 5 mm, subhedral, strong pleochroism (green ~yellowish green), C/AZ = 16°. Augite : < 1 mm subbedral, pale green, C/AZ = 42°. Sphene : < 0.3 mm, brown. Much sphenes are distributed in the hornblende and augite. A few wollastnite stringers (0.2 mm in width).	
DR-9	do	do	Quartz-plagioclase garnet-hornblende schist	Dark gray schistose rock with red garnet and white stringers	HolocrySTALLINE. The rock is principally made up of quartz, plagioclase, hornblende and garnet. Quartz : < 2 mm irregular form. plagioclase: replaced thoroughly by sericite and chlorite. Hornblende : < 1 mm, strong pleochroism (brown yellowish brown) C/AZ = 18°. Garnet : < 7 mm, pale pinkish red, including many quartz and magnetite grains.	See PL-1B
DR-10	Dingalan	Intrusives	Hornblende diorite	Gray, holocrySTALLINE	HolocrySTALLINE. The principal minerals are twinned and zoned plagioclase (< 3 mm), pale green hornblende (< 2 mm, C/AZ = 16°), ilmenite (< 1 mm) and sphene. Epidote grains and zoisite stringers are also present.	

Sample No.	Location	Group or Formation	Rock	Macroscopic feature	Microscopic observations	Remarks
DR-12	Lubingan R.	Basement Complex	Quartz-plagioclase epidote schist	Greenish gray, schistose	This rock contains lenticular quartz (0.01 mm), acicular plagioclase parallel to the schistosity, and granular epidote (<0.2 mm).	
DR-17	do	do	Muscovite-quartz-plagioclase-hematite	Reddish black, schistose	Banded texture. Main components are quartz (<0.5 mm), twinned plagioclase (<0.5 mm) partially altered to sericite, calcite (<1 mm), fibrous hematite and muscovite.	
DR-18	do	do	Quartz-plagioclase-epidote-two mica schist	Greenish gray, schistose	Distinct schistosity. Quartz (<0.02 mm), plagioclase (<0.1 mm), flakes of biotite and muscovite, epidote with accessory sphene and apatite. Quartz-epidote stringers cut the schistosity.	
DR-24	Villa Aurora	Caraballo G-I	Andesitic lapilli	Greenish gray rock with rock fragments	Chips of andesite, quartz and plagioclase are cemented by chlorite. Most of the andesite are aphyric and consist of acicular plagioclase, granular pyroxene and glass.	
DR-25	do	do	Basaltic lapilli tuff	Dark gray rock with fine rock fragments	Rock fragments of basalt and a few andesite are embedded in a few amount of chlorite. Basalt : porphyritic. Abundant phenocrysts consisting of plagioclase and augite (partially altered to celadonite) occur in a matrix of plagioclase laths, granular pyroxene and magnetite. Andesite : porphyritic. Phenocrysts of plagioclase and augite are in a matrix of plagioclase laths, pyroxene and magnetite. Most of the minerals in the matrix are altered to chlorite and calcite.	
DR-26	Villa Aurora	Intrusives	Granophyre	Gray, compact	A few euhedral plagioclase phenocrysts (<3mm) are observed in a matrix of quartz, plagioclase, epidote, zoisite, chlorite and magnetite, with weak parallelism. Quartz grains have irregular forms and show a mosaic texture. Plagioclase laths are less than 0.2 mm in length and are also included in the quartz grains poikilitically.	
DR-30	Dalatan R.	do	Hornblende-quartz diorite	Leucocratic, granitic	Holocrystalline. The essential minerals are anhedral quartz (<2 mm), zoned and twinned plagioclase (idiomorphic ~ hypidiomorphic, 2 mm, partially altered to epidote), hornblende (hypidiomorphic ~ xenomorphic, C/Z = 20° altered to chlorite) and magnetite. Narrow veinlets (1 ~ 2 mm in width) of quartz, hornblende and plagioclase or chlorite are present.	
DR-44	Talavera R.	Caraballo G-II	Augite basalt	Gray rock with mafic crystals	Augite phenocrysts, sometimes in clusters, occur in a matrix of plagioclase laths (<0.2 mm), acicular augite and magnetite, with a flow texture.	
DR-45	do	do	Pyroxene basalt	Gray, compact	A few pyroxene phenocrysts are enclosed in plagioclase laths and granular pyroxene. Texture : intergranular. A weak flow texture is recognizable.	

Sample No.	Location	Group or Formation	Rock	Macroscopic feature	Microscopic observations	Remarks
DR-46	Bunga R.	Intrusives	Quartz bearing hornblende spessartite	Gray, compact	Holocrystalline. All minerals are anhedral. The principal minerals are hornblende (<0.2 mm, pleochroic : green~yellowish green, CAZ = 20°) and twinned plagioclase (<0.4 mm) with a little magnetite, intersertal quartz and sphene. Some epidote veinlets.	
DR-48	Digdig R.	Caraballo G-III	Altered basalt	Dark gray, compact	Phenocrysts of plagioclase (Carlsbad-twinned) occur in a matrix of acicular plagioclase (<0.3 mm, arranged radially), pyroxene altered thoroughly to chlorite, acicular hematite (?) and secondary quartz and chlorite which fill cavities. Calcite and quartz stringers are developed like a network.	
DR-50	do	Basement Complex	Crystalline limestone schist	White, schistose	Finely granulated calcite and quartz (both <0.2 mm) with a distinct schistosity. Same granular chlorite bands also occur in them.	See PL-1C
DR-56	do	Intrusives	Dacite	Reddish gray, porphyritic	Phenocrysts of quartz (with rounded, corroded edges), zoned and twinned plagioclase (<3 mm) and magnetite are distributed in a fine-grained matrix of plagioclase (<0.05 mm), quartz (<0.1 mm), pyroxene and hematite.	
DR-64	do	Caraballo G-I	Quartz-spessartite	Greenish gray, fine-grained	Holocrystalline. The texture is quite similar to DR-46. A few intersertal quartz are present.	
DR-70	do	Intrusives	Biotite-hornblende andesite	Gray, porphyritic	Phenocrysts of zoned and twinned plagioclase with poikilitic hornblende, hornblende (CAZ = 18°) and biotite are scattered in a matrix of plagioclase laths, quartz, magnetite and chlorite. Calcite is recognized as secondary minerals.	
DR-72	do	do	Hornblende-augite	Greenish gray	Dominant minerals are twinned plagioclase (<4 mm, labradolite), hornblende (<6 mm, flexured, altered locally to actinolite and epidote), and augite (with a well-marked parting). An accessory is magnetite.	
DR-75	Puncon R.	Caraballo G-III	Andesitic lapilli tuff	Reddish gray rock with rock fragments	Rock fragments of andesite (<5 mm) and chips of plagioclase and augite are cemented by ferruginous materials. Andesite is porphyritic. Phenocrysts of plagioclase, altered partially to sericite, and clinopyroxene occur in a glassy matrix or a matrix of plagioclase laths, granular pyroxene and magnetite. Generally andesite is affected by silicification.	
DR-81	Daugrug R.	Caraballo G-II	Augite basalt	Black, compact rock with tiny white stringers	Phenocrysts of twinned plagioclase (<1.2 mm, partially altered to chlorite) and augite (<1 mm) are in a fine-grained matrix which is composed of plagioclase laths (<0.2 mm), acicular or granular augite (<0.2 mm), magnetite and chlorite. The texture is intergranular. Some quartz-epidote stringers are present.	

Sample No.	Location	Group or Formation	Rock	Macroscopic features	Microscopic observations	Remarks
DR-82	do	Intrusives	Epidote granophyre	Dark gray, porphyritic	HolocrySTALLINE and porphyritic. Glomeroporphyritic phenocrysts of twinned plagioclase (<1.2 mm) and epidote (<1.5 mm) occur in a matrix of quartz, plagioclase laths, magnetite and chlorite with micrographic texture. Alterations are very weak.	
DR-84	do	do	Porphyritic grano-phyre	Pale greenish, porphyritic	Porphyritic. Similar to DR-82. Phenocrysts of much quartz (<8 mm, with corroded edges) and twinned plagioclase (<6 mm, altered partially to sericite and epidote) are in a micrographic matrix. A few epidote stringers.	
DR-90	Barak R.	do	Quartz-hornblende microdiorite	Dark gray, compact	HolocrySTALLINE. The main minerals are twinned plagioclase (0.3 ~ 2 mm), quartz (<0.5 mm, intersertal to plagioclase), hornblende (<1 mm, C/AZ = 17°) and magnetite (<0.5 mm).	
Polished Section						
C-45	Benneng R.	Intrusives	Diorite			A few pyrite with chalcopyrite are disseminated in an altered diorite or fill its cracks.
C-46	do	do	do			Sphalerite, chalcopyrite and pyrite grains are disseminated in a quartzose matrix.
C-73	Bolo R.	do	do			Fractured chalcopyrites are healed with a gangue.



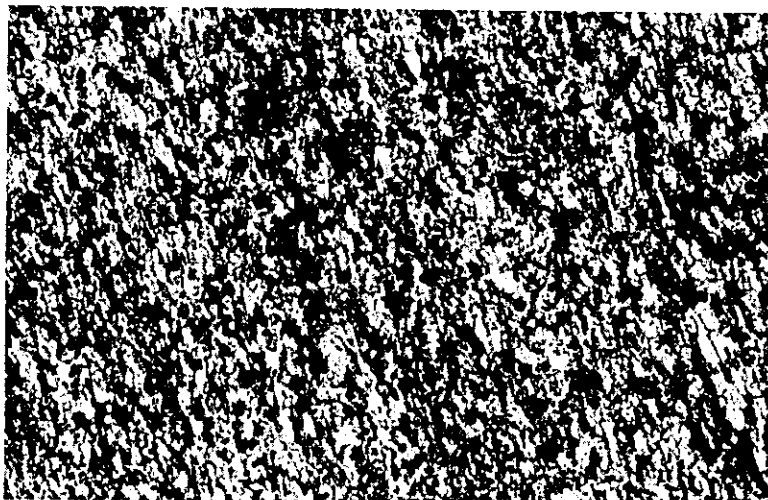
A: Hornblende-augite-schist
 (Sample No. B-36)
 The essential minerals are plagioclase(pl), augite(aug), magnetite (mag) and quartz (q).

x 75



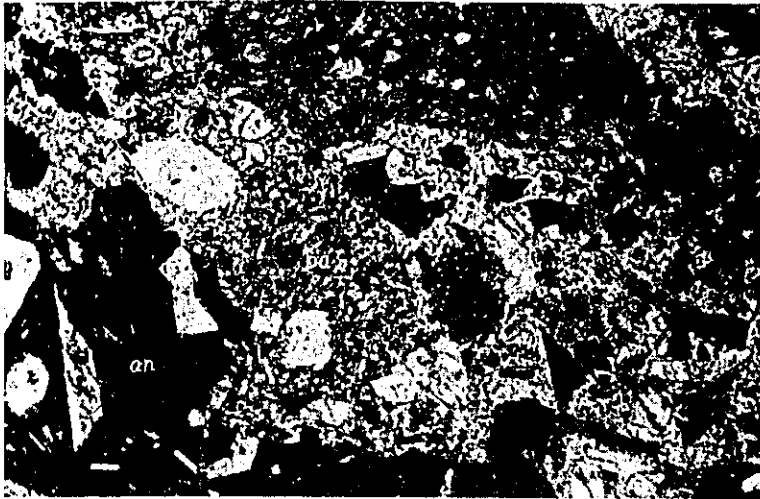
B: Quartz-plagioclase-garnet-hornblende-schist
 (Sample No. DR-9)
 Quartz(q), plagioclase(pl), garnet (gar) and hornblende(hb), make up this rock.

x 50



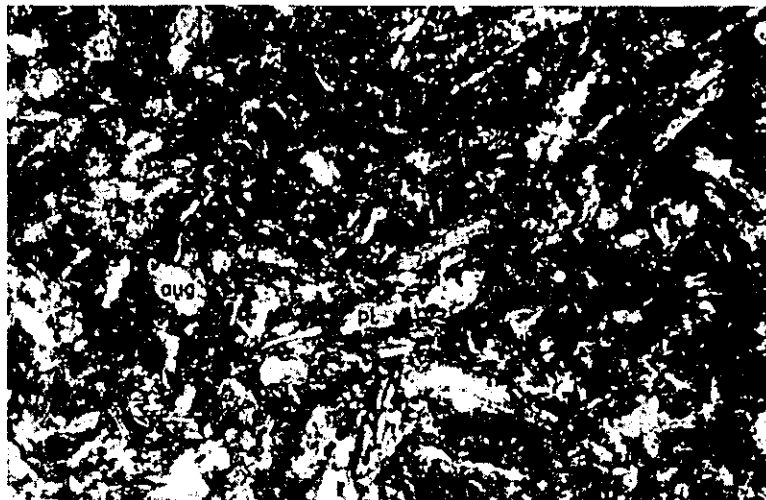
C: Crystalline limestone schist
 (Sample No. DR-50)
 Finely granulated calcite and quartz with a distinct schistosity.

x 75



A: Basaltic lapilli tuff
 (Sample No. DR-25)
 Rock fragments of basalt(ba)
 and a few andesite(an) are cement-
 ed by a few amount of chlorite.

x 75



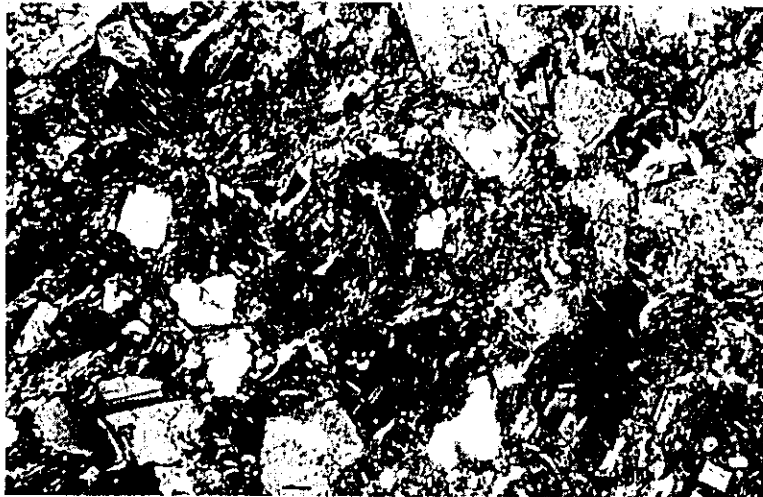
B: Altered augite basalt
 (Sample No. B-7)
 Tiny phenocrysts of plagioc-
 clase(pl) and augite(aug) occur in a
 devitrified matrix.

x 75



C: Olivine augite basalt
 (Sample No. B-96)
 Phenocrysts of plagioclase(pl),
 augite(aug) and olivine(ol) are in a
 matrix.

x 75



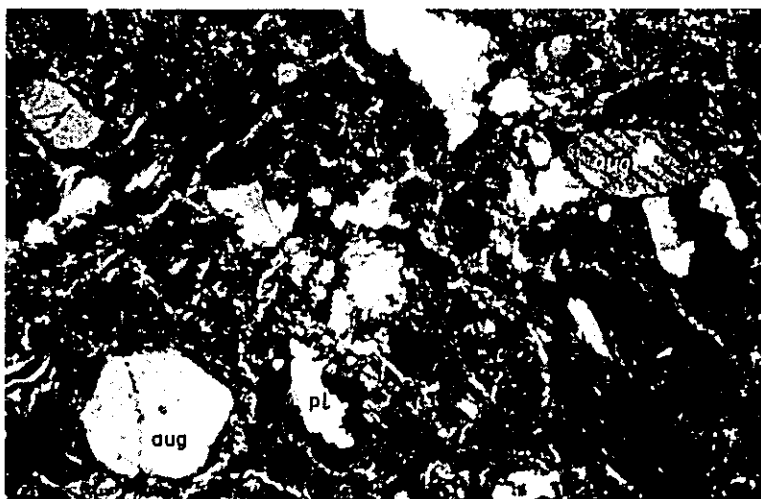
A: Andesitic fine tuff
(Sample No. C-25R)
About 50% of lithic fragments and the rest of crystal chips and few matrix compose this rock.

x 75



B: Two-pyroxene basalt
(Sample No. A-9)
Plagioclase(pl), augite(aug) and hyperthene(hyp) are phenocrysts.

x 75



C: Pitchstone
(Sample No. B-23)
Plagioclase(pl) altered to kaoline and zeolite, and augite(aug) are in a glassy matrix.

x 75

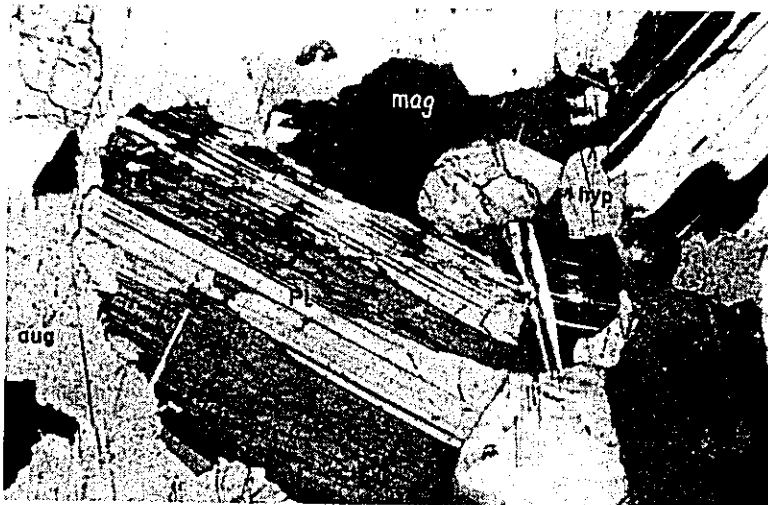


A: Peridotite

(Sample No. A-2568)

The essential minerals are augite (aug), hyperthene (hyp) and serpentine (serp) after olivine.

x 75



B: Two-pyroxene gabbro
(Sample No. A-294)

Plagioclase (pl), augite (aug), hyperthene(hyp) and accessory magnetite (mag).

x 50



C: Augite-basalt
(Sample No. PA-9)

Phenocrysts of plagioclase (pl) and augite (aug) are enclosed in a holocrystalline matrix.

x 75

PL-V



**A: Hornblende granite
(Sample No. A-31)**

The essential minerals are plagioclase (pl), hornblende (hb) and microcline (mic). Some magnetite.

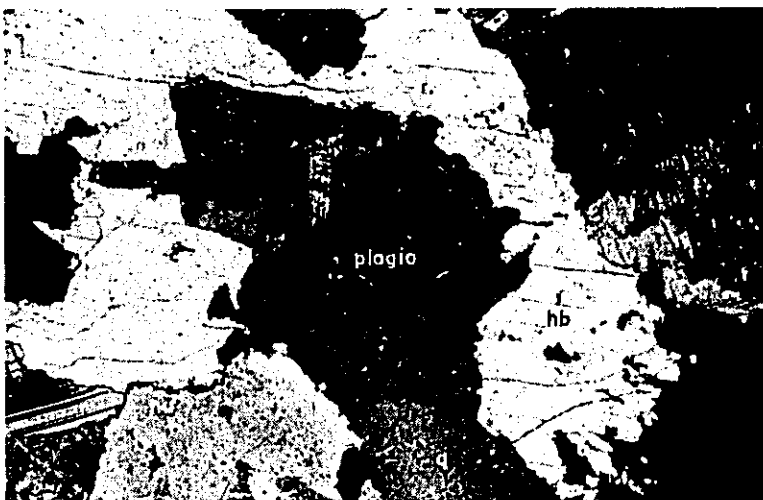
x 75



**B: Monzonite
(Sample No. B-93)**

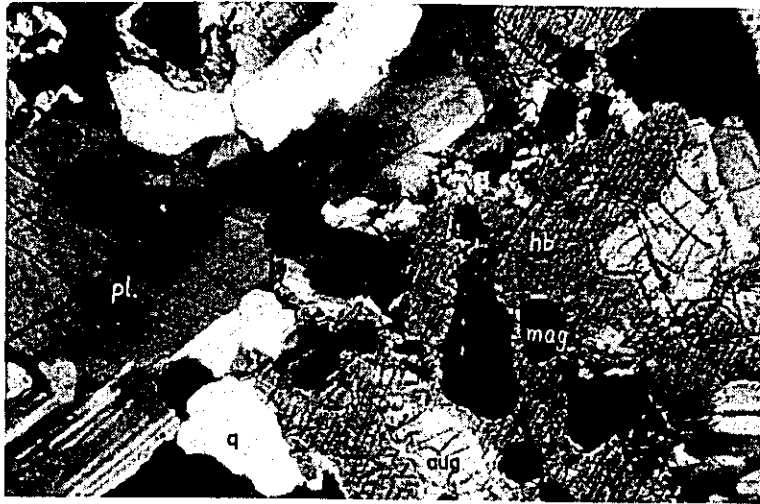
K-feldspar (K-fr), plagioclase (pl) and biotite (bio) are the main components.

x 50



**C: Quartz diorite
(Sample No. PA-14)**
Plagioclase(pl), hornblende(hb) and quartz (q).

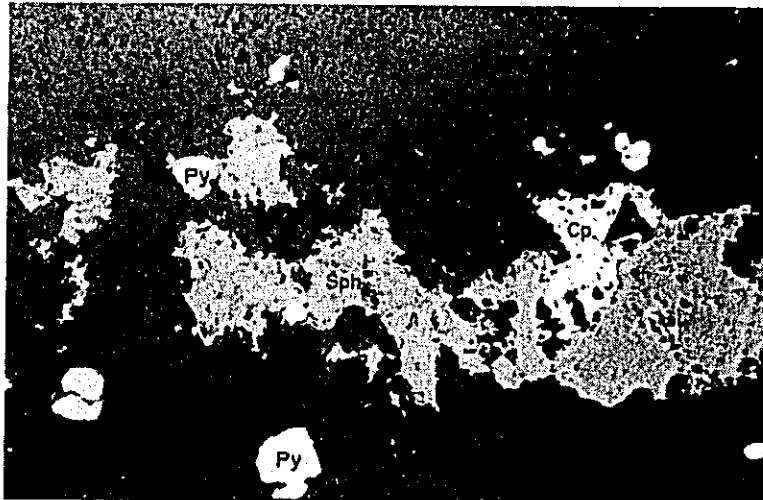
x 75



A: Biotite-hornblende-gabbro
(Sample No. B-34)
Plagioclase(pl), hornblende(hb)
augite (aug), quartz (q) and mag-
netite (mag). A few hyperthen are
out of this field.

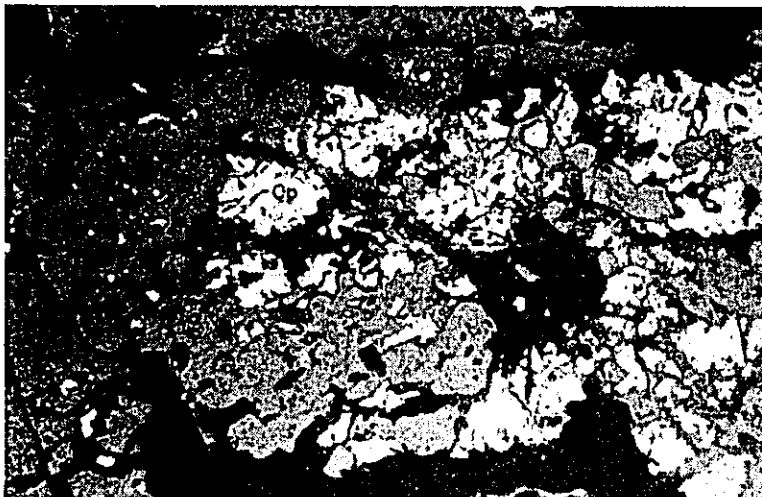
x 50

Ore



B: Sphalerite-chalcopyrite
-pyrite
(Sample No. C-65)
Sphalerite (sph), chalcopyrite
(cp) and pyrite (py).

x 50



C: Chalcopyrite
(Sample No. C-73)
Fractured chalcopyrite (cp).

x 50

Table 4. Chemical analysis of rock samples

(A) Rock

Sample No.	Location	Formation	Rock	SiO ₂	TiO ₂	Al ₂ O ₃	Fe ₂ O ₃	FeO	MnO	MgO	CaO	Na ₂ O	K ₂ O	P ₂ O ₅	H ₂ O	H ₂ O	Total
A-200	Dibutunan R.	Intrusives	Granite	75.15	0.58	11.72	1.68	1.12	0.02	1.00	4.30	3.51	0.50	0.02	0.60	0.27	100.47
PA-14	Bazal R.	do.	Quartz diorite	54.98	0.71	16.89	5.07	2.06	0.01	5.26	9.23	3.86	0.94	0.05	0.69	0.20	100.55
B - 34	Smapanuan R.	do.	Gabbro	51.46	0.85	18.72	3.87	5.83	0.18	5.67	11.11	1.98	0.53	0.07	0.23	0.11	100.61
B - 93	Sulong R.	do.	Monzonite	51.64	0.92	19.10	2.04	2.70	0.03	3.85	7.93	3.40	3.97	0.03	2.92	0.80	99.33
C- 5D	Benneng R.	do.	Micro-diorite	49.03	0.55	19.56	1.94	4.44	0.15	5.64	11.62	3.23	1.09	0.07	2.25	0.34	99.92

(B) Mineralized rock

Sample No.	Location	Rock	Au	Ag	Cu	Mo	S	Remarks
A - 23	Pacucan R.	Altered basalt	-	-	0.01	-	2.10	Weak pyrite dissemination.
B - 26	Campote R.	Porphyritic andesite	-	-	0.01	-	3.12	Weak pyrite dissemination with silicification. Close to a diorite porphyry body.
B - 52	Mapayao R.	Diorite	0.6	-	0.64	-	0.05	Malachite stain along joints.s.
B - 95a	Sulong R.	Porphyritic andesite	0.3	-	0.01	-	6.49	Strong silicification and dissemination. Close to a monzonite body.
B - 119	Maasin R.	Silicified rock	0.2	-	0.13	-	2.01	Strong silicification and dissemination. Very close to a monzonite body.
C - 72	Boto R.	Diorite	0.5	20	0.17	0.02	2.50	North extension of Tawi-Tawi ore deposits.

Table 5. X-ray diffractive analysis

Sample No.	Location	Group or Formation	Rock	Kao	Halloy	Seri	Chl.	Laum	Preh	Qz	Felds	Horn	Cal	Py	Remarks
A-281	Cabatangan R.	Caraballo G-II	Fine grained sandstone		0		0			0	0				Argillized
B-26	Campote R.	do.	Porphyritic andesite			0	0			0	0			0	Silicified and pyritized
B-52	Santa Cruz R.	Intrusives	Diorite	0		0	0			0	0			0	Mineralized
B-95a	Sulong R.	Caraballo G-II	Porphyritic andesite			0				0				0	Strongly silicified
B-119	do.	do.	Andesitic volcanic breccia	0		0				0	0			0	Strongly silicified and phritized
C-50a	Benneng R.	Intrusives	Diorite				0	0	0		0	0			Strongly argillized
C-50b	do.	do.	do.				0	0	0		0	0			Weakly argillized
C-69	Bokod R.	Caraballo G-III	Tuff breccia			0	0			0			0	0	Argillized
DR-58	Digdig R.	Caraballo G-I	do.			0	0			0	0			0	Strongly argillized

Remarks : Kao : Kaolinite Chl : Chlorite Cal : Calcite O : Present
 Halloy: Halloysite Laum: Laumontite Py : Pyrite
 Seri : Sericite Preh : Prehnite Qz : Quartz Felds: Feldspar
 Horn : Hornblende

Table 6. Metal content of geochemical samples

										(ppm)				
Ser. No.	Sample No.	Cu	Zn	Mo	Ser. No.	Sample No.	Cu	Zn	Mo	Ser. No.	Sample No.	Cu	Zn	Mo
1	A - 1	36	281	< 2	56	A - 58	39	256	< 2	111	A - 118	78	244	< 2
2	2	27	115	< 2	57	59	34	129	< 2	112	119	37	77	< 2
3	3	47	281	< 2	58	60	73	205	< 2	113	120	20	56	< 2
4	4	49	409	< 2	59	61	51	307	< 2	114	121	16	192	< 2
5	5	81	256	< 2	60	62	47	281	< 2	115	122	14	64	< 2
6	6	58	230	< 2	61	63	23	256	< 2	116	123	6	77	< 2
7	7	72	153	< 2	62	64	47	205	< 2	117	124	28	72	< 2
8	8	116	435	< 2	63	65	50	154	< 2	118	125	16	95	< 2
9	9	49	102	< 2	64	66	55	205	< 2	119	126	10	154	< 2
10	10	49	435	< 2	65	67	41	244	< 2	120	127	10	92	< 2
11	11	51	230	< 2	66	69	43	218	< 2	121	128	6	78	< 2
12	12	58	205	< 2	67	70	65	90	< 2	122	129	4	29	< 2
13	13	40	153	< 2	68	71	30	128	< 2	123	130	17	44	< 2
14	14	40	230	< 2	69	72	54	169	< 2	124	131	15	20	2
15	15	47	281	< 2	70	74	34	141	< 2	125	132	22	46	4
16	16	58	77	< 2	71	75	46	82	< 2	126	133	13	32	< 2
17	17	67	384	< 2	72	76	43	128	< 2	127	134	22	32	< 2
18	18	49	115	< 2	73	78	39	179	< 2	128	135	7	24	< 2
19	19	67	102	< 2	74	79	50	154	< 2	129	136	20	20	< 2
20	20	81	716	< 2	75	80	44	103	< 2	130	137	23	73	< 2
21	21	60	102	< 2	76	81	65	154	< 2	131	138	37	122	< 2
22	22	58	486	< 2	77	82	117	410	< 2	132	139	16	85	< 2
23	23	41	205	< 2	78	83	157	244	< 2	133	140	30	102	< 2
24	24	41	205	< 2	79	84	57	244	< 2	134	141	21	44	< 2
25	25	43	358	< 2	80	85	83	218	< 2	135	142	27	93	< 2
26	26	47	691	< 2	81	86	100	192	< 2	136	143	28	117	< 2
27	27	56	473	< 2	82	87	61	326	< 2	137	144	32	41	< 2
28	28	77	153	< 2	83	88	63	167	< 2	138	145	37	51	< 2
29	29	62	384	< 2	84	89	30	174	< 2	139	146	66	207	< 2
30	30	60	435	< 2	85	90	98	167	< 2	140	147	33	73	2
31	31	69	153	< 2	86	91	61	90	< 2	141	148	32	98	3
32	32	69	537	< 2	87	93	133	108	< 2	142	149	33	78	< 2
33	33	39	793	< 2	88	95	63	77	< 2	143	150	28	78	< 2
34	35	47	179	< 2	89	96	50	154	< 2	144	151	29	76	< 2
35	37	39	230	< 2	90	97	109	77	< 2	145	152	9	15	< 2
36	38	51	281	< 2	91	98	70	103	< 2	146	154	11	54	< 2
37	39	30	230	< 2	92	99	67	103	< 2	147	154	13	68	< 2
38	40	43	307	< 2	93	100	102	97	< 2	148	155	11	24	< 2
39	41	41	486	< 2	94	101	104	82	< 2	149	156	19	98	< 2
40	42	51	409	< 2	95	102	36	77	< 2	150	157	11	39	< 2
41	43	43	409	< 2	96	103	39	77	< 2	151	158	12	34	< 2
42	44	28	179	< 2	97	104	47	82	< 2	152	159	12	98	< 2
43	45	21	205	< 2	98	105	94	308	< 2	153	160	4	37	< 2
44	46	30	230	< 2	99	106	96	436	< 2	154	161	4	44	< 2
45	47	43	435	< 2	100	107	38	87	< 2	155	162	5	44	< 2
46	48	36	256	< 2	101	108	54	108	< 2	156	163	11	85	< 2
47	49	51	256	< 2	102	109	43	64	< 2	157	164	10	146	< 2
48	50	73	205	< 2	103	110	43	90	< 2	158	165	5	24	6
49	51	13	332	< 2	104	111	135	713	< 2	159	166	4	112	< 2
50	52	58	281	< 2	105	112	87	397	< 2	160	167	27	90	< 2
51	53	54	358	< 2	106	113	113	500	< 2	161	168	3	41	< 2
52	54	34	741	< 2	107	114	48	210	< 2	162	169	5	88	< 2
53	55	47	281	< 2	108	115	33	79	< 2	163	170	3	80	< 2
54	56	34	256	< 2	109	116	83	256	< 2	164	171	12	97	< 2
55	57	34	256	< 2	110	117	33	167	< 2	165	172	5	34	< 2

												(ppm)		
Ser. No.	Sample No.	Cu	Zn	Mo	Ser. No.	Sample No.	Cu	Zn	Mo	Ser. No.	Sample No.	Cu	Zn	Mo
166	A - 173	5	53	< 2	231	A - 239	6	13	< 2	296	A - 308	23	71	< 2
167	174	10	59	< 2	232	240	16	65	< 2	297	309	14	114	< 2
168	175	11	97	< 2	233	241	57	139	< 2	298	310	36	71	< 2
169	176	12	83	< 2	234	242	90	120	< 2	299	311	58	129	< 2
170	177	13	134	< 2	235	243	89	61	< 2	300	B - 2	40	235	< 2
171	178	20	23	< 2	236	244	65	161	< 2	301	3	65	110	< 2
172	179	26	34	< 2	237	245	56	213	< 2	302	4	50	100	< 2
173	180	22	34	< 2	238	246	58	133	< 2	303	5	65	145	< 2
174	181	16	38	< 2	239	247	68	159	< 2	304	6	50	115	< 2
175	182	28	57	< 2	240	248	38	170	< 2	305	8	55	115	< 2
176	183	30	75	< 2	241	249	59	62	< 2	306	10	110	130	< 2
177	184	20	91	< 2	242	250	66	179	< 2	307	11	90	120	< 2
178	185	32	1000	< 2	243	251	48	86	< 2	308	13	70	225	< 2
179	186	49	491	< 2	244	252	15	223	< 2	309	14	45	90	< 2
180	187	33	925	< 2	245	253	7	464	< 2	310	15	55	120	< 2
181	188	48	59	< 2	246	254	9	161	< 2	311	16	35	200	< 2
182	189	186	870	< 6	247	255	12	112	< 2	312	17	45	110	< 2
183	190	33	70	< 2	248	256	9	196	< 2	313	18	40	185	< 2
184	191	31	41	< 2	249	257	5	77	< 2	314	19	45	260	< 2
185	192	20	37	< 2	250	258	7	107	< 2	315	20	49	95	< 2
186	193	43	56	< 2	251	259	19	71	< 2	316	21	125	1165	< 2
187	194	32	74	< 2	252	260	12	98	< 2	317	23	75	250	< 2
188	195	28	74	< 2	253	261	4	107	< 2	318	24	45	85	< 2
189	196	35	59	< 2	254	262	10	54	< 2	319	25	50	130	< 2
190	197	28	106	< 2	255	263	15	89	< 2	320	26	65	105	< 2
191	198	9	31	< 2	256	264	24	54	< 2	321	27	60	440	< 2
192	199	27	48	< 2	257	265	19	41	< 2	322	28	40	120	< 2
193	200	70	65	< 2	258	266	23	36	< 2	323	29	50	205	< 2
194	201	64	56	< 2	259	267	15	34	< 2	324	31	10	35	< 2
195	202	24	22	< 2	260	268	22	62	< 2	325	32	30	35	< 2
196	203	40	52	< 2	261	269	15	45	< 2	326	35	15	45	< 2
197	204	41	46	< 2	262	270	7	34	< 2	327	36	25	65	< 2
198	205	113	104	< 2	263	271	6	36	< 2	328	37	15	105	< 2
199	206	64	59	< 2	264	272	10	61	< 2	329	39	10	35	< 2
200	208	60	93	< 2	265	273	22	57	< 2	330	41	10	25	< 2
201	209	50	93	< 2	266	274	72	107	< 2	331	42	5	15	< 2
202	210	39	65	< 2	267	275	19	36	< 2	332	44	15	30	< 2
203	211	19	78	< 2	268	276	19	32	< 2	333	45	20	50	< 2
204	212	49	65	< 2	269	277	10	39	< 2	334	46	45	95	< 2
205	213	68	69	< 2	270	278	15	42	< 2	335	48	10	20	< 2
206	214	44	24	< 2	271	279	37	38	< 2	336	49	40	80	< 2
207	215	32	41	< 2	272	280	33	45	< 2	337	50	15	45	< 2
208	216	34	28	< 2	273	281	11	32	< 2	338	52	5	30	< 2
209	217	36	46	< 2	274	282	21	64	< 2	339	53	15	40	< 2
210	218	42	11	< 2	275	283	17	48	< 2	340	56	170	155	< 2
211	219	48	56	< 2	276	284	12	49	< 2	341	56	185	400	< 2
212	220	44	50	< 2	277	285	5	32	< 2	342	59	205	230	< 2
213	221	47	102	< 2	278	286	2	34	< 2	343	60	210	715	< 2
214	222	77	78	< 2	279	287	4	32	< 2	344	61	160	415	< 2
215	223	25	33	< 2	280	288	2	27	< 2	345	62	170	400	< 2
216	224	23	31	< 2	281	291	42	89	< 2	346	64	140	415	< 2
217	225	33	56	< 2	282	292	4	43	< 2	347	65	95	190	< 2
218	226	22	89	< 2	283	293	15	29	< 2	348	66	130	275	< 2
219	227	35	56	< 2	284	294	14	46	< 2	349	68	105	245	< 2
220	228	10	30	< 2	285	295	19	50	< 2	350	69	75	180	< 2
221	229	19	39	< 2	286	296	41	84	< 2	351	70	110	500	< 2
222	230	30	30	< 2	287	297	35	98	< 2	352	71	55	165	< 2
223	231	31	65	< 2	288	298	44	134	< 2	353	72	75	440	< 2
224	232	19	57	< 2	289	299	12	54	< 2	354	73	45	190	< 2
225	233	16	111	< 2	290	301	20	143	< 2	355	74	50	135	< 2
226	234	24	139	< 2	291	302	64	89	< 2	356	75	60	120	< 2
227	235	48	185	< 2	292	304	39	129	< 2	357	77	50	125	< 2
228	236	7	41	< 2	293	305	72	107	< 2	358	78	85	115	< 2
229	237	49	83	< 2	294	306	41	89	< 2	359	79	95	105	< 2
230	238	18	78	< 2	295	307	70	98	< 2	360	80	110	130	2

					(ppm)									
Ser. No.	Sample No.	Cu	Zn	Mo	Ser. No.	Sample No.	Cu	Zn	Mo	Ser. No.	Sample No.	Cu	Zn	Mo
361	B - 83	180	275	< 2	426	B - 173	120	335	2	491	B - 354	105	285	< 2
362	84	80	135	< 2	427	174	135	190	< 2	492	356	100	135	< 2
363	85	95	210	< 2	428	175	150	190	3	493	358	75	165	< 2
364	86	90	110	< 2	429	176	140	125	34	494	359	75	210	< 2
365	88	105	115	< 2	430	177	110	140	2	495	360	110	300	< 2
366	89	100	205	< 2	431	178	90	150	2	496	362	135	205	< 2
367	91	55	135	< 2	432	180	85	230	< 2	497	364	195	230	< 2
368	95	45	30	< 2	433	181	60	105	< 2	498	365	195	325	< 2
369	100	40	20	< 2	434	182	70	140	< 2	499	366	175	280	< 2
370	101	40	25	< 2	435	184	65	130	< 2	500	367	160	235	< 2
371	102	40	30	< 2	436	185	95	185	< 2	501	368	215	175	< 2
372	104	45	50	< 2	437	189	75	200	< 2	502	369	190	170	< 2
373	105	50	40	< 2	438	190	80	105	< 2	503	371	245	120	< 2
374	107	50	50	< 2	439	192	85	130	< 2	504	373	240	150	< 2
375	108	45	50	< 2	440	193	90	100	< 2	505	375	200	125	< 2
376	109	25	45	< 2	441	194	95	145	< 2	506	377	230	465	< 2
377	110	30	45	< 2	442	195	80	115	< 2	507	379	170	390	< 2
378	112	15	50	< 2	443	196	130	190	< 2	508	381	245	375	< 2
379	114	35	55	< 2	444	197	70	140	< 2	509	382	180	305	< 2
380	115	20	45	< 2	445	198	125	190	< 2	510	384	190	350	< 2
381	116	30	50	< 2	446	199	45	60	< 2	511	385	20	215	< 2
382	117	40	40	< 2	447	200	110	95	< 2	512	386	175	225	< 2
383	119	40	35	< 2	448	201	115	90	< 2	513	388	80	120	< 2
384	120	45	50	< 2	449	202	110	130	< 2	514	390	125	390	< 2
385	121	35	55	< 2	450	203	130	115	< 2	515	391	115	125	< 2
386	123	20	50	< 2	451	204	85	95	< 2	516	392	90	330	< 2
387	124	50	30	< 2	452	205	110	100	< 2	517	394	140	220	< 2
388	126	60	80	< 2	453	206	100	230	< 2	518	395	150	245	< 2
389	127	50	80	< 2	454	207	95	150	< 2	519	396	170	305	< 2
390	128	60	85	< 2	455	208	85	125	< 2	520	397	130	135	< 2
391	130	40	75	< 2	456	209	110	120	< 2	521	398	75	155	< 2
392	131	20	35	< 2	457	210	70	115	< 2	522	399	95	140	< 2
393	132	40	85	< 2	458	211	60	170	< 2	523	400	110	275	< 2
394	133	90	120	< 2	459	212	85	135	< 2	524	403	145	315	< 2
395	134	60	85	< 2	460	213	115	145	< 2	525	405	45	75	< 2
396	135	40	40	< 2	461	214	95	120	< 2	526	406	45	40	< 2
397	136	195	140	< 2	462	215	50	110	< 2	527	411	45	90	< 2
398	137	20	140	< 2	463	216	50	150	< 2	528	413	55	65	< 2
399	138	105	80	< 2	464	217	55	45	< 2	529	415	25	30	< 2
400	139	200	165	< 2	465	218	70	305	< 2	530	417	25	40	< 2
401	140	65	70	< 2	466	219	55	125	< 2	531	421	25	40	< 2
402	141	90	120	< 2	467	220	55	120	< 2	532	422	20	55	< 2
403	142	80	135	< 2	468	221	55	135	< 2	533	427	65	65	< 2
404	143	355	255	< 2	469	222	50	665	< 2	534	430	110	45	< 2
405	144	610	365	< 3	470	302	65	185	< 2	535	432	60	50	< 2
406	145	245	195	< 2	471	304	60	260	< 2	536	434	75	55	< 2
407	147	105	105	< 2	472	308	45	135	< 2	537	435	75	65	< 2
408	149	180	160	< 3	473	309	75	130	< 2	538	437	60	45	< 2
409	150	160	120	< 2	474	310	35	130	< 2	539	438	95	45	< 2
410	151	175	105	< 4	475	313	30	125	< 2	540	441	20	25	< 2
411	152	205	145	< 4	476	315	30	150	< 2	541	443	405	40	< 2
412	153	90	90	< 2	477	318	50	85	< 2	542	445	55	30	2
413	154	75	225	< 2	478	319	70	105	< 2	543	446	70	55	3
414	156	110	125	< 2	479	320	35	120	< 2	544	447	55	95	< 2
415	157	110	90	< 2	480	323	60	135	< 2	545	450	80	100	< 2
416	159	70	130	< 2	481	324	10	60	< 2	546	451	130	105	4
417	160	54	95	< 2	482	328	25	70	< 2	547	452	65	90	< 2
418	161	40	105	< 2	483	332	15	70	< 2	548	454	205	125	7
419	164	140	170	< 2	484	334	25	70	< 2	549	456	100	120	< 2
420	166	145	140	< 2	485	342	75	160	< 2	550	457	76	73	< 2
421	167	165	140	< 2	486	344	55	120	< 2	551	459	52	66	< 2
422	168	85	150	< 2	487	348	50	140	< 2	552	461	80	75	< 2
423	169	100	215	10	488	350	30	115	< 2	553	462	71	69	< 2
424	171	90	150	5	489	352	40	105	< 2	554	463	84	66	< 2
425	172	125	275	2	490	353	80	60	< 2	555	465	49	61	< 2

(ppm)														
Ser. No.	Sample No.	Cu	Zn	Mo	Ser. No.	Sample No.	Cu	Zn	Mo	Ser. No.	Sample No.	Cu	Zn	Mo
556	B - 467	39	68	< 2	621	C - 22	39	176	< 2	686	C - 122	39	101	< 2
557	469	44	63	< 2	622	23	65	139	< 2	687	124	39	70	< 2
558	470	77	63	< 2	623	24	64	111	< 2	688	126	37	101	< 2
559	471	73	79	< 2	624	25	42	74	< 2	689	128	37	103	< 2
560	477	56	39	< 2	625	26	56	130	< 2	690	130	32	99	< 2
561	481	70	50	< 2	626	27	46	81	< 2	691	132	37	84	< 2
562	483	75	20	< 2	627	28	48	131	< 2	692	134	34	125	< 2
563	485	91	57	< 2	628	29	66	115	< 2	693	136	45	70	< 2
564	487	77	57	< 2	629	30	40	157	< 2	694	138	39	101	< 2
565	488	47	21	< 2	630	31	45	152	< 2	695	140	41	174	< 2
566	490	34	60	< 2	631	32	78	130	< 2	696	142	41	90	< 2
567	491	75	57	< 2	632	33	46	120	< 2	697	144	47	99	< 2
568	492	53	59	< 2	633	34	54	93	< 2	698	146	30	209	< 2
569	494	103	110	< 2	634	35	60	107	< 2	699	148	37	157	< 2
570	495	97	71	< 2	635	36	62	70	< 2	700	150	47	122	< 2
571	496	99	56	< 2	636	37	76	111	< 2	701	152	37	115	< 2
572	497	67	109	< 2	637	38	47	143	< 2	702	154	47	89	< 2
573	498	79	139	< 2	638	39	29	52	< 2	703	157	39	87	< 2
574	499	62	203	< 2	639	40	51	124	< 2	704	159	43	160	< 2
575	500	66	168	< 2	640	41	38	102	< 2	705	160	47	78	2
576	501	40	94	< 2	641	42	52	148	< 2	706	161	43	330	< 2
577	502	71	78	< 2	642	43	48	148	< 2	707	162	20	52	< 2
578	505	58	94	< 2	643	44	1819	944	< 2	708	163	36	84	< 2
579	506	54	94	< 2	644	45	64	176	< 2	709	164	36	66	< 2
580	508	77	94	< 2	645	46	41	157	< 2	710	166	34	87	< 2
581	509	23	70	< 2	646	47	48	120	< 2	711	168	36	70	< 2
582	512	37	85	< 2	647	48	59	115	< 2	712	170	32	108	< 2
583	514	25	72	< 2	648	49	37	200	< 2	713	172	30	87	< 2
584	515	75	89	< 5	649	50	33	98	< 2	714	174	37	139	< 2
585	516	66	83	< 2	650	52	37	102	< 2	715	176	24	54	< 2
586	517	40	68	< 2	651	54	51	126	< 2	716	178	39	66	< 2
587	518	61	82	< 2	652	56	44	120	< 2	717	180	22	44	< 2
588	521	93	86	< 2	653	58	34	126	< 2	718	182	36	52	< 2
589	525	99	86	< 2	654	60	58	93	< 2	719	184	21	30	< 2
590	526	84	86	< 2	655	62	50	130	< 2	720	186	24	52	< 2
591	527	87	79	< 2	656	64	38	102	< 2	721	188	32	57	< 2
592	530	68	85	< 2	657	66	38	93	< 2	722	189	41	73	< 2
593	536	62	84	< 2	658	68	31	115	< 2	723	190	27	50	< 2
594	537	43	97	< 2	659	70	45	107	< 2	724	192	28	50	< 2
595	538	126	82	< 2	660	72	49	102	< 2	725	194	24	6	< 2
596	540	61	77	< 2	661	74	91	37	< 2	726	196	32	62	< 2
597	541	82	90	< 2	662	76	39	80	< 2	727	198	30	68	< 2
598	542	67	90	< 2	663	78	26	87	< 2	728	200	30	68	< 2
599	543	81	98	< 2	664	80	43	85	< 2	729	202	35	71	< 2
600	C - 1	54	124	< 2	665	82	49	83	< 2	730	204	28	45	< 2
601	2	25	296	< 2	666	84	75	45	3	731	206	32	50	< 2
602	3	33	130	< 2	667	86	46	78	< 2	732	207	34	59	< 2
603	4	113	133	< 2	668	88	39	90	< 2	733	208	29	71	< 2
604	5	72	111	< 2	669	90	45	84	< 2	734	209	64	73	< 2
605	6	38	189	< 2	670	92	51	87	< 2	735	210	78	86	< 2
606	7	89	115	< 2	671	94	59	73	< 2	736	212	36	71	< 2
607	8	98	89	< 2	672	96	43	77	< 2	737	213	188	268	3
608	9	41	1313	< 2	673	98	43	87	< 2	738	215	16	54	< 2
609	10	41	111	< 2	674	100	51	87	< 2	739	216	47	107	< 2
610	11	47	93	< 2	675	102	40	70	< 2	740	217	54	70	< 2
611	12	51	130	< 2	676	104	57	61	< 2	741	218	22	39	< 2
612	13	107	148	< 2	677	106	63	66	< 2	742	220	47	52	< 2
613	14	56	83	< 2	678	108	36	78	< 2	743	222	34	32	< 2
614	15	57	126	< 2	679	110	51	82	< 2	744	224	40	89	< 2
615	16	44	93	< 2	680	112	39	108	< 2	745	226	66	107	< 2
616	17	60	111	< 2	681	114	47	104	< 2	746	227	32	64	< 2
617	18	45	89	< 2	682	116	37	101	< 2	747	229	56	111	< 2
618	19	63	96	< 2	683	118	43	104	< 2	748	231	42	39	< 2
619	20	40	52	< 2	684	120	47	84	< 2	749	233	32	45	< 2
620	21	48	207	< 2	685	121	34	104	< 2	750	235	140	223	2

					(ppm)									
Ser. No.	Sample No.	Cu	Zn	Mo	Ser. No.	Sample No.	Cu	Zn	Mo	Ser. No.	Sample No.	Cu	Zn	Mo
751	C - 237	33	161	< 2	816	D - 17	75	70	< 2	881	D - 105	40	60	< 2
752	239	34	98	< 2	817	18	68	88	< 2	882	106	42	60	< 2
753	241	51	93	< 2	818	19	72	75	< 2	883	107	95	54	< 2
754	243	37	107	< 2	819	21	58	75	< 2	884	108	42	38	< 2
755	245	52	125	< 2	820	22	50	50	< 2	885	109	35	32	< 2
756	247	56	71	< 2	821	23	68	78	< 2	886	110	50	66	< 2
757	249	45	164	< 2	822	24	68	78	< 2	887	111	45	70	< 2
758	251	48	129	< 2	823	25	72	75	< 2	888	115	35	28	< 2
759	253	51	118	< 2	824	26	66	75	< 2	889	118	50	49	< 2
760	255	47	125	< 2	825	27	78	90	< 2	890	122	50	76	< 2
761	257	48	77	< 2	826	28	66	98	< 2	891	124	60	54	< 2
762	259	48	125	< 2	827	29	52	107	< 2	892	125	75	57	< 2
763	261	84	59	< 2	828	30	62	73	< 2	893	131	45	64	< 2
764	263	49	134	< 2	829	31	65	64	< 2	894	134	45	64	< 2
765	265	37	154	< 2	830	32	60	75	< 2	895	136	45	60	< 2
766	267	52	107	< 2	831	33	50	70	< 2	896	137	40	57	< 2
767	269	38	121	< 2	832	34	60	66	< 2	897	139	40	70	< 2
768	271	48	157	< 2	833	35	56	57	< 2	898	141	30	23	< 2
769	273	46	89	< 2	834	36	60	64	< 2	899	143	45	72	< 2
770	274	47	98	< 2	835	38	54	55	< 2	900	147	44	44	< 2
771	276	47	179	< 2	836	39	60	72	< 2	901	150	42	53	< 2
772	278	50	136	< 2	837	40	88	60	< 2	902	152	60	92	< 2
773	280	52	107	< 2	838	41	40	58	< 2	903	155	35	18	< 2
774	282	62	125	< 2	839	42	72	55	< 2	904	158	40	23	< 2
775	284	52	116	< 2	840	43	58	53	< 2	905	160	40	69	< 2
776	286	36	286	< 2	841	44	60	53	< 2	906	162	50	41	< 2
777	288	46	87	< 2	842	46	26	37	< 2	907	165	45	61	< 2
778	290	46	121	< 2	843	47	28	44	< 2	908	166	25	28	2
779	292	49	105	< 2	844	48	38	48	< 2	909	169	45	60	< 2
780	294	51	98	< 2	845	49	38	48	< 2	910	171	147	247	< 2
781	296	40	75	< 2	846	50	30	44	< 2	911	172	55	157	< 2
782	298	52	119	< 2	847	51	46	63	< 2	912	173	25	78	< 2
783	300	40	170	< 2	848	53	55	58	< 2	913	175	82	184	< 2
784	302	46	121	< 2	849	54	56	55	< 2	914	176	52	129	< 2
785	304	84	107	< 2	850	55	34	52	< 2	915	179	60	170	< 2
786	305	54	130	< 2	851	58	48	52	< 2	916	180	42	101	< 2
787	306	70	104	< 2	852	61	56	63	< 2	917	183	72	175	< 2
788	307	33	143	< 2	853	62	60	58	< 2	918	184	48	72	2
789	310	82	125	< 4	854	64	80	58	< 2	919	188	55	122	< 2
790	311	36	170	< 2	855	65	62	46	< 2	920	189	40	97	< 2
791	313	36	205	< 2	856	67	78	40	< 2	921	190	45	42	< 2
792	315	80	139	< 6	857	70	62	71	< 2	922	192	42	101	< 2
793	317	40	121	< 2	858	71	52	64	< 2	923	194	45	87	< 2
794	319	51	143	< 2	859	72	46	64	< 2	924	196	52	57	< 2
795	321	48	152	< 2	860	73	48	91	< 2	925	198	45	72	< 2
796	323	188	1446	< 2	861	75	62	65	< 2	926	202	35	30	< 2
797	325	64	232	< 2	862	76	50	81	< 2	927	203	60	59	< 2
798	327	36	250	< 2	863	78	104	43	< 2	928	204	71	60	< 2
799	329	592	1018	< 14	864	79	112	68	< 2	929	208	20	22	< 2
800	331	1184	241	< 20	865	82	92	55	< 2	930	210	48	39	< 2
801	D - 332	412	286	< 7	866	83	108	55	< 2	931	211	52	54	< 2
802	1	85	82	< 2	867	85	74	58	< 2	932	213	121	63	< 2
803	2	90	83	< 2	868	86	60	45	< 2	933	215	61	70	< 2
804	3	72	68	< 2	869	87	55	48	< 2	934	216	50	51	< 2
805	4	118	60	< 2	870	88	55	45	< 2	935	220	66	55	< 2
806	6	138	88	< 2	871	90	50	61	< 2	936	222	69	56	< 2
807	7	112	75	< 2	872	91	135	61	< 2	937	223	39	47	< 2
808	8	100	75	< 2	873	92	120	92	< 2	938	225	42	45	< 2
809	9	98	98	< 2	874	94	92	59	< 2	939	227	50	60	< 2
810	10	55	88	< 2	875	96	75	56	< 2	940	228	36	60	< 2
811	11	92	90	< 2	876	97	94	59	< 2	941	229	47	64	< 2
812	12	85	70	< 2	877	98	80	59	< 2	942	231	31	56	< 2
813	13	78	70	< 2	878	99	50	63	< 2	943	232	36	54	< 2
814	15	74	75	< 2	879	100	55	60	< 2	944	233	40	50	< 2
815	16	78	60	< 2	880	104	40	57	< 2	945	244	21	73	< 2

(ppm)				
Ser. No.	Sample No.	Cu	Zn	Mo
1141	J - 150	64	104	< 2
1142	151	68	439	< 2
1143	152	57	145	< 2
1144	153	54	63	< 2
1145	154	32	87	< 2
1146	155	39	119	< 2
1147	156	36	148	< 2
1148	157	27	72	< 2
1149	158	36	133	< 2
1150	159	43	102	< 2
1151	160	46	104	< 2
1152	161	54	333	< 2
1153	162	36	126	< 2
1154	163	29	350	< 2
1155	164	29	351	< 2
1156	165	25	79	< 2
1157	166	29	82	< 2
1158	167	61	151	< 2
1159	168	146	129	< 2
1160	169	46	137	< 2
1161	170	54	114	< 2
1162	171	50	158	< 2
1163	172	50	60	< 2
1164	174	46	91	< 2
1165	175	64	158	< 2
1166	176	43	180	< 2
1167	177	61	491	< 2
1168	178	125	135	< 2

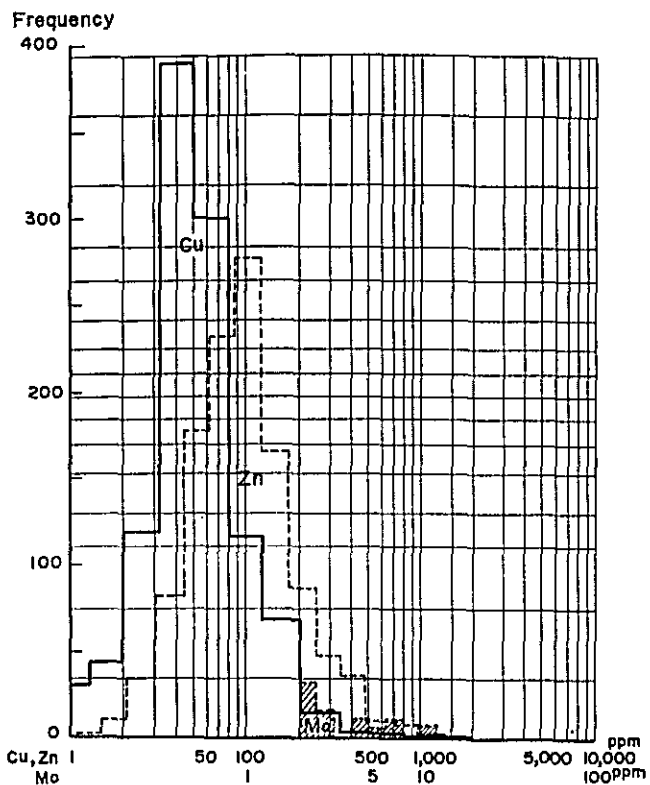


Fig. 1. Histogram of Cu, Zn and Mo

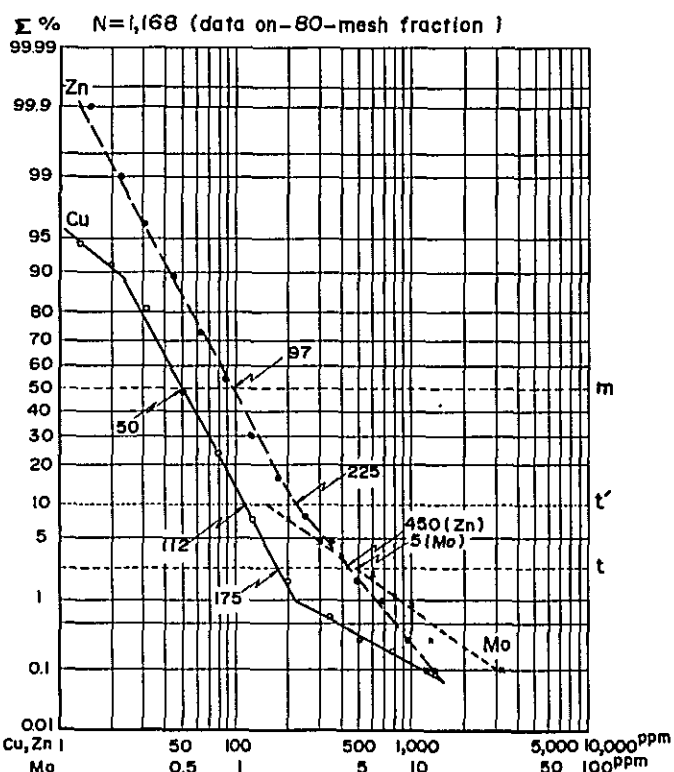


Fig. 2. Cumulative frequency distribution of Cu, Zn and Mo

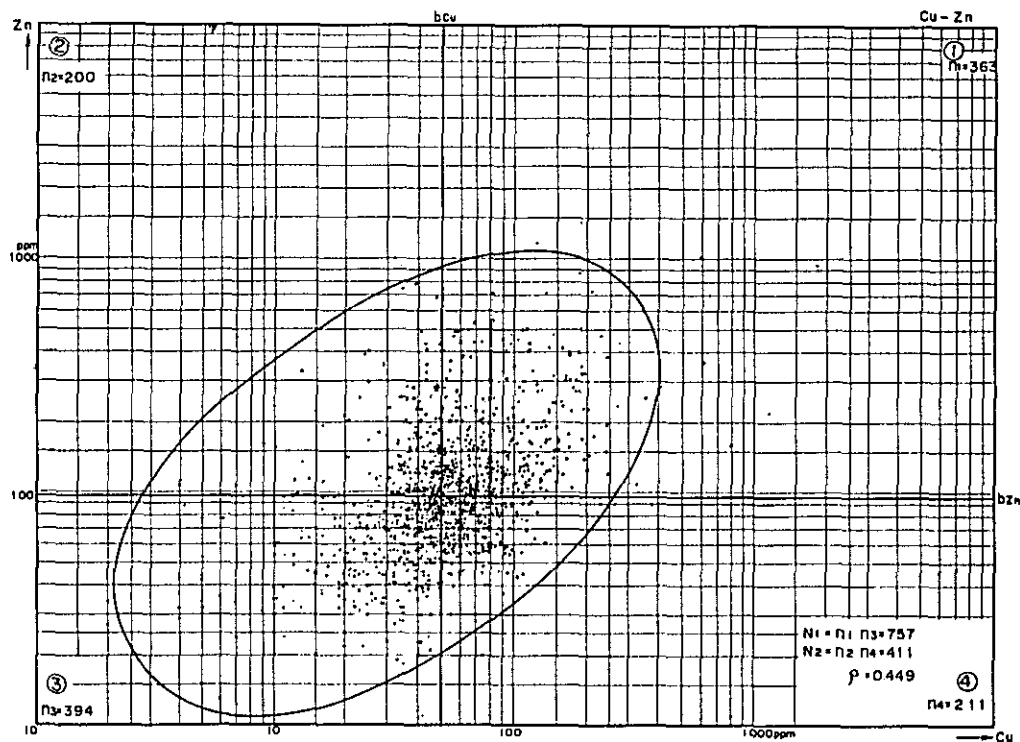


Fig. 3. Correlation diagram Cu-Zn

